Curriculum Vitae

Robert A Brown

rabrown@som.umaryland.edu

https://www.linkedin.com/in/robert-brown-5b031986/

Doctor of Philosophy, May 2023

Education

2018-2023 Ph.D in Molecular Medicine, Graduate Program in Life Sciences University of Maryland, Baltimore – Baltimore, MD

2017-2018 Masters Student, Graduate Program in Cellular and Molecular Biomedical Science University of Maryland, Baltimore- Baltimore, MD

2007-2011 B.S. in Biology, Loyola University Maryland- Baltimore, MD

Research Experience

9/2018-current Graduate Student Research Assistant, Department of Biochemistry and Molecular Biology-University of Maryland School of Medicine

2017-9/2018 Graduate Student Research Assistant, Center for Shock, Trauma and Anesthesiology Research-University of Maryland School of Medicine

2/2018-5/2018 Graduate Laboratory Rotation, Department of Physiology-University of Maryland School of Medicine

4/2016-9/2017 Laboratory Research Assistant, Department of Microbiology and Immunology -University of Maryland SoM

8/2014-4/2016 Laboratory Research Technician, Department of Endocrinology, Diabetes and Nutrition-University of Maryland SoM

Institutional Service – University of Maryland School of Medicine

Medical Student Instructor

2021-2022 Foundation course preceptor (2 sessions, a total of 4 contact hours, >80 first year medical students each)

- Gene and Chromatin Regulation
- Oxidative phosphorylation

2019- 2021 Summer Student Mentorship. Total of 4 undergraduate summer interns as they pursued their respective projects in the Zalzman lab.

Publications

1. Gupta A., Hwang BJ., Benyamien-Roufaeil D., Jain S., Liu S., Gonzales R., **Brown RA**, Zalzman M, and Lu AL. Mammalian MutY homolog (MYH or MUTYH) is critical for telomere integrity under oxidative stress. 2022. *OBM Geriatrics* doi:10.21926/obm.geriatr.2202196

2. Arad M*, **Brown RA***, Khatri R, Taylor RJ, Zalzman M. Direct differentiation of tonsillar biopsy-derived stem cells to the neuronal lineage. *Cell Mol Biol Lett*. 2021 PMID: 34407767 *denotes co-first authorship

3. Qian K, Yu D, Wang W, Jiang M, Yang R, **Brown R**, Gong DW. STK38 is a PPARγ-interacting protein promoting adipogenesis. 2021. *Adipocyte*. PMID: 34670478

4. Portney BA, Arad M, Gupta A, **Brown RA**, Khatri R, Nay-Lin P, Hebert AM, Angster KH, Silipino LE, Meltzer WA, Taylor RJ, Zalzman M. ZSCAN4 facilitates chromatin remodeling and promotes the cancer stem cell phenotype. 2020. *Oncogene*. PMID: 32507861

5. Zalzman M, Meltzer WA, Portney BA, **Brown RA**, Gupta A. The Role of Ubiquitination and SUMOylation in Telomere Biology. 2020. *Current Issues in Molecular Biology*. PMID: 3142293

6. Xu F, Zhou H, Wu M, Zhang H, Zhang Y, Zhao Q, **Brown R**, Gong DW, Miao L. Fc-Elabela fusion protein attenuates lipopolysaccharide-induced kidney injury in mice. 2020 *Biosci Rep*. PMID: 32808659

7. **Brown RA**, Voit A, Srikanth MP, Thayer JA, Kingsbury TJ, Jacobson MA, Lipinski MM, Feldman RA, Awad O. mTOR hyperactivity mediates lysosomal dysfunction in Gaucher's disease iPSC-neuronal cells. 2019. *Disease Models and Mechanisms*. PMID: 31519738.

8. Gong DW, Yu D, Zhang H, Wang J, Zhao Q, Qian Q, **Brown R**, Yang R, Wang W, Li Y, Xi Y, Shi Z, Tian Z. Recombinant Elabela-Fc Fusion Protein Has Extended Plasma Half-life and Mitigates Post-infarct Heart Dysfunction in Rats. 2019. *International Journal of Cardiology*. PMID: 31101543.

9. Zhou H, Yang R, Wang W, Xu F, Xi Y, **Brown R**, Zhang H, Shi L, Zhu D, Gong DW. Fc-apelin fusion protein attenuates lipopolysaccharide-induced liver injury in mice. 2018. *Scientific Reports*. PMID: 30061611.

10. Wang W, Zhang D, Yang R, Xia W, Qian K, Shi Z, **Brown R**, Zhou H, Xi Y, Shi L, Sun X, Chen L, Zhu D, Gong DW. Hepatic and Cardiac Beneficial Effects of Long-acting Fc-apelin Fusion Protein in Diet-induced Obese Mice .2018. *Diabetes/Metabolism Research and Reviews*. PMID: 29577579.

11. Awad O, Panicker LM, Deranieh RM, Srikanth MP, **Brown RA**, Voit A, Peesay T, Park TS, Zambidis ET, Feldman RA. Altered Differentiation Potential of Gaucher's Disease

iPSC Neuronal Progenitors due to Wnt/β-Catenin Downregulation. 2017. *Stem Cell Reports*. PMID: 29198828.

Conference Abstracts

1. **Brown RA**, Gupta A, Portney BA, Benyamien-Roufaeil DS, and Zalzman M. ZSCAN4-RNF20 Interactions Regulate Chromatin De-condensation and Pluripotency Gene Expression. 2022. Abstract: UMB Graduate Research Conference. Baltimore, MD
2. **Brown RA**, Gupta A, Portney BA, Benyamien-Roufaeil DS, and Zalzman M. Regulation of Cancer Stem Cell Gene Expression through Chromatin Remodeling. 2022. Abstract: Baltimore Area Repair Symposium. Baltimore, MD
3. **Brown RA**, Arad M, Zalzman M. Rapid Differentiation of Tonsil-Derived Mesenchymal Stem Cells to the Neuronal Lineage. 2020. Abstract: UMB Biochemistry and Molecular Biology Annual Retreat. Baltimore, MD
4. **Brown RA**, Arad M, Zalzman M. Direct Differentiation of Tonsillar-Biopsy Derived Stem Cells to the Neuronal Lineage. 2019. Abstract: American Society for Gene and Cell Therapy Annual Meeting. Washington, DC
5. **Brown RA**, Arad M, Zalzman M. Direct Differentiation of Neuron-Like Cells from Tonsillar-Biopsy Derived Multipotent Stem Cells. 2019. Abstract: International Society for Stem Cell Research Annual Meeting. Los Angeles, CA
6. Sarkar C, **Brown RA**, Awad O, Feldman R, Lipinski MM. Neuronal differentiation of neuronal stem cells by autophagy induction in an oxidative environment to treat TBI. 2018. Abstract: Annual Joint Symposium of the International and National Neurotrauma Societies. Toronto, Canada
7. **Brown R**, Awad O, Srikanth M, Voit A, Feldman R. Mechanisms of TFEB dysfunction by GBA1 mutations in an iPSC model of neuropathic Gaucher disease. 2017. Abstract: Society for Neuroscience Annual Meeting. Washington, DC
8. Sarkar C, Awad O, **Brown RA**, Feldman R, Lipinski MM. Neuronal differentiation of neuronal stem cells by autophagy induction in an oxidative environment to treat TBI. 2017. Abstract: Maryland Stem Cell Research Fund Annual Meeting. Baltimore, MD.
9. Feldman RA, Awad O, Panicker LM, Deranieh RM, Srikanth M, **Brown RA**, Park TS, Zambidis ET. WNTED: A Link Between GBA1 and Neurodegeneration. 2017. Abstract: Maryland Stem Cell Research Fund Annual Meeting. Baltimore, MD

Book Chapters

Zalzman M, Meltzer WA, Portney BA, **Brown RA**, Gupta A. "The Role of Ubiquitination and SUMOylation in Telomere Biology" SUMOylation and Ubiquitination, Current and Emerging Concepts. (Edited by: Van G. Wilson). Caister Academic Press, U.K. (2019) Pages: 289-302

Awards

- Graduate Research Assistantship-University of Maryland, Baltimore 2018-2023
- Best Poster Award-UMB Graduate Research Conference 2022

Abstract

ZSCAN4-Mediated Stem Cell Potency in Adult and Cancer Stem Cells

Robert A. Brown, Doctor of Philosophy, 2023
Dissertation Directed by:
Michal Zalzman, PhD, Assistant Professor
Department of Biochemistry and Molecular Biology
Department of Otorhinolaryngology – Head and Neck Surgery
University of Maryland School of Medicine

The replication and differentiation capacity of stem cells (stem cell potency) are important determinants in a variety of human diseases. Impaired potency of endogenous stem cells is a contributing factor to aging-related diseases, including neurodegenerative disease. Cell therapies, aimed at treating neurodegenerative disease, use exogenous stem cells, whose efficacy varies based on their potency. Previous reports have demonstrated that mesenchymal stem cells (MSCs), are a promising source for stem cell therapies in neurodegenerative disease. We previously reported the generation of fully defined MSCs from palatine tonsil (T-MSC) biopsies of less than 1g of tissue, with extremely high efficiency compared to extraction protocols from other sources.

However, clinical applications of MSCs are still limited by low replication potential and telomere shortening in cells derived from elderly individuals. Furthermore, after expansion in culture, T-MSCs show a reduced ability to differentiate due to accelerated aging *in vitro*. Therefore, methods to control survival and enhance the differentiation capacity of aged MSCs are urgently needed for the scale-up needs of regenerative medicine. This is a key

obstacle to the engineering of cell therapies for neurodegenerative diseases, as cells not only need to be able to self-renew, but also to efficiently differentiate for clinical applications. In these studies, we first developed a procedure to generate neuron-like cells from T-MSCs and defined their neurogenic potential. Our results demonstrate that T-MSCs extracted from pediatric donors have high neurogenic potency for 6-10 passages, compared to bone-marrow derived MSCs. Next, we assessed the potential of ZSCAN4, an early embryonic gene associated with developmental potency, to increase the differentiation potential of aged MSCs with the future goal of enhancing their efficacy for the treatment of neurodegenerative diseases. Our data indicate that expression of ZSCAN4 in these cells increases stem cell characteristics and their ability to differentiate to neural stem-like cells.

In the next part of our work we studied the mechanism of ZSCAN4, the effect of its interaction with another factor, RNF20, and their mutual significance to pluripotency gene expression in cancer cell lines. Aberrant increases in stem cell potency factors in a small number of transformed tumor cells, creates a sub-population of Cancer Stem Cells (CSCs). Such cells are responsible for seeding metastases and driving tumor aggressiveness, while being comparatively slower growing and more resistant to radiation and common chemotherapies, versus bulk tumor cells. Thus, methods to reduce stem cell potency in cancers may be beneficial. Previous findings in our lab show that ZSCAN4, while not normally expressed in post-embryonic human cells, is expressed in human cancers and cancer cell lines, leading us to theorize that ZSCAN4 may be mediating the cancer stem cell phenotype in the same manner it has been reported to regulate stem cell potency in pluripotent stem cells. Our results indicate that ZSCAN4 expression is associated with cancer stem cells, and enhances pluripotency gene expression in cancer

stem cells. We further found that while ZSCAN4 can exert epigenetic effects independently of RNF20, both proteins need to be present for ZSCAN4's effects on telomere length and expression of pluripotency genes.

Altering stem cell potency is important in regenerative medicine, where increased stem cell potency is desirable, and for oncology, where reduced stem cell potency is sought. Our results indicate that ZSCAN4, whose expression is otherwise restricted to early development, positively regulates stem cell potency when expressed in either T-MSCs or in cancer cell lines. Thus, ZSCAN4 is a promising target for use in regenerative medicine and inhibition in cancers.

ZSCAN4-Mediated Stem Cell Potency in Adult and Cancer Stem Cells

by
Robert Andrew Brown

Dissertation submitted to the Faculty of the Graduate School of the
University of Maryland, Baltimore in partial fulfillment
of the requirements for the degree of
Doctor of Philosophy
Spring 2023

Acknowledgements

First and foremost, I'd like to thank my mentor Dr. Michal Zalzman. Michal, despite the challenges of the last few years, you've been able to keep both my project and multiple collaborative projects in the lab progressing. Thank you for your support and encouragement to pursue my interests, even when they diverged off from my original project, as well as helping me to understand that "the data is the data" and to never be too locked into a hypothesis. You've helped me to become a better scientist.

A big thank you goes out to my committee members Drs. Ronna Hertzano, Michael Seidman, Marta Lipinski, Ola Awad and Tami Kingsbury. Your guidance and constructive criticism over the last few years has significantly improved my work. I'd also like to thank my pre-doctoral mentors. Dr. Da-Wei Gong, thank you for giving someone with no research background a launching pad in science. Drs. Ricardo Feldman and Ola Awad, thank you both for giving me the opportunity to learn, publish and hone my skills as a researcher, while treating me as a graduate student, even prior to my joining the program here. Drs Marta Lipinski and Chinmoy Sarkar, thank you for the chance to continue learning and helping me to translate knowledge and techniques from one research area to another. Dr. Tami Kingsbury, thank you for giving a rotation student a "cool" project that resulted in successful knockout cells.

I would be remiss not to mention our collaborators Dr. Rodney Taylor and Yaping Ji. Our regular meetings and presentations have provided a sounding board for my ideas and a constructive environment for evaluating my data. Likewise, I'd like to thank former members of the Zalzman lab for their contributions to my projects and allowing me to contribute to theirs. Aditi, thank you for helping to orient me to the Zalzman lab, despite

only joining a few months before me, as well as your preliminary data for many of my experiments. Alok, thanks for being my bench-mate and for introducing a biologist to the world of materials science. Phyo, thanks for your help in characterizing our knockout lines and for your Instant Pot. Daniel, thank you for your contributions to my project, particularly your ChIP expertise. To our summer students Alex, Katrina, Sara, and Sophie thank you for your help in the lab and infectious enthusiasm for science.

I'd further like to thank the Molecular Medicine program, its director Dr. Toni Antalis, and my track leaders Dr. Matthew Trudeau and Dr. Megan Rizzo for their support in navigating the program. I'd also like to thank Chelsea Leonard and Elice Garcia-Baca for keeping me on track with gentle reminders to turn in required forms. An additional thank you to the Biochemistry departmental staff, specifically Bruce, Heather, Kathleen, Koula, and Melissa.

Finally, I'd like to thank my friends and family, whose support during my graduate career kept me going. In particular, I'd like to thank my parents, Richard and Marian, my sister Kathleen, and my dog Malcolm, all of whom helped to support me and thereby, this project. Without you all, this would not have been accomplished.

Table of Contents

List of Figures

List of Abbreviations

ABCG2	ATP-binding cassette super-family G member 2
ACTA2	Alpha Actin 2
AD	Alzheimer's Disease
ALDH1A1	Aldehyde dehydrogenase 1 family, member A1
ALT	Alternative Lengthening of Telomeres
BMI1	Polycomb complex protein BMI-1
BM-MSC	Bone Marrow-derived Mesenchymal Stem Cell
CD105	Cluster of Differentiation 105
CD44	Cluster of Differentiation 44
CD73	Cluster of Differentiation 73
CD90	Cluster of Differentiation 90
ChART	Chromatin Accessibility by Real Time Polymerase Chain Reaction
ChIP	Chromatin Immunoprecipitation
CNS	Central Nervous System
CRISPR	Clustered Regularly Interspaced Short Palindromic Repeats
CSC	Cancer Stem Cell
DAPI	4′,6-diamidino-2-phenylindole
DCX	Doublecortin

DOPA	L-Dopamine
DOX	Doxycycline
ELDA	Extreme Limiting Dilution Assay
ESC	Embryonic Stem Cell
H2Bub1	Mono-ubiquitylated histone H2B at Lysine 120
HNSCC	Head and Neck Squamous Cell Carcinoma
HSC	Hematopoetic Stem Cell
iCas9	inducible Cas9
iPSC	induced Pluripotent Stem Cell
KD	Knockdown
KO	knockout
L-GLUT	L-Glutamate
MAP2	Microtubule Associated Protein 2
MDR1	Multi-Drug Resistance 1
MSC	Mesenchymal Stem Cell
MSI1	Musashi-1
NANOG	Homeobox Protein NANOG
NCAM1	Neural Cell Adhesion Molecule 1
NEFL	Neurofilament light chain
NSC	Neural Stem Cell
NTC	Non-targeting control
OCT4	Octamer binding transcription factor 4
PD	Parkinson's Disease

POLR2A	RNA Polymerase 2, subunit A
PSC	Pluripotent Stem Cell
PSD95	Post-synaptic Density 95
RNF20	Rin finger protein 20
RT-PCR	Reverse Transcriptase Polymerase Chain Reaction
SCR	Scrambled
SOX1	SRY-Box Transcription Factor 1
SOX2	SRY-Box Transcription Factor 1
SYP	Synaptophysin
TERC	Telomerase RNA component
TERT	Telomerase Reverse Transcriptase
T-MSC	Tonsil-derived Mesenchymal Stem Cell
Tuj1	Beta 3 Tubulin
WT	Wild Type
ZGA	Zygotic Genome Activation
ZSCAN4	Zinc Finger and SCAN domain containing 4

Chapter 1: Introduction

1.1 Stem Cells

Stem Cells are developmentally primitive cells characterized by their ability to self-renew and to differentiate into more specialized lineages of tissue specific cells. The range of specialized cells that a stem cell is capable of differentiating into is called stem cell potency. Stem cell potency varies widely, from a totipotent zygote, capable of differentiating into any embryonic and extraembryonic cell type, to more lineage-restricted multipotent stem cells such as neural stem cells or mesenchymal stem cells (1). Endogenous stem cells play crucial roles in early development, as cells differentiate from totipotent stem cells to pluripotent stem cells, to germ layer-restricted multipotent stem cells and finally tissues-specific cells and their progenitors, which are cells with a limited capacity for self-renewal and are lineage-restricted to one type of mature cell (Figure 1). This process of progressive differentiation in development can be mimicked *in vitro* with cultured stem cells.

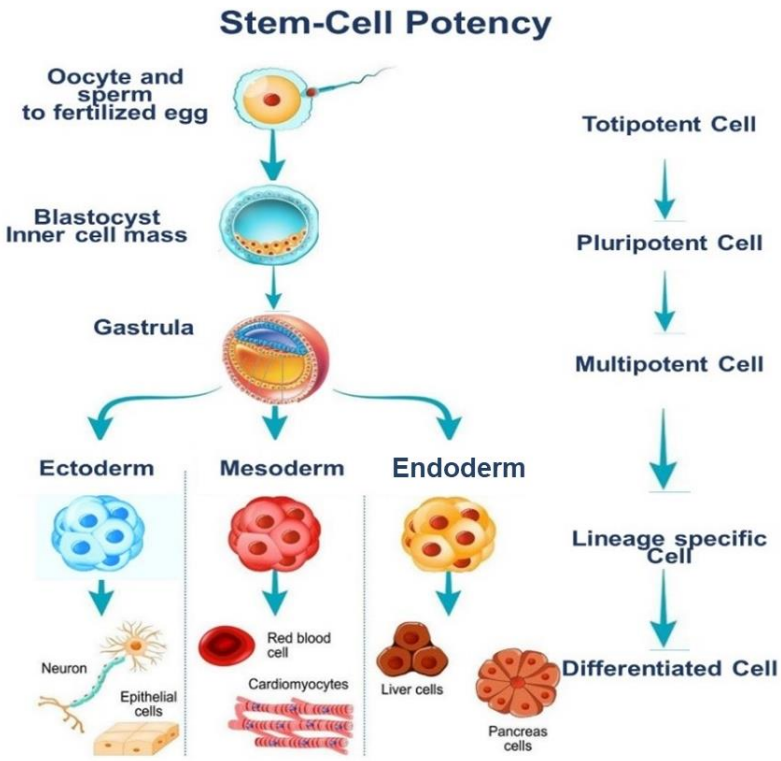

Figure 1: Stem cell hierarchy of potency
The most potent cell is the fertilized egg, which then develops into the blastocyst. Pluripotent stem cells can be derived from the inner cell mass which, like in the gastrula, can generate the three germ layers: the ectoderm, mesoderm and the endoderm. These cells are multipotent and can generate many lineage-specific stem cells, which in turn, can differentiate to tissue specific stem cells and finally to terminally differentiated functional cells.

1.1A. Stem Cell Phenotype

Aside from their ability to self-renew and to differentiate, stem cells can be characterized by several other attributes. The stem cell phenotype can be distinguished by distinct gene expression patterns, governed by generally loose, accessible DNA, as well as by relatively long telomeres, a bulwark against attrition during cell division. These aspects are intertwined and co-dependent, with all three working in concert to maintain cell stemness.

1.1.B. Pluripotent Stem cells

In vitro Pluripotent Stem Cells (PSCs) are either derived from early embryonic tissue (embryonic stem cells or ESCs) or can be engineered by a de-differentiation process from

mature cell types (induced Pluripotent Stem Cells or iPSC). These cells are capable of surviving, proliferating and, importantly, retaining their stem cell potency in cell culture conditions. Their undifferentiated state can be maintained across hundreds of cell divisions by the use of serum-free media and the presence of either exogenous growth factors or "feeder cells" that secrete them. Withdrawal of these factors results in PSC differentiation (2) to form embryoid bodies, which are 3D structures consisting of lineage-restricted stem cells from all three germ layers (endoderm, mesoderm, ectoderm) (3). By altering the composition of culture media during and after embryoid body development, one can select for cells of a particular lineage. For instance, co-inhibition of TGF-B and BMP signaling skews embryoid bodies towards the ectodermal lineage at the expense of endoderm and mesoderm, while also inducing differentiation from ectodermal stem cells to yet more restricted neural stem cells (4). Similar approaches can be used to generate a vast variety of cell types from each germ layer (5, 6) As a result, PSCs can be used to generate nearly any cell type needed for either research or therapeutic purposes.

1.1.C. Multipotent Stem Cells

Multipotent Stem Cells are more lineage-restricted, less potent stem cells either found in post-embryonic tissues or generated *in vitro* by partial differentiation of PSCs as mentioned above. Multipotent stem cells exist in a variety of tissues, such as intestinal stem cells in intestinal crypts, responsible for the regular re-generation of intestinal epithelium (7).

Mesenchymal Stem Cells (MSCs) are a type of multipotent stem cell that (at least classically) are restricted to the mesenchymal lineages of bone, fat, cartilage, and muscle (8). MSCs are derived either from developmental mesoderm or neural crest cells

(ectoderm-derived) (9). MSCs exist perivascularly (pericytes), lining the blood vessels of many tissues (8). *In vivo*, MSCs typically exist as quiescent cells which can be activated by local environmental cues (typically injury) to proliferate, secrete immunomodulatory factors, or differentiate in an effort to repair or replace damaged cells. *Ex vivo*, MSCs can be extracted from various tissues and cultured adherently. MSCs have been reported from bone marrow (10), adipose tissue (11), skin (12), skeletal muscle (13), dental pulp (14), and fetal/neonatal tissues like amniotic fluid (15), or umbilical cord (16). Recently, MSCs have been generated from tonsil tissue, both by our lab and others (17, 18). Interestingly, MSCs have been reported to generate a variety of cell types outside of the mesenchymal lineages, such as liver cells, pancreatic cells, and neural cells (19-21).

1.2 Epigenetics

As stem cells and their progeny share the same DNA, the differentiation process involves major epigenetic changes to the chromatin, in order to open or close tissue specific programs. Epigenetics is the study of the changes to the structure of the chromatin without changes in the DNA sequence. Unlike the relatively loose and unstructured genome of prokaryotes, eukaryotic DNA exists in complex with structural scaffold proteins known as histones. Histones are globular proteins that form a hetero-octamer of two H2A-H2B dimers and a tetramer of H3-H4 proteins. Together, this histone octamer interacts with the DNA, resulting in a more structured genome. Histones have high abundances of positively charged amino acids (Lysines and Arginines) that generate an overall positive charge to the octamer, enabling electrostatic interactions with the negatively charged DNA.

1.2.A. Histones Acetylation and Chromatin Accessibility

Changes in the charge of histones affects the strength of the interaction between them and their associated DNA. The N-terminal tails of the histones are generally outward facing and can undergo post-translational modifications by cellular enzymes. The amino acids Serine, Threonine and Tyrosine can be phosphorylated, while Lysine and Arginine can be methylated (mono-, di-, or tri-) or acetylated. The addition of a phosphate group strongly dispels the electrostatic interactions between DNA and histones and results in loosely bound DNA. The addition of acetyl groups serves to reduce the positive charge of the histones and results in a less dramatic, though still substantial loosening of the DNA-histone interaction. Histone acetylation is promoted by histone acetyltransferase (HAT) enzymes and antagonized by histone deacetylases (HDACs), the expression and activity of these two classes thus underlie total acetylation levels in the cell (22).

1.2.B. Histone Mono-ubiquitylation

In a separate category is histone mono-ubiquitylation. While less studied than histone acetylation, some histone lysines can also be mono-ubiquitinated, with an E3 ubiquitin ligase attaching an 8.6kDa ubiquitin molecule to a lysine. While, like acetylations, this does serve to mask the basic charge of a histone, the bulk of its effect is actually due to steric interactions between nucleosomes. Nucleosomes can be understood as “beads on a string” with stretches of free DNA between nucleosomes (Figure 2). In tightly packed DNA, nucleosomes are effectively stacked adjacent to one another with little spacing and resultantly, little accessibility for transcription. The addition of a ubiquitin molecule to a histone serves to sterically break up that tight stacking (“ubiquitin crowbar”) and increase

separation between nucleosomes (23) (Figure 2). Ubiquitylation of histones is performed by E3 ubiquitin ligases (RNF20/40, RING1A/1B) and antagonized by deubiquitnases (BAP1, UBP8) the balance between their respective activities dictating the level of histone ubiquitylation in a given cell (24-26).

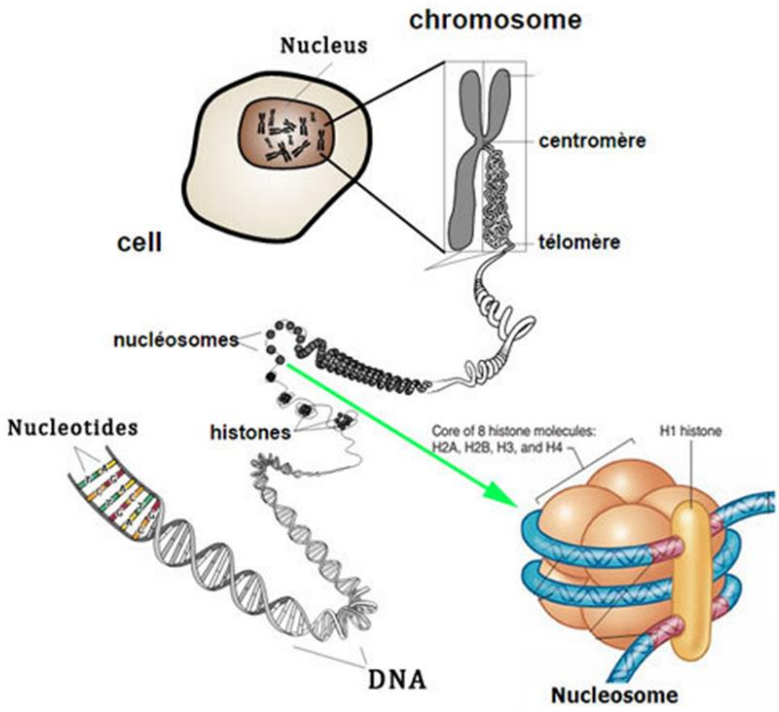

Figure 2: Overview of nucleosome structure.
DNA exists in complex with an octamer of histone proteins, forming a nucleosome. The strength of the interaction between the DNA and histone proteins is dictated by relative levels of histone acetylation. The relative spacing between the nucleosomes themselves is mediated by histone mono-ubiquitylation.

1.2.C. Histone Modifications and Gene Expression

The aforementioned histone acetylation and ubiquitylation govern the relative compaction of chromatin and therefore, its accessibility for gene expression. In addition to these marks, histones can be methylated with 1, 2, or 3 methyl groups (mono-, di-, or tri-methylation). Unlike acetylation, histone methylation does not alter the underlying charge of the histone and therefore does not affect the compaction of the chromatin directly (23). Depending on

their location on a histone tail, methylations can either be repressive for gene expression or facilitative. Tri-methylation of Histone H3 at lysine 4 (H3K4Me3) for example is activating and is believed to function in the recruitment of chromatin remodeling enzymes, as well as the recruitment of RNA polymerase II to transcriptional start sites of genes(24) Conversely, Tri-methylation of Histone H3 at lysine 9 (H3K9Me3) is repressive, serving as a scaffold for additional histone methylases, DNA methylases, and transcriptionally repressive proteins (24). Histone methylations are performed by Histone methyltransferases (KMTs) and removed by histone demethylases (KDMs) the balance of which, akin to that in histone acetylation and ubiquitylation, is responsible for overall histone methylation levels in the cell.

1.2.D. DNA Methylation

Finally, there is one epigenetic modification that occurs on DNA itself, not the histones. DNA can be methylated on the 5-carbon of the base cytosine, resulting in 5-methylcytosine (5mC). DNA methylation is strongly repressive for gene expression, acting to inhibit the binding of transcription factors to promoters, inhibit the binding of RNA polymerase, and to further prevent RNA polymerase processivity in the event it does bind(24, 25). Methylated DNA further recruits methyl binding domain proteins (MBD1, MBD2, etc.) which serve to recruit additional repressive proteins and sterically inhibit transcription factor and RNA polymerase binding to genes(26). DNA methylation levels are maintained by the balance of DNA methyltransferase (DNMTs) and DNA demethylase (TET enzymes) activity. Thus, while histone acetylation and ubiquitylation affect the accessibility of DNA, and thereby gene expression, directly by altering DNA-histone

interaction strength, histone methylation and DNA methylation can affect gene expression indirectly by recruitment of activating or inhibitory factors. The balance of all of these effects in a given cell and at a given gene loci, determine whether, and to what extent, a gene is expressed.

1.2.E. Stem Cell Epigenetics

Stem cells are characterized by globally open, transcriptionally accessible chromatin. This phenotype is facilitated by high levels of histone acetylation and low levels of repressive histone methylation, together contributing to a globally transcriptionally accessible genome. This open chromatin phenotype is maintained by the balance of enzymes responsible for the modification, or removal of, histone modifications. In order to maintain the epigenetic phenotype of open, accessible chromatin, stem cells either express high levels or have high activity of KATs, KDMs, and E3 Ubiquitin ligases, and low levels or low activity of HDACs, KMTs, and DUBs. With loss of stem cell potency (due to differentiation or cellular aging) this balance is shifted, leading to an epigenetic phenotype of progressively closed chromatin (27-29).

The local epigenetic environment is even more important for the stem cell phenotype. The chromatin state at the genes regulating pluripotency is an important regulator of their expression. Expression of the core pluripotency factors NANOG, OCT4, and SOX2 are regulated epigenetically, by a combination of histone acetylation, histone methylation, and DNA methylation (30-32). Interestingly, expression of the core pluripotency factors has been reported to reciprocally regulate the epigenetic state of the cell, through regulation of chromatin modifiers (33).

Likewise, the chromatin status at telomeres is an important arbiter of telomere length. Telomere length depends on the relative accessibility of telomeric chromatin to extension machinery (34). The more open, accessible state of telomeric chromatin in stem cells thereby enables telomere extension. The epigenetic state of stem cells is an important factor underlying pluripotency gene expression and telomere extension.

1.3 Pluripotency Gene Expression

Differential gene expression is what gives a cell its phenotype. The gene expression patterns of a keratinocyte, for example, will differ significantly from that of a neuron. The phenotype of a stem cell is similarly underlain by the expression of specific genes. Most importantly, and upstream to most potency-associated pathways, is the expression of the core pluripotency factors NANOG, OCT4, and SOX2. These core factors work in concert with one another to maintain a stem cell in an undifferentiated state, suppressing differentiation. In stem cells, multiple self-renewal signaling pathways (Wnt, Notch, Akt) converge to independently activate expression of OCT4 (aka POU5F1) and the self-renewal factor BMI1 (35-38). BMI1 subsequently activates expression of SOX2 (39). Finally, OCT4 and SOX2 cooperatively bind the promoter of NANOG, inducing its expression (40). NANOG, OCT4, and SOX2 then cooperatively bind to and activate expression of a variety of self-renewal and potency related genes, driving the undifferentiated phenotype of a stem cell. As mentioned previously, the expression of NANOG-OCT4-SOX2 depends on the epigenetic state of their promoters. Once expressed, these factors then regulate expression of chromatin modifying genes that alter the epigenetics of the whole genome, including their own promoters (41). NANOG-OCT4-

SOX2 have also been implicated in activating expression of TERT and TERC, the major components of the enzyme telomerase, thereby contributing to telomere elongation (42). Expression of the core pluripotency factors thus regulates telomere length, as well as reciprocally regulating the cell's epigenetic state.

1.4 Telomeres

Stem cells exhibit longer telomeres than differentiated cells, as well as better ability to maintain those telomeres across cell divisions (43). Telomeres are regions of repetitive hexomeric DNA sequences (TTAGGG) present at the end of eukaryotic chromosomes, functioning to prevent the loss of genomic regions across cell divisions. Due to the linear chromosomes of eukaryotes, every cell division (DNA replication) results in a mismatched strand length between the newly synthesized lagging strands and their complementary parental strands. This "end replication problem" causes one strand to be shorter than its complement, leaving a 3' overhang of roughly 50-200bp at the end of each chromosome. To prevent the single-stranded overhang from activating the DNA damage response (DDR), several telomere-specific proteins, known as the Shelterin complex, bind the single stranded overhang and protect it from activating the DDR. However, since 50-200 bp are lost from one strand during each cell division, over many cell divisions, unless maintained, telomeres shorten considerably. When telomeres become critically short, shelterin no longer fully protects the telomeres and DDR is activated, leading to cell senescence or apoptosis (44). Telomeres thus serve as a biological clock setting a maximum number of cell divisions for a given cell. As stem cells need to maintain long-term self-renewal

capability, even across many cell divisions, they typically employ mechanisms to mitigate telomere attrition. The most common mechanism of telomere maintenance is telomerase.

1.5 Telomerase

Telomerase is a reverse transcriptase, comprised of multiple subunits, with a major protein component (TERT) and an RNA component (TERC), and is capable of adding TTAGGG repeats ends of the telomere (45-47). Telomerase is highly expressed in the embryo (and derived cells such as ESCs), with expression levels declining precipitously with differentiation or aging (48). Lineage-restricted stem cells, such as HSCs or NSCs have some telomerase expression, while MSCs and fully differentiated cell types have negligible expression.

1.6 Alternative Lengthening of Telomeres

Telomerase, however, is not the only mechanism for telomere maintenance. Several proposed mechanisms have been reported for telomerase-independent maintenance or extension of telomeres, collectively described as Alternative Lengthening of Telomeres (ALT) (49, 50) . ALT mechanisms are typically offshoots of DNA repair pathways, wherein telomeres can be extended by homologous recombination, using homologous DNA sequences from the same chromosome, a different chromosome, or from extrachromosomal telomeric DNA (C-circles)(51). ALT has been reported in the cleavage stage embryo, but not in stem cells, however, it is present in some telomerase negative of human cancers (52).

1.7 Telomeres in Pluripotent Stem Cells

As seen in Figure 3, the status of telomeric chromatin is important for mediating telomere extension, whether via Telomerase or ALT. More open, accessible telomeric chromatin in the presence of active telomere extension mechanisms, allows either the telomerase complex or ALT (RAD52-RPA, among others) to bind to and subsequently extend the telomere (53, 54). As the NANOG-OCT4-SOX2 pluripotency factors contribute to the global open chromatin characteristic of stem cell and promote telomerase expression (55), they positively regulate telomere length. Telomeres themselves can indirectly regulate the chromatin state of the cell and thereby, affect pluripotency gene expression (56). Thus, all three aspects of the stem cell phenotype, as detailed above, are co-dependent, and underly the self-renewal and differentiation capacity of undifferentiated stem cells (3).

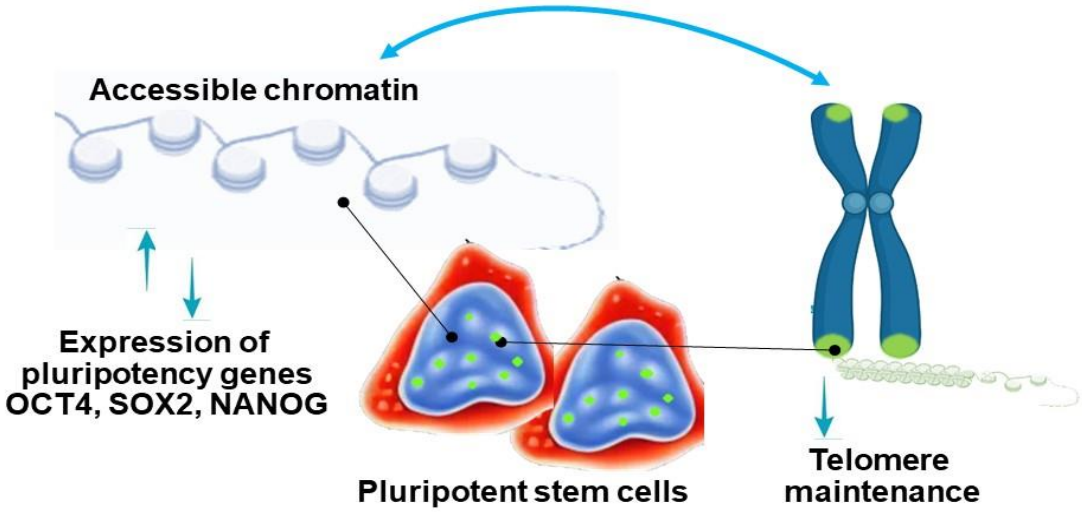

Figure 3: Chromatin accessibility, stem cell pluripotency and telomere maintenance. Accessible chromatin facilitates both the expression of the pluripotency genes SOX2, OCT4 and NANOG and enables telomere maintenance. Pluripotency genes can affect the regulation of telomerase and ALT and thereby contributes to telomere extension. It can also regulate chromatin accessibility through regulation of chromatin modifying enzymes. Finally, the telomeres can indirectly regulate changes in chromatin structure and potentially alter pluripotency gene expression.

1.8 Stem Cells in Disease

Stem cells play a significant role in many human diseases. After development, remaining reservoirs of stem cells are responsible for replacing cells lost or dysfunctional due to aging, injury or disease state. As such, they must retain substantial stem cell potency to retain their function across a human lifetime. A failure to preserve sufficient stem cell population or differentiation capacity, can result in disease. Conversely, cancer cells can aberrantly gain stem cell characteristics, rendering them more drug resistant, metastatic, and aggressive than they would otherwise be. Understanding how altered stem cell potency underlies disease is important for designing stem cell therapies.

1.8.A. Loss of Stem Cell Potency in Disease

Throughout a lifetime and across tissue types, there is a process of mature cells becoming dysfunctional, senescent and/or dying (57). To retain tissue function, these cells are replaced by the differentiation of endogenous stem cells. In response to microenvironmental cues, resident stem cells both proliferate and differentiate, generating the desired differentiated cell type, while retaining the reserve of undifferentiated stem cells. Over the course of normal aging, this injury response becomes skewed, with a progressively greater percentage of cells either failing to self-renew or failing to differentiate. This results in a depletion of stem cell reservoirs and to human aging (58).

One example is seen in age-related cognitive decline. Even in the absence of a specific disease process, with increasing age, there is increased incidence of mild cognitive impairment (MCI) (59). Here too, loss of stem cell potency has been implicated. While the

majority of neurogenesis occurs from development through adolescence, adults retain several reservoirs of neural stem cells (NSCs) (60). Throughout life, upon loss of mature neural cells due to injury or dysfunction, these losses are mitigated by neural stem cell differentiation, replacing lost cells, and retaining cognitive function. However, as seen with other adult stem cells, this population declines with age, failing either to self-renew or differentiate (61). Therefore, even "normal aging" appears to involve a pathology of impaired stem cell potency.

In addition to disease states inducing excessive stem cell activation and subsequent exhaustion, several disease states alter stem cell potency directly. Models of PINK1 mutation-associated Parkinson's Disease (PD) have shown that neural stem cells harboring the mutation are unable to efficiently differentiate into dopaminergic neurons, which are lost in PD (62). In the lysosomal storage disorder Gaucher's Disease (GD), GBA1 mutant NSCs show a remarkably impaired ability to differentiate to dopaminergic neurons (63) Similarly, in models of APP and APOE4 Alzheimer's Disease, there is an impairment of proliferation and neuronal differentiation of endogenous neural stem cells (64-66). Together, these results suggest that decreased stem cell potency via depletion, exhaustion, or impaired differentiation contributes not only to human disease, but even phenotypically normal aging. There is thus a significant need for research into ways to restore or increase stem cell potency, whether from endogenous or exogenous stem cell sources.

1.8.B. Gain of pluripotency-like characteristics in cancer cells

Many of the qualities of stem cell potency can be commandeered by a small population of tumor cells in cancers. These cells, variously referred to as tumor-initiating cells,

circulating tumor cells or cancer stem cells (CSCs), drive the phenotype of drug resistance, metastasis and invasiveness in many cancers (67). The stem cell phenotype adopted by these cells leads to more open chromatin (68, 69), enhanced expression of pluripotency-associated genes (particularly the expression of the NANOG-OCT4-SOX2 network) (70-72), and enhanced telomere maintenance (73-76).

The open chromatin of CSCs allows for important differences vs somatic stem cells. CSCs, typically have epigenetically silenced tumor suppressor genes and epigenetically activated pro-growth genes (77). Normal stem cell metabolism relies on glycolysis to a greater degree than differentiated cells do. Due to the Warburg effect, tumor cell metabolize is heavily skewed towards glycolysis compared to normal stem cells or normal differentiated cells. Thus, the slower growing CSC population generally has more of a balanced metabolism between glycolysis and oxidative phosphorylation, relative to bulk tumor cells (78). Normal stem cells, as they need to divide frequently, also have upregulated DNA repair mechanisms to minimize replication errors or DNA-damage (79) CSCs likewise employ enhanced expression of DNA repair genes, giving them a significant resistance to common chemoradiation therapies that work well against bulk tumor cells (80). Finally, like normal stem cells, CSCs have greater telomerase expression than bulk tumor cells, at least in telomerase positive cancers (81). These characteristics of normal stem cells have thus been repurposed by CSCs, making them significant drivers of cancer progression. Understanding the mechanisms by which CSCs are able to acquire their stem cell phenotype will allow the development of therapeutics that can inhibit cancer stemness, and thereby, more effectively treat cancer.

1.9 Zinc Finger and SCAN domain-containing 4 (ZSCAN4)

ZSCAN4 is an early developmentally-expressed gene (82) associated with stem cell potency and telomere regulation (83). While its structure remains unsolved, it is known to consist of an N-terminal SCAN domain, facilitating protein-protein interactions, as well as 4 zinc finger domains that facilitate the binding of DNA. ZSCAN4 is well conserved in mammals, existing as a cluster of 6 expressed genes and 3 pseudogenes in mice (82). In humans, the ZSCAN4 locus has been reduced to a single expressed gene. In both mice and humans, ZSCAN4 is expressed transiently and with great specificity at the 2-cell stage of the mouse embryo and the 8-cell stage of the human embryo (84). ZSCAN4 is also expressed in mouse embryonic stem cells (mESCs) as well as in mouse iPSCs (82, 85) In such systems, ZSCAN4 has been variously associated with chromatin remodeling, the expression of pluripotency genes, long term culture survival, the maintenance and extension of telomeres, and developmental potency (Figure 4).

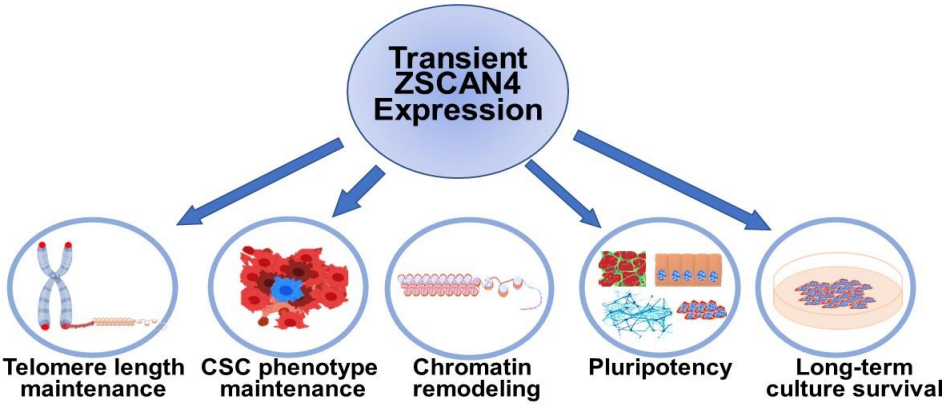

Figure 4: An illustration of the various and inter-related effects of transient ZSCAN4 expression.

1.9A ZSCAN4 in development

ZSCAN4 is transiently expressed in the early embryo (human 8-cell stage) where it is associated with zygotic genome activation (ZGA) (86). The resultant epigenetic changes beget gene expression changes that shift from the maternal and paternal programs to the zygote (87). Of particular importance are the pluripotency genes in the developing inner cell mass (needed to generate all downstream tissues), and the continued need to maintain telomeres in the face of the massive proliferation required during development. The importance of ZSCAN4 for ZGA has been demonstrated by knockdown and knockout studies in mice, showing ZSCAN4 expression during ZGA is indispensable for uterine implantation (88). ZSCAN4 expression in early development is short-lived, and it no longer expressed in the 4-cell stage of mice (16-cell stage human) (82). Thereafter, ZSCAN4 expression is negligible in all post-embryonic tissues.

1.9.B. ZSCAN4 and chromatin remodeling

ZSCAN4 is expressed transiently in mESCs and was found to be associated with significant epigenetic changes, paralleling what is seen during the ZGA (89). In particular, ZSCAN4 positive mESCs showed much higher levels of H3 histone acetylation at lysines 9 (H3K9ac), 14(H3K14Ac), 18(H3K18Ac) and 27 (H3K27Ac), as well as higher levels of the activating tri-methylation H3K4Me3 (89). Ectopic expression of ZSCAN4 in mESCs lead to increased levels of H3K27Ac and decreased levels of DNA methylation, specifically at ZGA related genes that were previously silenced (90). Taken together, this implicated ZSCAN4 as associated with epigenetic changes. However, it remained to be found if ZSCAN4 asserts these effect or marks cells with open chromatin.

1.9.C. ZSCAN4 and telomeres

Interestingly, while ZSCAN4 is transiently expressed during the 2-cell stage of embryogenesis, it is transcribed in short bursts of expression in mESCs (83, 91). These bursts are coupled with the expression of other genes that are specifically expressed during the two-cell stage, suggesting that this may in part drive a pluripotent phenotype (91). Further consequences of these outbreaks are a global shift from the heterochromatin state to a euchromatin state and rapid telomere expansion (92, 93). ZSCAN4 knockdown ES cells show significant reductions in telomere length followed by culture crisis, while ZSCAN4 rescue increases telomere length, doing so in a telomerase-independent manner (83). More recently, the telomerase-independent telomere lengthening was confirmed in ESCs as well as implicated in telomerase-negative, ALT positive cancer cells (94, 95).

1.9.D. ZSCAN4 and stem cell pluripotency

ZSCAN4 is associated with the expression of the pluripotency associated genes NANOG, OCT4 and SOX2 (82, 83). ZSCAN4 was also shown by our lab and others, to enhance gene expression of the pluripotency factors Rex1, Nanog, Oct3/4, and Sox2, suggesting an upstream, regulatory role in the expression of pluripotency genes (96, 97). ZSCAN4 is also associated with stem cell potency. ZSCAN4 has been reported to promote the maintenance of undifferentiated mESCs (98), as well as improving the reprogramming of mouse fibroblasts to generate iPSCs (96). In the later study, ZSCAN4 was found to be transiently activated during the reprogramming process, present in roughly 1% of iPSCs at a given time.

Furthermore, ectopic expression of ZSCAN4 during fibroblast reprogramming leads to improved efficiency of iPSC generation, and ZSCAN4 was capable of replacing the Yamanaka factor c-Myc in the process. Notably the effect of ectopic ZSCAN4 was long lasting, with a short pulse early in reprogramming leading to improved iPSC efficiency weeks later, analogous to ZSCAN4's transient, but lasting effects in development. Whether ZSCAN4 enhanced stem cell potency was assessed in a pair of studies showing that respectively, ZSCAN4-overexpressing mouse iPSCs and mouse ESCs were much more capable of generating viable embryos via tetraploid complementation assay (99, 100). In the later work, highly passaged ESCs were shown to have severely compromised potency, resulting in an inability to form viable embryos beyond 24 passages (an example of the previously mentioned *in vitro* aging/loss of potency). With intermittent pulses of ectopic ZSCAN4 every 3-4 passages, these ESCs were capable of forming viable embryos beyond 48 passages (100). Overall, ZSCAN4 appears to exhibit conserved functionality whether expressed embryonically, in mESCs, or iPSCs. Paralleling the process of ZGA, ZSCAN4 expression leads to telomere extension, increased open chromatin histone marks, decreased DNA methylation, increased pluripotency gene expression, and increased stem cell potency.

1.7 SCOPE OF WORK

Given the association of ZSCAN4 with stem cell potency, in this work we used ZSCAN4 as a tool to enhance the stem cell potency of aged stem cells for regenerative applications, while we knocked it out to reduce stem cell potency and thereby CSCs in cancer. In the first part of the work, we developed a procedure to differentiate a small biopsy-derived

MSCs to the neuronal lineage. We then assessed the effect of ZSCAN4 on MSC potency and neuronal differentiation of young and aged MSCs in order to enhance stem cell potency for a future neuro-restorative therapies. Finally, we defined the interaction of ZSCAN4 with another factor, RNF20, and assessed their roles in cancer stemness. Our results identify RNF20 as a functional partner needed to mediate the effects of ZSCAN4 on potency genes. Establishing ZSCAN4 as a regulator of stem cell potency provides a foundation on which to develop future therapies to modify stemness in both regenerative medicine and oncology.

Chapter 2: Enhancing the differentiation potential of young and aged tonsillar-biopsy derived MSCs to the neuronal linage

2.1 Introduction

Cell-based regenerative therapies are an active and promising area of research, involved involving the transplantation of exogenous cells to promote tissue repair. There are 22 FDA approved cell-based therapies, and 416 active MSC-based clinical trials with 114 assessing their use in CNS disease . Transplanted cells may either promote repair via interaction with resident cells to stimulate endogenous regeneration or differentiate to replace lost endogenous cells (cell replacement therapy).

The epigenetic and gene expression patterns of stem cells change with differentiation, but also with aging. These changes can induce a reduction in stem cell potency with aging both *in vivo* (with physiological aging) and when expanded *in vitro* (*in vitro* aging). Several studies have demonstrated that a few passages in culture are enough to cause a reduction in MSC potency (101-103). While pluripotent stem cells (ESCs and iPSCs) are more resistant to *in vitro* aging, here too, highly passaged cells show impaired differentiation capacity (100, 104). Stem Cell aging thus hinders stem cell-based therapies.

2.1A Neurodegenerative Diseases

Neurodegenerative diseases are a cluster of severe, progressive neurological disorders characterized by the death and dysfunction of cells in the central nervous system. Neurodegenerative diseases are differentiated from one another by symptoms, which in turn are caused by the dysfunction of different neural cell types and different areas of the

brain. Current therapeutics are mostly aimed at slowing disease progression by restoring neurotransmitters levels depleted due to neuronal cell death (105). Due to the progressive nature of neurodegenerative diseases, by the time of diagnosis, significant downstream damage has occurred, and therefore, regaining neurological function through these approaches would be unlikely. A promising potential therapeutic avenue for neurodegenerative diseases is therefore cell replacement therapy to restore the lost cells and function.

2.1B Cell replacement therapy in neurodegenerative disease

The concept of cell replacement therapy in neurodegenerative diseases, was first reported with the use of fetal ventral midbrain (FVM) tissue transplants in Parkinson's Disease (PD) models (106-108). Much of the clinical symptoms of PD, can be attributed to loss of Dopaminergic neurons in the basal ganglia, specifically at the substantia nigra (109). Therefore, cell replacement of dopaminergic neurons is an attractive approach as functional cure PD. The majority of clinical trials to date has focused on the use of embryonic or fetal derived stem cells or iPSCs (110). While the neurogenic potency of ESCs or fetal tissue is high, these are inherently non-autologous, raising issues of immune rejection. Furthermore, both ESCs and iPSCs can be tumorigenic, generating teratomas upon transplant. The relative prevalence and ease of extraction of MSCs, and particularly T-MSCs, makes them a promising stem cell source, but their neurogenic capacity has not been sufficiently characterized.

2.1C Tonsillar-biopsy derived mesenchymal stem cells (T-MSCs)

Tonsil-derived Mesenchymal Stem Cells (T-MSCs) are a promising source of stem cells for neurogenic applications and were reported to generate Schwann cell-like cells and Motor neuron-like cells (111, 112). Previous work in our lab has demonstrated that T-MSCs extracted from a small tonsillar biopsies, can be extracted with higher efficiency than other MSC sources, are highly proliferative, and can readily differentiate to mesenchymal lineages (18). However, like all somatic stem cells, T-MSCs are subject to cellular aging, both physiologic aging *in vivo* and culture aging *in vitro*. This replicative aging process results in progressively shorter telomeres, eventually leading to growth arrest and cellular senescence. Even prior to senescence, aged cells experience changes in their phenotype, illustrated by changes in gene expression, and a loss of differentiation capacity (113). Given the scale-up demands of clinical therapies where tens of millions of highly potent stem cells may be required, cellular aging thus represents a barrier to the use of MSCs in general, including T-MSCs.

2.1.D. Using ZSCAN4 to enhance stem cell potency

Prior work in mouse embryonic stem cells (mESCs) and induced pluripotent stem cells (iPSCs) has posited a role for ZSCAN4 in maintaining or enhancing stem cell potency (96, 99, 100). ESCs and iPSCs will also lose differentiation capacity with extensive *in vitro* culture. In mouse ESCs, however, intermittent expression of ectopic ZSCAN4 has been shown to nearly double the passage number at which cells retain full developmental

potency (100). Based on these findings, we hypothesized that a transient expression of ZSCAN4 in aged T-MSCs may restore stem cell potency (Figure 5).

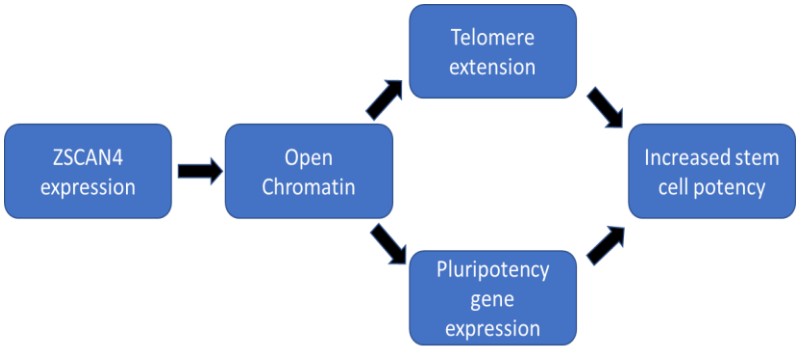

Figure 5: Proposed mechanism of the involvement ZSCAN4 in telomere extension and pluripotency.
In this model, the induction of ZSCAN4 may lead to chromatin remodeling which will then increase pluripotency gene expression and telomere extension. Together, these aspects will increase stem cell potency.

2.2 Results

2.2.A. Neurogenic Differentiation of T-MSCs

Current sources of MSCs generate a relatively low number of stem cells per gram of tissue(114). Extraction from Bone marrow, the most common source of MSCs, typically requires an inpatient procedure and risk to the donor (115, 116). Importantly, the proliferative and differentiation capacities of MSCs vary by tissue source, with some sources having a higher neurogenic capacity than others (117). MSCs generated from full tonsillectomies (T-MSCs) have been shown to generate both motor neurons and Schwann cells (111, 112). We have recently reported that small volume biopsies of palatine tonsils (<1g tissue) can generate tens of millions of T-MSCs (18). These biopsies can be performed as an outpatient procedure and offer little risk to the donor. T-MSCs, thus generated, express an MSC marker profile comparable to Bone Marrow-derived MSCs (BM-MSCs),

while demonstrating superior proliferation and the capacity to differentiate to mesenchymal lineages (18). Here we developed a procedure to induce the differentiation of tonsil biopsy-derived T-MSCs to the neuronal lineage and determined the neurogenic potency of T-MSCs. We further assessed the effects of transient, ZSCAN4 expression to enhance the neuronal differentiation of *in vitro* aged T-MSCs.

In our procedure, adherently cultured T-MSCs are seeded in ultra-low attachment plates and cultured in non-adherent conditions in a neuronal induction/neuronal stem cell media. (Figure 6A) After 72h of such culture, resultant spheres are dissociated and plated adherently in Poly-D-Lysine and Laminin coated plates in a growth factor-reduced, neuronal medium. (Figure 6B) After a further 72h, these cells then receive neuronal medium with the neurotrophic factors BDNF, GDNF and cyclic AMP, which is partially replaced every 3 days through the end of the protocol (Day 28). Cells exhibit significant morphologic changes during the protocol, with a neuroblast-like morphotype by Day 11 (Figure 6C) and a neuron-like morphology by Day 28, replete with neurite-like projections (Figure 6D).

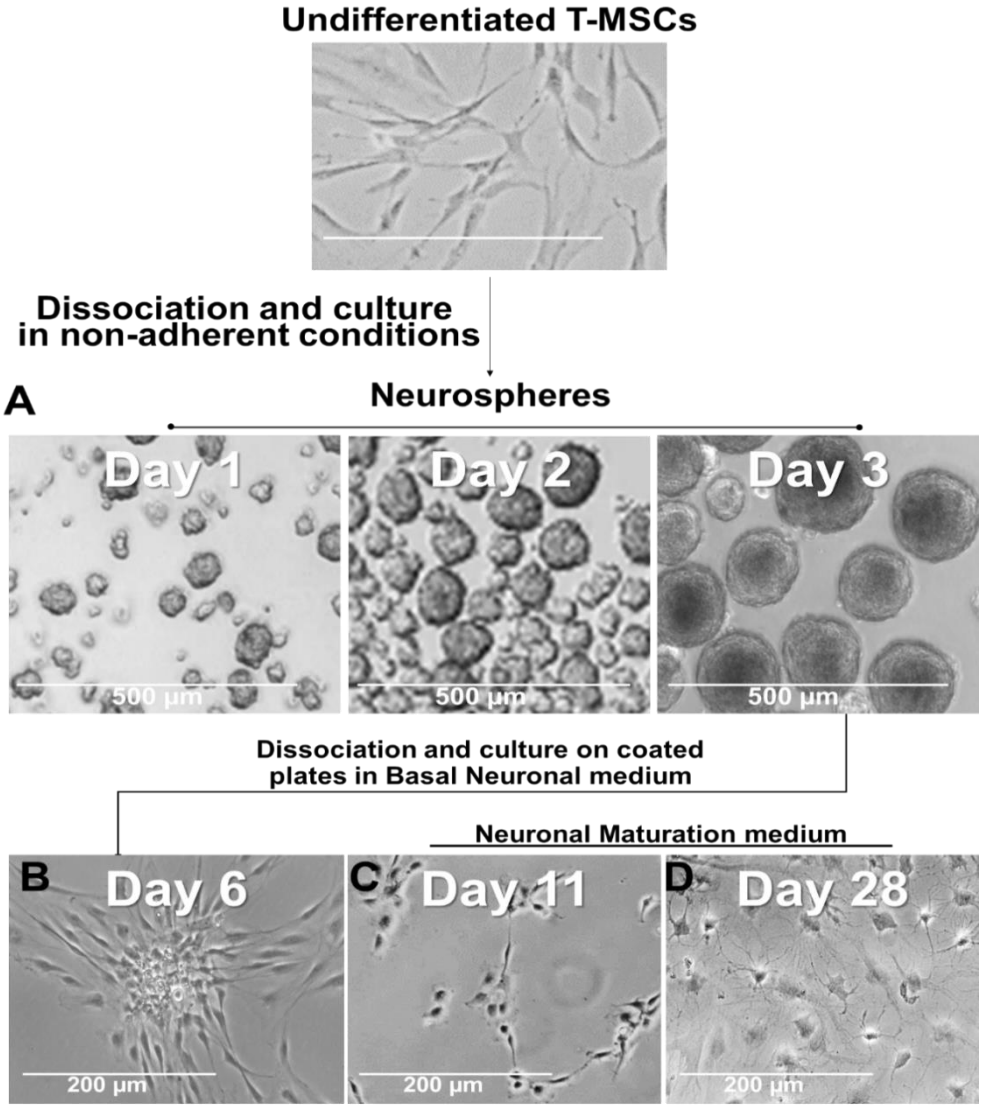

Figure 6: Procedure to generate neuronal-like cells from biopsies of tonsillar MSCs. **A)** Adherently cultured T-MSCs are dissociated and plated in non-adherent conditions in neural induction media for 72h. B) Resultant neurospheres are then dissociated and plated adherently and cultured in basal neuronal media without growth factors for an additional 72h at which point they acquire a neuroblast-like morphology. C) Further differentiation leads to a more pronounced neuron-like phenotype at Day 11 and a neuron-like phenotype at Day 28 D). (Adapted from Arad & Brown et. al. CMBL. 2021. Data generated by Dr. Michal Arad and Robert Brown. (118))

2.2.B. T-MSCs differentiate to neural stem-like cells with high efficiency

MSCs from a variety of tissues sources have been used to generate neuron-like cells, albeit with varying efficiencies (117). We thus compared the neurogenic differentiation of T-MSCs to that of BM-MSCs in our protocol. Seeding an equal number of MSCs in non-

adherent, neural induction conditions for 72h led to formation of neurosphere-like clusters. Notably, T-MSC derived spheres (Figure 7A) were significantly larger and more numerous than BM-MSC derived spheres (Figure 7B). Quantification of the spheres resulted in T-MSC's generating 1.9-fold more total spheres (Figure 7C), and 5.9-fold large spheres (>100um) than BM-MSCs (Figure 7D). These data show that T-MSCs exhibit better survival and proliferation in neurosphere conditions, characteristics suggestive of higher neurogenic potency.

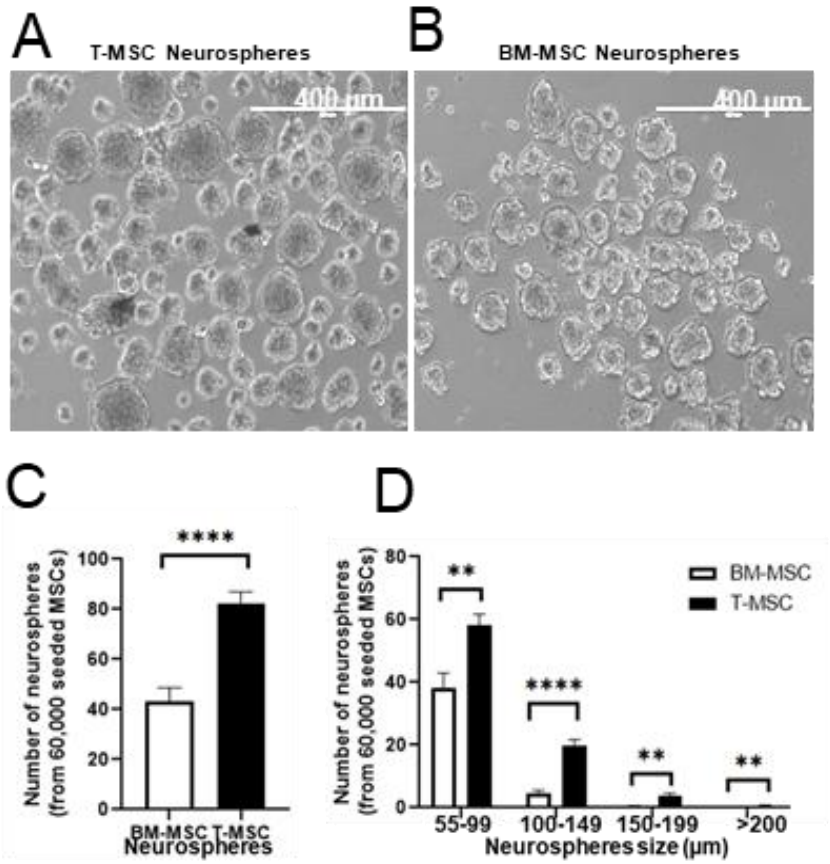

Figure 7: T-MSCs generate neurospheres with high efficiency.
Culture of T-MSCs (A) and BM-MSCs (B) in non-adherent, neural induction conditions for 72h results in formation of 3D neurospheres. Representative images illustrate T-MSCs generate more numerous and larger spheres compared to BM-MSCs. C) Quantification of sphere number confirms this with T-MSCs generation more spheres as well as D) larger spheres. Statistical significance was determined by student t-tests. All data shown as mean ± S.E.M. *p<0.05, **p<0.01, ***p<0.001, ****P<0.0001. (Adapted from Arad & Brown et. al. CMBL. 2021. Data generated by Robert Brown. (118))

Neurospheres are non-adherent, 3D clusters consisting mainly of neural stem/progenitor cells. To determine if our MSC-derived spheres were indeed enriched for neural stem-like cells, we performed RT-qPCR on collected spheres after 72h of culture. Our data show drastic, significant upregulations of the neural stem cell markers Nestin (Figure 8A), Musashi-1 (Figure 8B), and SOX2 (Figure 8C) in all 3 donor T-MSC lines tested. We also observed significant upregulation in Nestin and Musashi-1 in BM-MSC derived spheres, but no detectable SOX2.

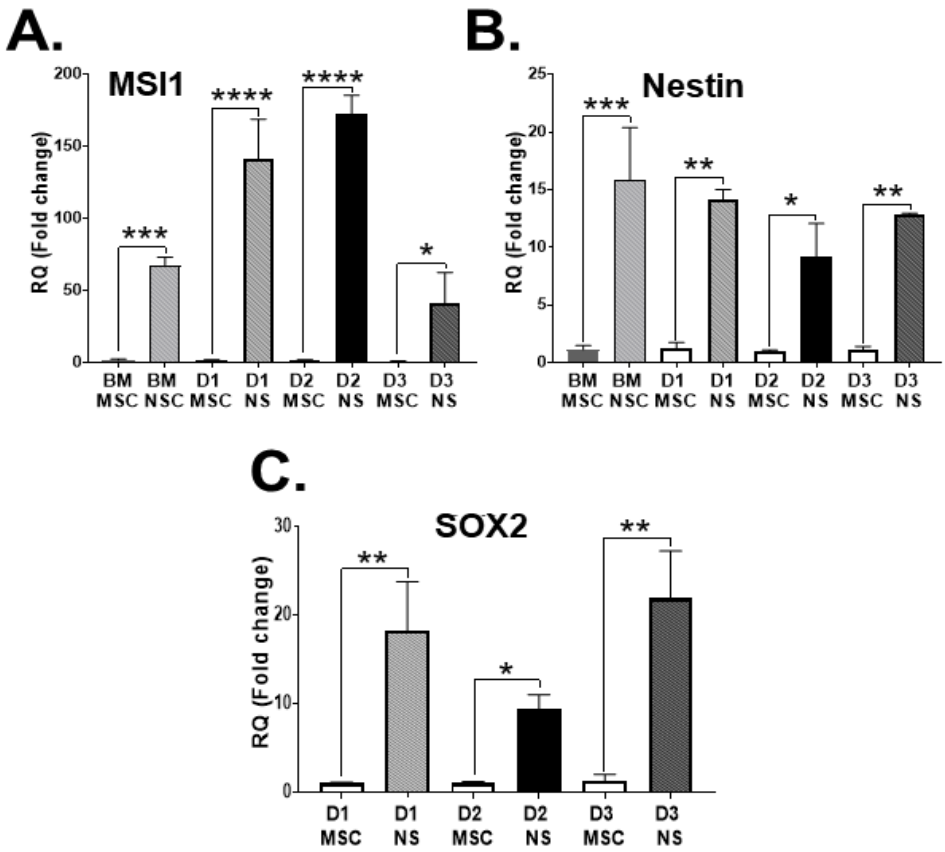

Figure 8: Upregulation of neural stem cell markers in MSC-derived neurospheres
RT-PCR of neurospheres from 5 T-MSC donors and BM-MSCs show that 72h of culture as neurospheres, results in upregulation of neural stem cell markers: A) Nestin B) Musashi-1, and C) SOX2 compared to isogenic undifferentiated MSCs. Statistical significance was determined by student t-tests. All data shown as mean ± S.E.M. *p<0.05, **p<0.01, ***p<0.001, ****P<0.0001. (Adapted from Arad & Brown et. al. CMBL. 2021. Data generated by Robert Brown. (118)

To confirm these findings, we next dissociated spheres and plated them adherently on Poly-D-lysine and Laminin coated plates. 24h later, cells were fixed and immuno-stained for Nestin and Musashi-1, as well as the progenitor marker SOX1. Our results indicate substantial upregulation of all 3 marks in both T-MSC derived and BM-MSC derived cells (Figure 9A-B). Notably, MSI-1 localization was primarily nuclear in neurosphere-derived cells, indicative of active differentiation (124). Both staining intensity and the number of MSI-1 positive and SOX1 positive cells was greater in T-MSC derived cells than BM-MSC derived cells. Of further note, T-MSC derived cells showed a greater percentage of Nestin+/MSI1+ co-positivity compared to BM-MSCs, suggestive of a greater number of Neural stem-like cells in the population. Together, our data suggest that T-MSCs acquire a neural stem/progenitor-like phenotype with as little as 72-96h of differentiation and do so with a higher efficiency than BM-MSCs.

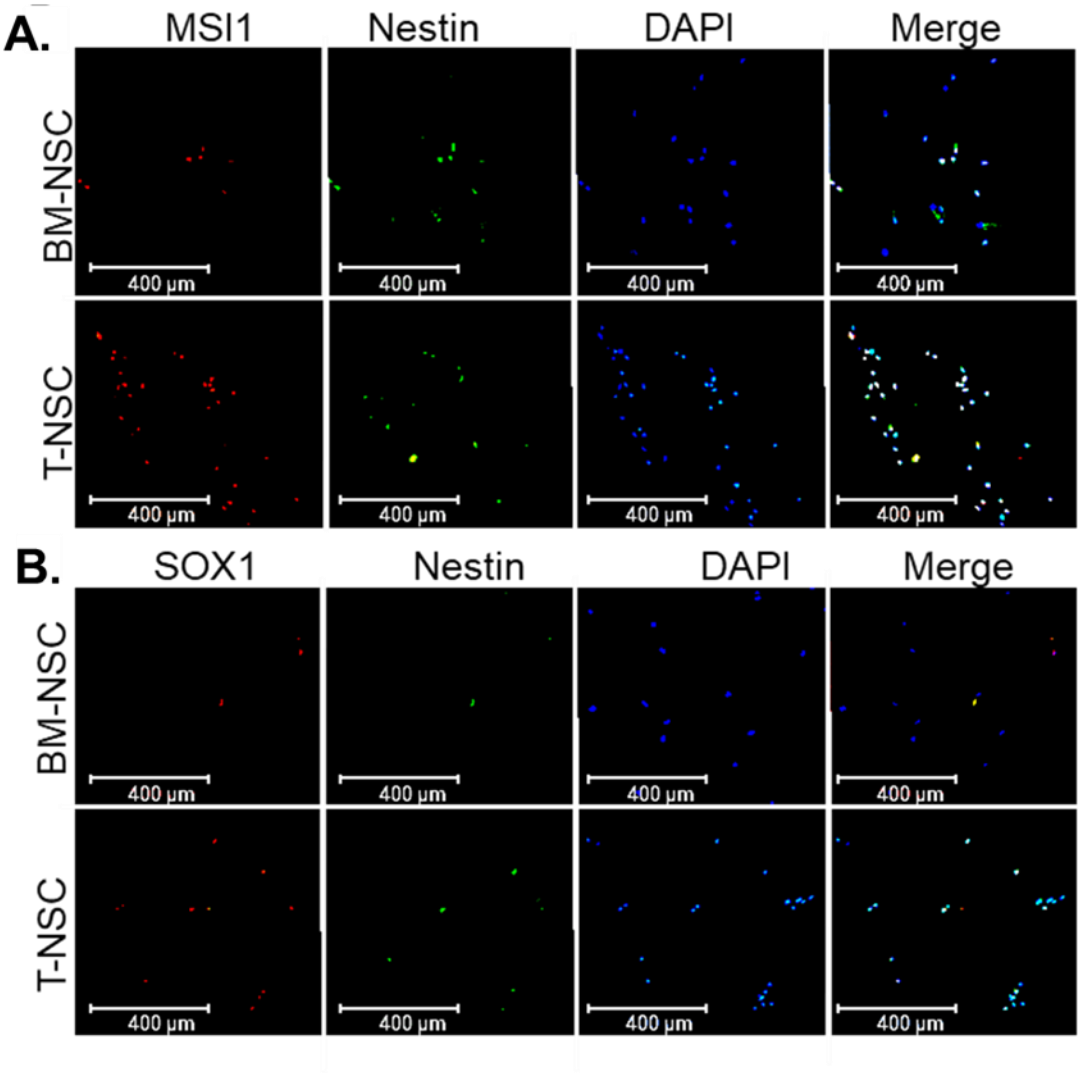

Figure 9: Expression of NSC markers after 96 hours of neurogenic differentiation.
Representative immunofluorescence staining of differentiated T-MSCs and BM-MSCs at Day 4. A) With differentiation, both T-MSC and BM-MSC derived cells show robust expression of Musashi-1 and Nestin, with T-MSC-derived cells showing more positive cells and particularly, more co-positive cells than BM-MSC derived cells. B) T-MSC derived cells, but not BM-MSC derived cells, express the neuronal progenitor marker SOX1, which is co-positive with Nestin in most cells. (Adapted from Arad & Brown et. al. CMBL. 2021. Data generated by Robert Brown. (118))

2.2.C. Neuronal differentiation of T-MSCs leads to upregulation of neuronal markers

As our T-MSCs demonstrated efficient differentiation to a neural stem/progenitor-like population, we next assessed whether they could be further differentiated to a neuron-like population. After 72h of neurosphere culture, dissociated cells were plated adherently on Poly-D-lysine and Laminin coated plates and differentiated further, in the presence of neurotrophic factors from Day 6 onward. At Day 11 and Day 28 cells were collected for RT-qPCR to assess neuronal gene expression. Our results indicate a robust, significant upregulation of the neuronal genes Doublecortin (DCX), Beta-3 Tubulin (Tuj1), Microtubule Associated Protein 2 (MAP2) , Neural Cell Adhesion Molecule 1 (NCAM-1), and Post-Synaptic Density 95 (PSD95) in both T-MSC donor lines assessed at Day 11. (Figure 10A) These genes remained significantly upregulated at Day 28, with the mature neuronal marker Neurofilament Light Chain (NEFL) also upregulated (Figure 10B).

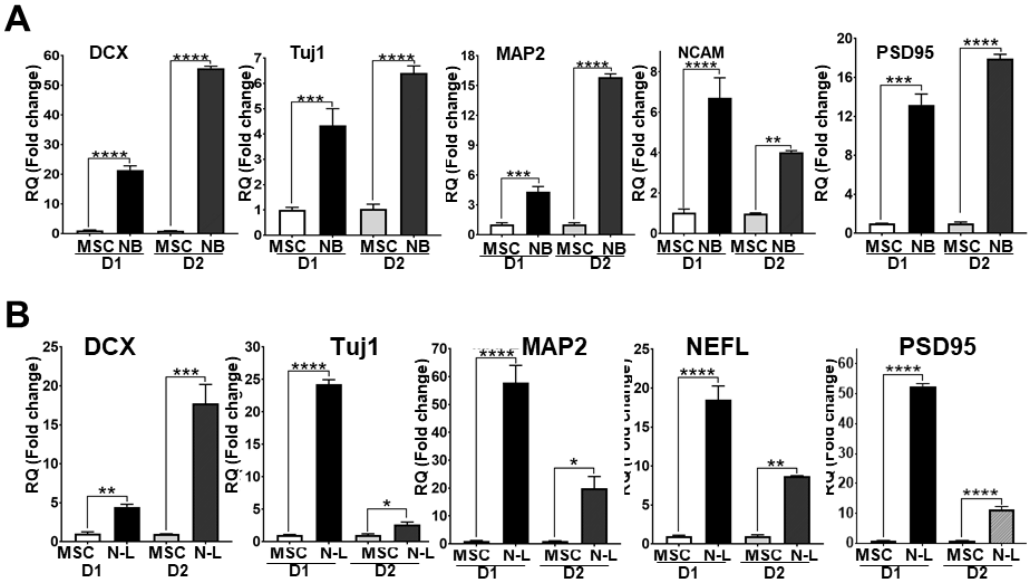

Figure 10: Neuronal genes are upregulated with neuronal differentiation.
RT-qPCR of neuronal genes after **A)** 11 days and **B)** 28 days of neurogenic differentiation in two representative donors. Gene expression was normalized to the housekeeping gene RPLP0 and presented as fold change compared to isogenic undifferentiated T-MSCs. Statistical significance was determined by student t-tests. All data shown as mean ± S.E.M. *p<0.05, **p<0.01, ***p<0.001, ****P<0.0001. (Adapted from Arad & Brown et. al. CMBL. 2021. Data generated by Dr. Michal Arad and Robert Brown. (118)).

To confirm these findings, we then performed immuno-staining of cells at Day 11 (Figure 11A-B) and Day 28 (Figure 11C-D). Consistent with our RT-qPCR results, we found the neuronal markers MAP2, Tuj1, and Pan-Neurofilament (marking neurofilament heavy, medium, and light chains) to be robustly upregulated in Day 11 cells. Notably, these cells were mostly stained co-positive for neuronal markers. Similarly, at Day 28, cells showed robust upregulation of MAP2, Pan-neurofilament, Synaptophysin (SYP) and NEFL. Intriguingly, some areas even showed a morphology similar to that of a neuronal network. (Figure 11C). Taken together, our results show significant upregulation of neuronal markers and phenotype, suggesting differentiation to neuron-like cells.

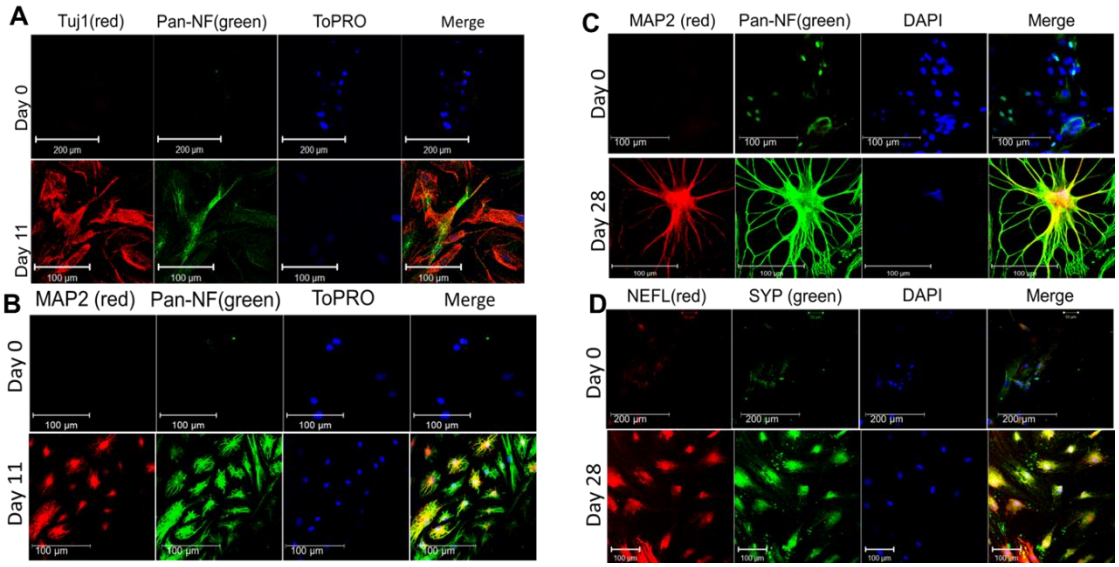

Figure 11: Increase in neuronal markers with neurogenic differentiation
Immunofluorescence staining at Day 11 (A-B) and Day 28 (C-D) showing neuronal markers compared to isogenic undifferentiated T-MSCs. Tuj1 and Pan-neurofilament (A) and MAP2 and Pan-neurofilament (B) were upregulated at Day 11, with MAP2 and Pan-neurofilament (C) and NEFL and synaptophysin also upregulated at Day 28. (Adapted from Arad & Brown et. al. CMBL. 2021. Data generated by Dr. Michal Arad (118))

2.2.D. T-MSCs derived neuron-like cells express neurotransmitters and post-mitotic neuronal markers

Aside from expression of neuronal markers, mature neuron-like cells can be identified by the expression of neurotransmitters and genes associated with their function. Our

differentiation protocol was designed for a general neuronal differentiation and was not intended to enrich for a specific neuronal-sub-lineage. To determine which, if any, neurotransmitters may be expressed by our differentiated cells, we performed RT-qPCR for sub-lineage specific markers in our Day 28 cells. Initially screening in a single donor line, we found that the noradrenergic marker Dopamine Beta-Hydroxylase (DBH), the cholinergic marker Choline Acetyltransferase (ChAT), and the GABAergic markers Vesicular GABA Transporter (VGAT) and Glutamate Decarboxylase (GAD65) were undetectable. (Figure 12A-D) Vesicular Acetylcholine Transporter (VAChT), another cholinergic marker, was detected, but not upregulated at Day 28 compared to undifferentiated T-MSCs (Figure 12E). Based on these data, we concluded that the Adrenergic, Cholinergic, or GABAergic phenotypes can be excluded in neuron-like cells using our protocol. Screening for the Glutamatergic lineage revealed high expression of Glutaminase-1 (GLS1), but no significant change between Day 28 and undifferentiated T-MSCs. (Figure 12F) As GLS1 is a widely expressed metabolic gene, not necessarily specific for neuronal cells, we also assessed expression of Vesicular Glutamate Transporter 1 (VGLUT1), a more neuron-specific Glutamatergic marker, which we did find to be upregulated at Day 28. (Figure 12G) Finally, we assessed a Dopaminergic phenotype with the markers Dopamine Active Transporter (DAT), nuclear receptor related 1 protein (NURR1), and Aromatic L-amino acid decarboxylase (AADC), all of which were found to be upregulated at Day 28. (Figure 12H-J) These Glutamatergic and Dopaminergic markers were further found to be upregulated at Day 28 in two additional T-MSC donor lines. (Figure 12G-J)

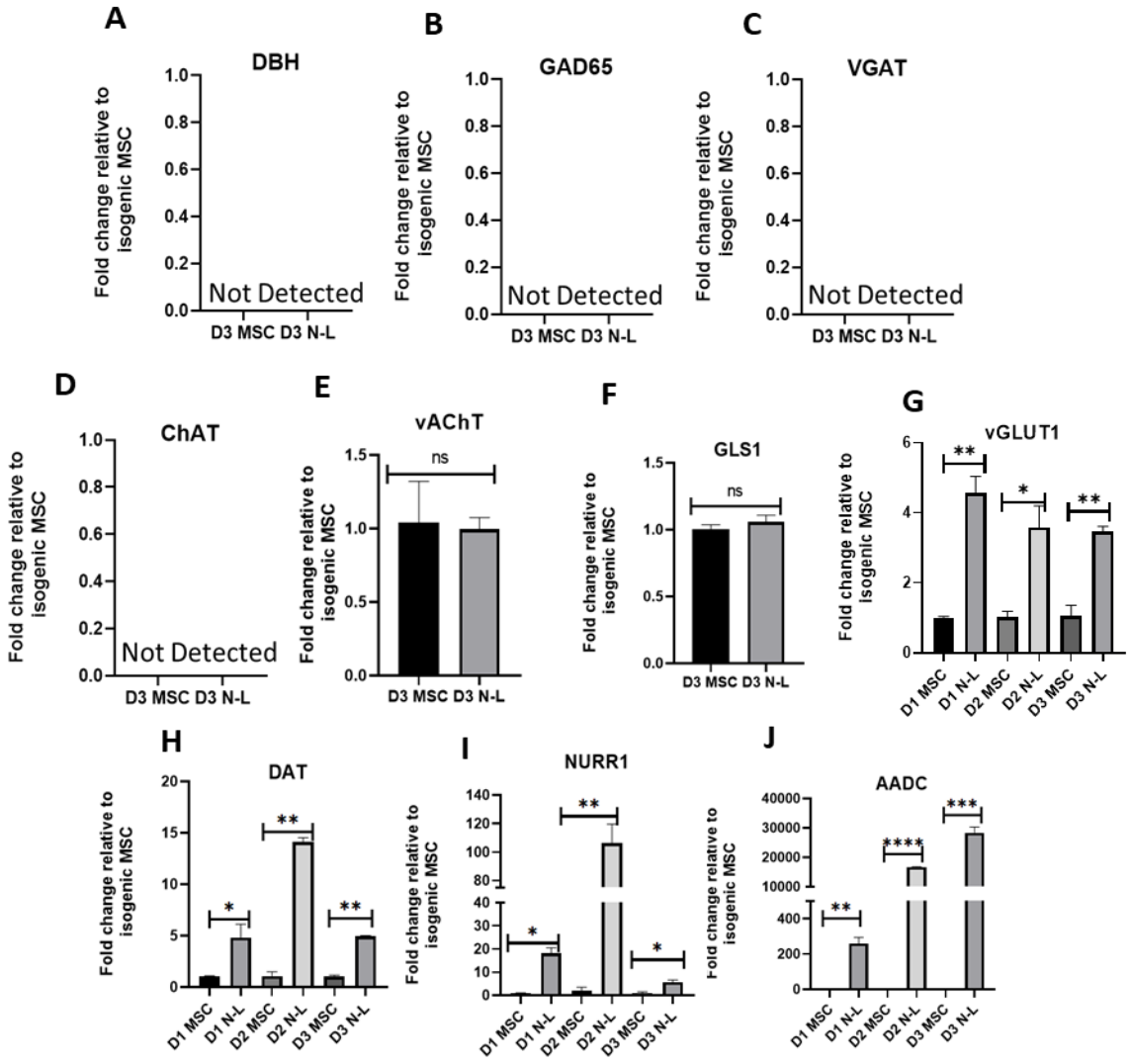

Figure 12: Neuronal-like cells express glutamatergic and dopaminergic markers.
Following 28 days of neuronal differentiation, gene Expression by RT-PCR screening showed no detectable expression of the adrenergic marker DBH (A), the GABAergic markers GAD65 and VGAT (B,C) and the cholinergic marker ChAT (D). Expression of the Cholinergic marker VChT (E) and the Glutamatergic marker GLS1 (F) were unchanged compared to undifferentiated T-MSCs. Expression of the Glutamatergic marker VGLUT1 (G) and the Dopaminergic markers DAT (H), NURR1 (I) and AADC (J) were all upregulated across three T-MSC donor lines. Expression was normalized to expression of the housekeeping gene RPLP0 and presented as fold change compared to undifferentiated T-MSCs. Statistical significance was determined by student t-tests. All data shown as mean ± S.E.M. *p<0.05, **p<0.01, ***p<0.001, ****P<0.0001 **(**Adapted from Arad & Brown et. al. CMBL. 2021. Data generated by Robert Brown (118))

Having identified Dopaminergic and Glutamatergic marker upregulation by RT-qPCR, we next performed immuno-staining for the neurotransmitters L-Dopamine and L-Glutamate. Staining for L-Dopamine revealed that roughly 15% of Day 28 cells express Dopamine

and that those cells also co-express the mature neuronal marker Pan-neurofilament and the mature, post-mitotic neuronal marker NeuN. (Figure 13A-B) Thus, ~15% of our Day 28 cells appear to be post-mitotic, dopaminergic, neuron-like cells. Staining for L-Glutamate revealed a similar, though slightly more abundant population with roughly 20% of cells expressing L-Glutamate. (Figure 13C-D) . Likewise, those cells also co-expressed Pan-neurofilament and NeuN, indicative of ~20% of our cells with a post-mitotic, Glutamatergic neuron-like phenotype.

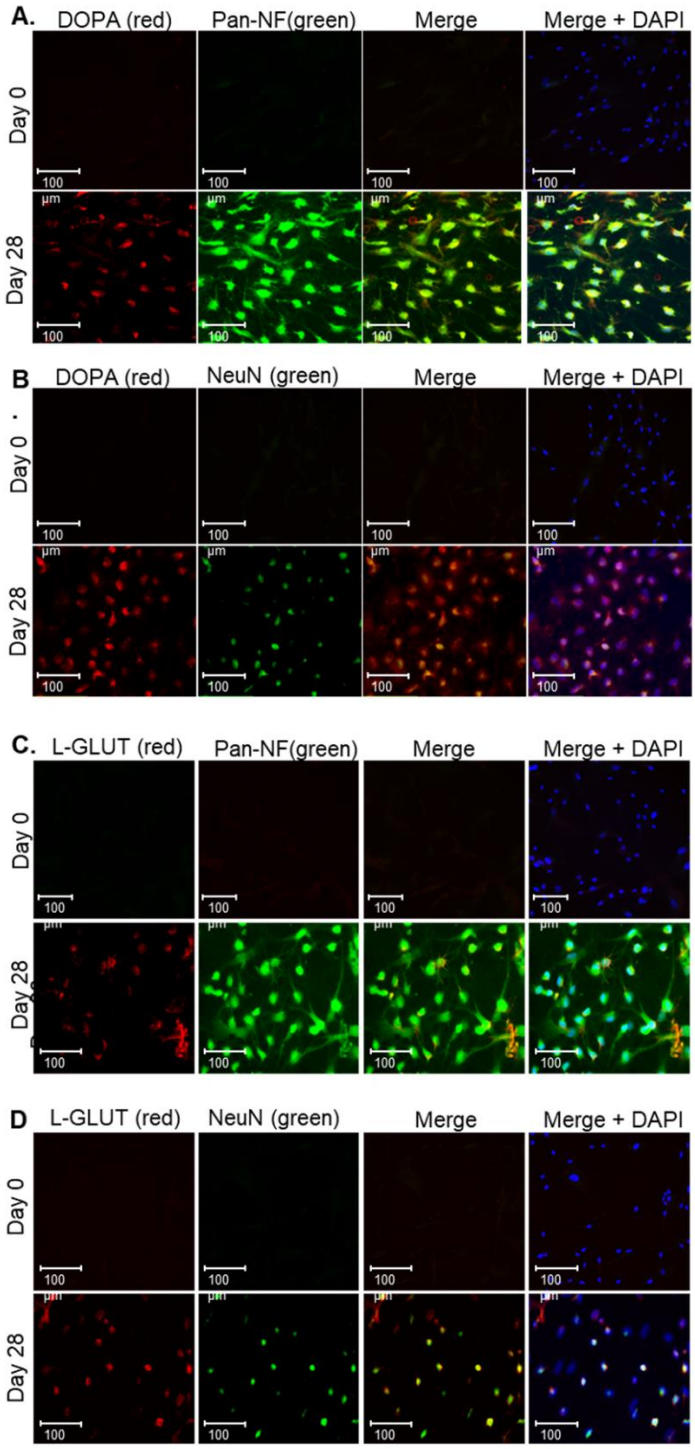

Figure 13: Neurotransmitters and mature markers after 28 days of differentiation.
A) Immunofluorescence staining at Day 0 and Day 28 showing co-expression of L-Dopamine with the mature neuronal marker Pan-neurofilament and B) the post mitotic marker NeuN. C) Immunofluorescence staining at Day 0 and Day 28 showing co-expression of L-Glutamate with Pan-neurofilament and D) NeuN. Images reflect positive staining areas with ~15% of overall cells expressing L-Dopamine and ~20% of cell expressing L-Glutamate. (Adapted from Arad & Brown et. al. CMBL. 2021. Data generated by Robert Brown (118))

2.2.E. Neuronal Differentiation is concomitant with the loss of the MSC phenotype

In assessing neuronal differentiation, it is important to determine that cells are lineage committed. Thus, with increased expression of neuronal lineage markers, there needs to be a concomitant decrease in markers of the T-MSC phenotype. T-MSCs are highly proliferative cells, with a population doubling time of ~33h (18). Despite 25 days in adherent culture during our differentiation protocol, we noticed that cells appeared to have ceased proliferation. Cells counts at Day 28 revealed that our differentiated cells had only undergone 1 to 2 population doublings across 25 days, a far cry from the doubling time of undifferentiated cells. (Figure 14A) To further assess proliferation, we immuno-stained Day 28 cells for the proliferative markers Ki67 and Cyclin A2. (Figure 14B). While undifferentiated T-MSCs showed a high percentage of Ki67 and CyclinA2 positive cells (86.1% and 82.9% respectively), by Day 28 only 18.2% and 14.5% of cells were Ki67-positive and CyclinA2-positive, respectively (Figure 14C-D). These results, coupled with the expression of the post-mitotic neuronal marker NeuN (Figure 14B, D), indicate a loss of the proliferative phenotype characteristic of T-MSCs.

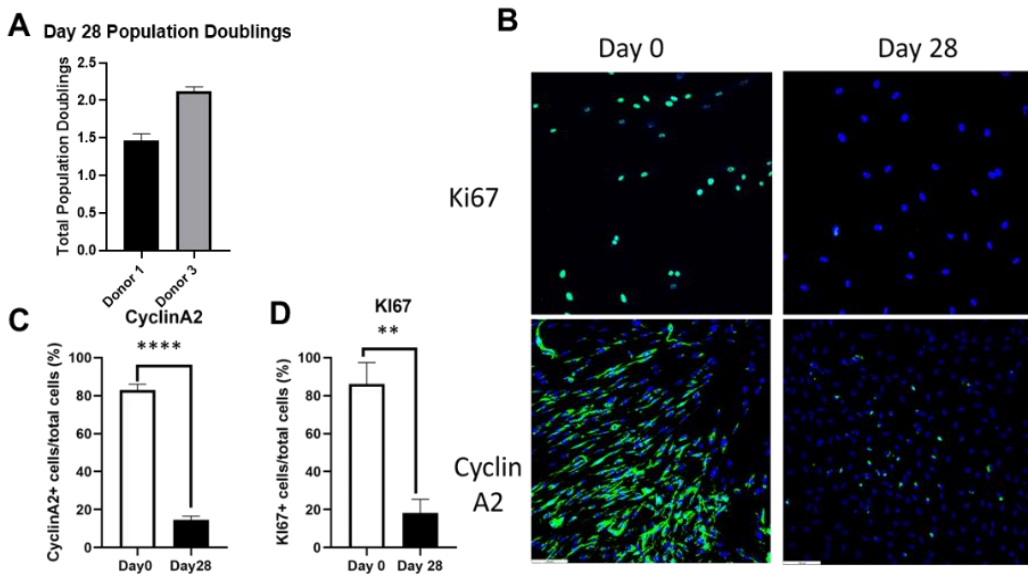

Figure 14: Neurogenic differentiation for 28 days results in reduced proliferation.
A) Population doublings in neurogenic conditions. Cells were counted after 25 days and compared to the numbers originally plated in two representative T-MSC donor lines. B) Representative images of immunofluorescence staining for the proliferative markers Ki67 and Cyclin A2 in undifferentiated T-MSCs and Day 28 neuro-differentiated cells. C) Quantification of KI67 and Cyclin A2 staining showing the percentage of positive cells at both points (n=6 per condition). Statistical significance was determined by student t-tests. Data shown as mean ± S.E.M. *p<0.05, **p<0.01, ***p<0.001, ****P<0.0001. (Adapted from Arad & Brown et. al. CMBL. 2021. Data generated by Robert Brown (118))

T-MSCs, and MSCs in general, are also characterized by cell surface markers. Among others, T-MSCs express high levels of CD73, CD90, and CD105, with undifferentiated cells having >97% of cells co-expressing these marks (18). Initial RT-qPCR based screening found that as little as 72h of differentiation (to the neurosphere/neural stem cell stage) resulted in significant reductions in CD90 (Figure 15A), while CD73 and CD105 were unchanged. As the MSC phenotype depends on co-expression of all markers, this reduction likely signifies a phenotypic loss. Undifferentiated T-MSCs also maintain a fibroblast-like morphology and express several fibroblast markers. In addition to CD90, we also found a downregulation of the fibroblast marker ACTA2, further suggestive of a loss of the MSC phenotype (Figure 15B). Further differentiation to Day 11 resulted in a downregulation of all 3 MSC cell surface marks as assessed by flow cytometry, with CD73,

CD90 and CD105 significantly decreased compared to undifferentiated cells (Figure 15C-E). Flow cytometry of co-stained cells revealed that less than 5% of Day 11 cells were co-positive for CD90/CD105, CD73/CD105, or CD73/CD90, further demonstrating a loss of the MSC phenotype (Figure 15F-H). Together, the robust reduction in proliferation and the compromised expression of MSC markers suggests loss of the MSC phenotype and commitment to the neuronal lineage.

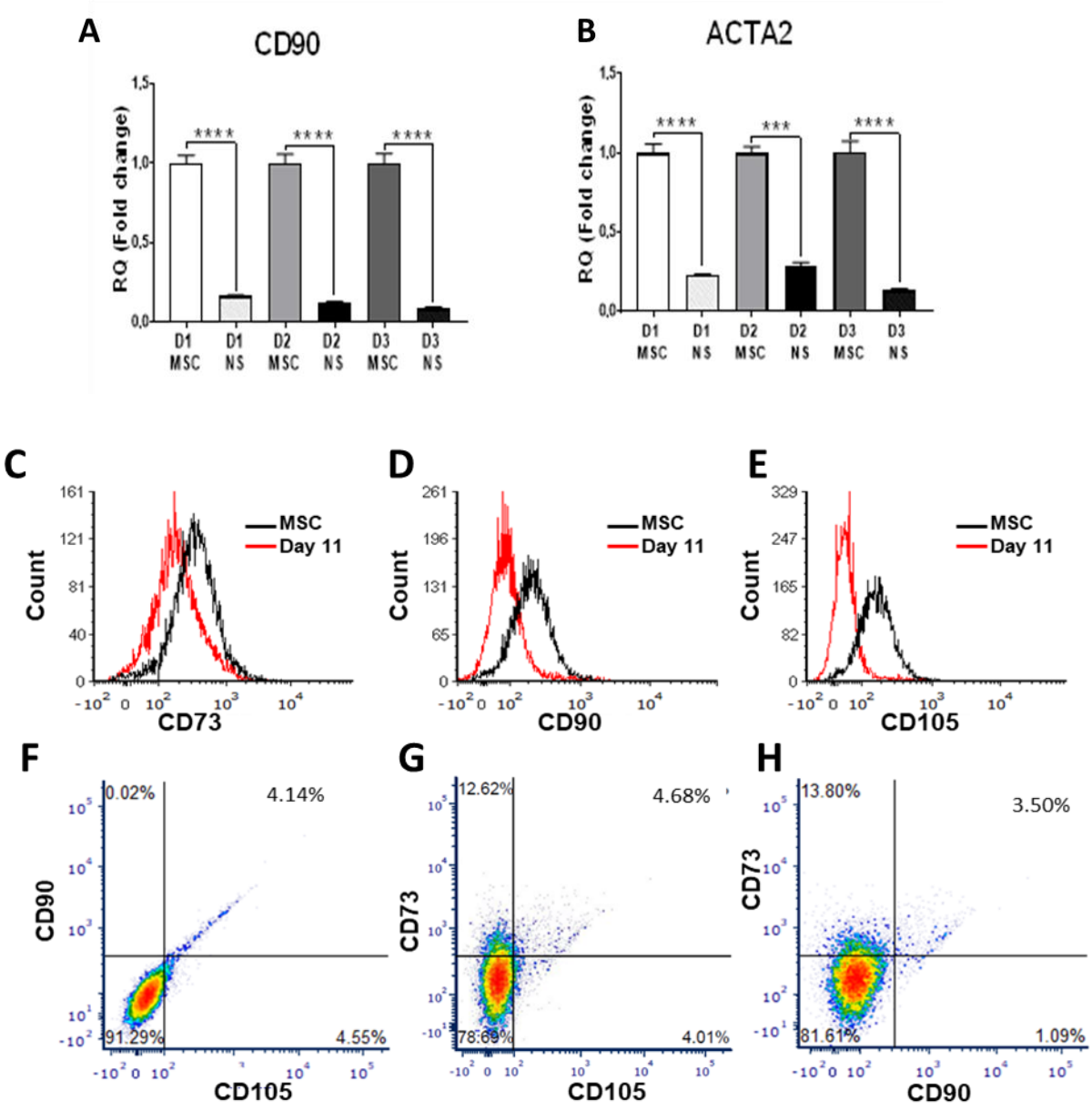

Figure 15: Loss of MSC-markers with neurogenic differentiation.
RT-qPCR in T-MSCs and neurospheres showing expression of A) the MSC marker CD90 and B) the fibroblast marker ACTA2 in three representative donors. Gene expression is normalized to the housekeeping gene RPLP0 and presented as fold change relative to undifferentiated T-MSCs. Statistical significance was determined by student t-tests. (C-E) Representative donor line flow cytometry analysis showing expression levels of the MSC markers CD73, CD90 and CD105 after 11 days of neurogenic differentiation compared to undifferentiated T-MSCs. (F-H) Representative donor line flow cytometry analysis showing co-expression of MSC markers after 11 days of neurogenic differentiation. All data shown as mean ± S.E.M. *p<0.05, **p<0.01, ***p<0.001, ****P<0.0001 (Adapted from Arad & Brown et. al. CMBL. 2021. Data generated by Robert Brown and Dr. Michal Arad (118))

2.2.F Applying ZSCAN4 to restore stem cell gene expression *in-vitro* aged T-MSCs

Unpublished data from our lab (generated by Dr. Michal Arad) demonstrated a marked reduction in neurogenic differentiation capacity from *in vitro* aged T-MSCs, reflecting a loss of stem cell potency. Stem Cell potency is associated with a phenotype of open, transcriptionally accessible chromatin and the expression of potency associated genes. Several reports across differently sourced MSCs indicate that expression of the pluripotency genes NANOG, OCT3/4, and/or SOX2 is associated with enhanced differentiation potency, in mesenchymal lineages (119-121). As T-MSCs do not express endogenous ZSCAN4, we hypothesized that ectopic expression of ZSCAN4 may lead to chromatin remodeling, which in turn, would enhance the neurogenic differentiation potency lost due to *in vitro* aging.

2.2.G. ZSCAN4 enhances pluripotency gene expression in *in-vitro* aged T-MSCs

Using aged T-MSC lines transduced with a tetracycline-inducible ZSCAN4 expression vector (Figure 16A), we cultured cells for 72h in the presence or absence of Doxycycline to induce ectopic ZSCAN4 expression. Remarkably, yet consistent with reports in mESCs and iPSCs, ZSCAN4 induction led to increased pluripotency gene expression across all 4 donor lines tested. (Figure 16B-E).

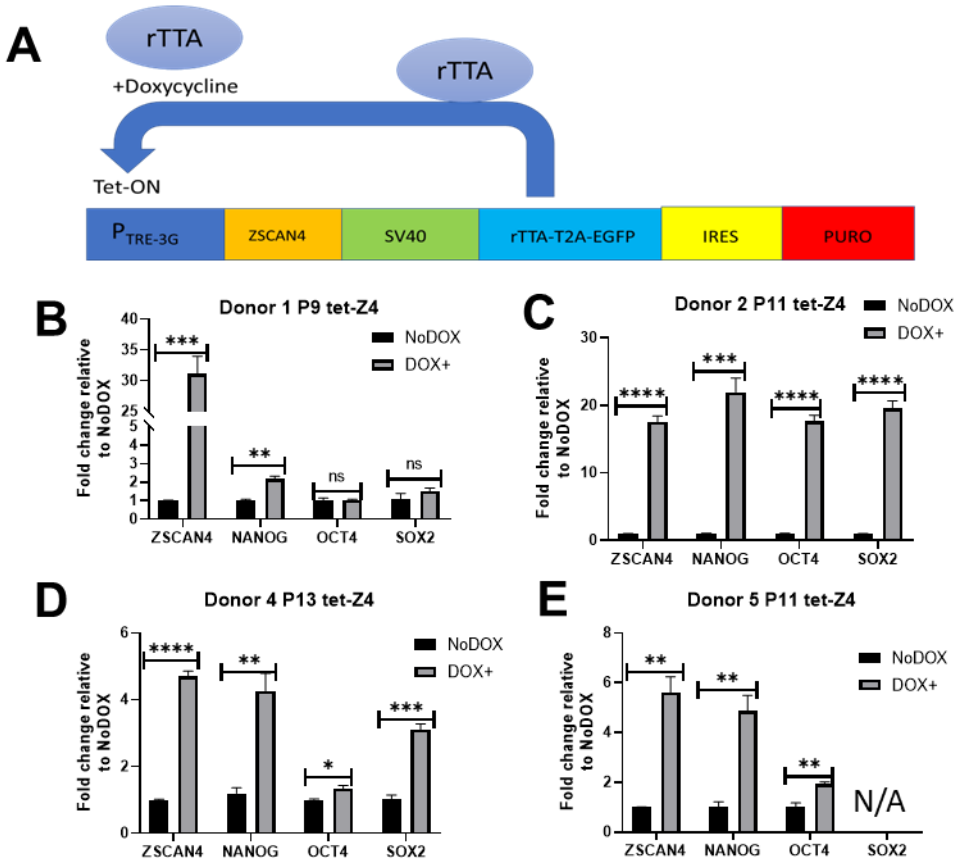

Figure 16: ZSCAN4 induction in T-MSCs increases pluripotency gene expression.
A) Illustration of Dox-inducible ZSCAN4 vector, wherein Doxycycline leads to expression of ZSCAN4. (B-E) RT-qPCR in three *in vitro* aged tet-ZSCAN4 T-MSC donor lines. Gene expression fold change was normalized to RPLP0 relative to uninduced cells (NoDOX). Significance was determined by multiple separate student t-tests. All data shown as mean ± S.E.M. *p<0.05, **p<0.01, ***p<0.001, ****P<0.0001 (Unpublished data generated by Robert Brown)

To determine if the effect of ZSCAN4 on pluripotency genes is mediated through chromatin remodeling, we then performed Chromatin Immunoprecipitation (ChIP) in Doxycycline treated or untreated T-MSCs using antibodies for the open chromatin marks H3K14ac and H4K8Ac. Consistent with the increased pluripotency gene expression in response to ZSCAN4, our results reveal that ZSCAN4 induction resulted in increased open chromatin marks at both pluripotency gene open reading frames (Figure 17A-C), and

pluripotency gene promoters (Figure 17D-F). This data suggest that ZSCAN4 induces open chromatin at pluripotency genes, leading to increased gene expression.

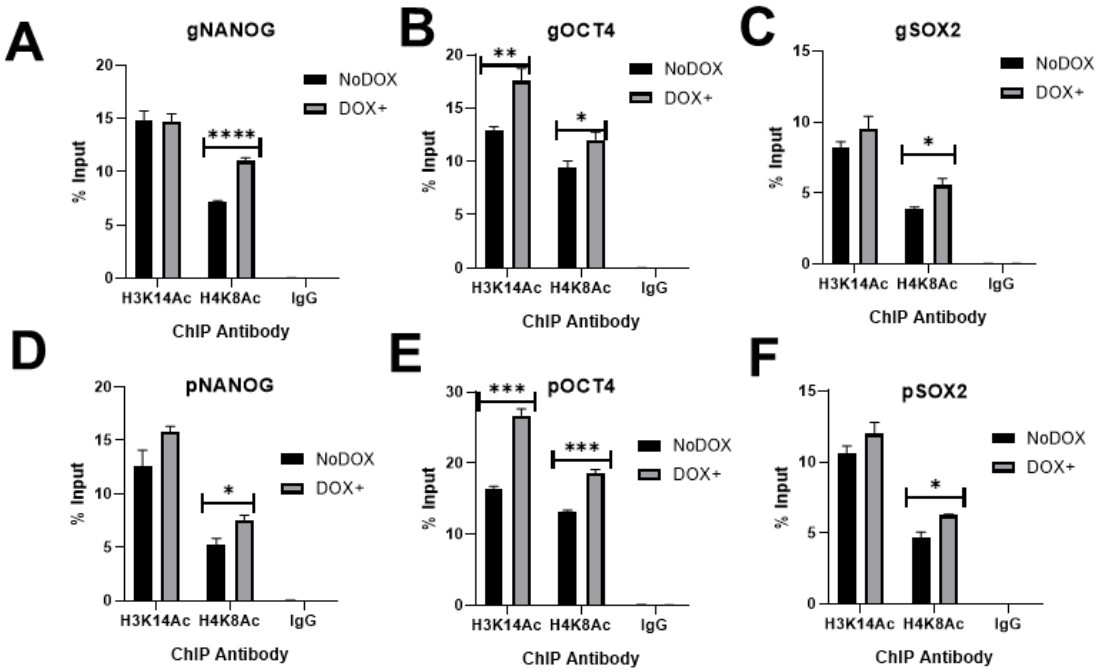

Figure 17: ZSCAN4 induction for 2 days in T-MSCs increases histone acetylation at pluripotency genes.

ChIP-PCR show relative histone acetylation at pluripotency gene open reading frames (A-C) and pluripotency gene promoters (D-F) in ZSCAN4-induced and uninduced T-MSCs. Results are shown as a percentage of ChIP input chromatin. Statistical significance was determined by student t-tests. All data shown as mean ± S.E.M. *p<0.05, **p<0.01, ***p<0.001, ****P<0.0001 (Unpublished data generated by Robert Brown)

2.2.H. ZSCAN4 facilitates histone acetylation and telomere extension of aged T-MSCs

ZSCAN4 has been reported to positively regulate telomere length and stability in pluripotent stem cells (83, 122) As telomere attrition is a driving force underlying stem cell aging(48), we expected that ZSCAN4 induction would lead to telomere extension in aged T-MSCs. Indeed, after induction of ZSCAN4, we found significant telomere extension of 27.7% in aged T-MSCs (Figure 18A). Previous studies have found that ZSCAN4-mediated extension of telomeres is telomerase-independent (87). As our T-MSCs are telomerase-

negative, for telomere extension to occur, the telomeric DNA must be accessible for ALT machinery(58). We therefore looked at the relative accessibility of telomeric chromatin after ZSCAN4 induction. Via ChIP, we found that there was a substantial increase in the open chromatin mark H3K14Ac (Figure 18B), suggesting, that, similar to its role at pluripotency genes, ZSCAN4 is inducing open chromatin at the telomeres, which may enable telomere extension.

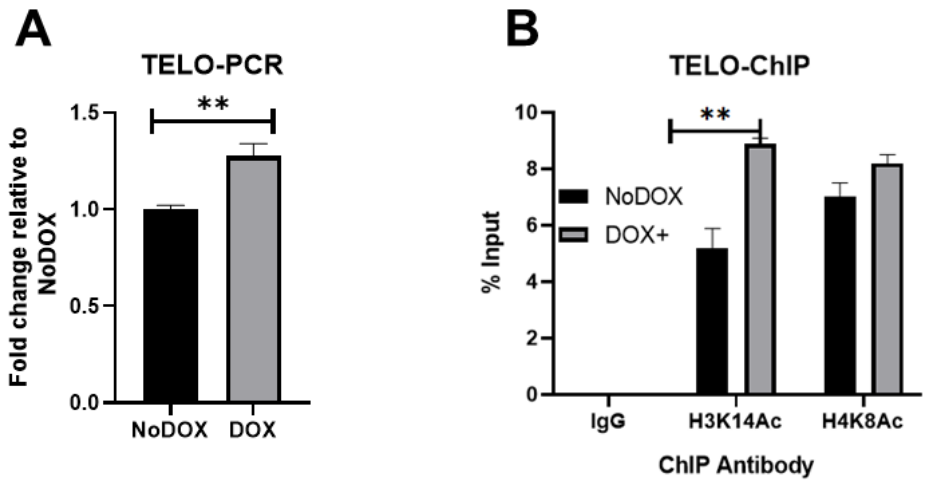

Figure 18: ZSCAN4 facilitates telomere lengthening and histone acetylation in T-MSCs.
A) Telomere qPCR showing relative telomere length in ZSCAN4-induced and uninduced T-MSCs. Telomere signal is normalized to the single copy gene RPLP0 and shown as fold change relative to uninduced cells B) ChIP-qPCR showing histone acetylation levels at the telomere in ZSCAN4-induced and uninduced T-MSCs. Results are presented as a percentage of ChIP input chromatin. Statistical significance was determined by student t-tests. All data shown as mean ± S.E.M. *p<0.05, **p<0.01, ***p<0.001, ****P<0.0001 (Unpublished data generated by Robert Brown)

2.3.I. ZSCAN4 enhances the differentiation of aged T-MSCs to neural stem-like cells.

Our findings that ZSCAN4 induces open chromatin, pluripotency gene expression, and telomere extension, are all suggestive of enhanced stem cell potency. We thus assessed whether ZSCAN4 induction, prior to neurogenic differentiation, would actually enhance the differentiation capacity of aged T-MSCs. After 72h of ZSCAN4 induction with Doxycycline, T-MSCs were plated in non-adherent neurosphere conditions for 72h. A

visible difference was shown, with fewer and larger spheres in the untreated compared to spheres of ZSCAN4-induced cells. (Figure 19A). Quantification of spheres revealed that there were indeed significantly more spheres in the ZSCAN4-induced condition (Figure 19B), suggestive of increased neurogenic potency. We further assessed the phenotype of our neurosphere-derived cells by RT-qPCR for the neural stem cell markers Vimentin, Nestin, and Mushashi-1, all of which showed increased expression in ZSCAN4-induced cells (Figure 19C)). Taken together, these data suggest that ZSCAN4 induction enhances the ability of aged T-MSCs to generate neural stem-like cells.

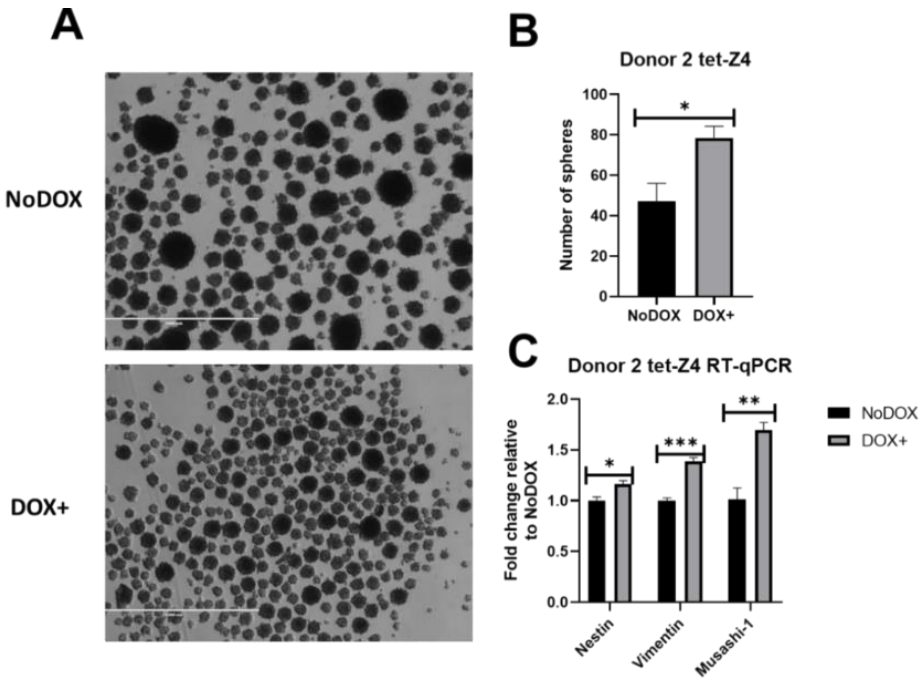

Figure 19: The effect of ZSCAN4 on neurosphere formation from aged MSCs.
A) Representative images of neurospheres (72h) generated from tet-ZSCAN4 MSCs with (Dox+) or without (Dox-) induction. **B).** Quantification of neurospheres via ImageJ in at least 6 wells per condition. Neurosphere defined as >75um. Significance was determined by student T-test. **C)** RT-PCR of neurospheres from tet-ZSCAN4 T-MSCs either with or without ZSCAN4 induction. Results presented as fold change relative to the uninduced cells and normalized to RPLP0. All data shown as mean ± S.E.M. *p<0.05, **p<0.01, ***p<0.001, ****P<0.0001. (Unpublished data generated by Robert Brown)

2.3J. ZSCAN4 enhances histone acetylation at Neural Stem Cell and Neuronal - associated genes

Our previous data suggest that ZSCAN4's enhancement of pluripotency gene expression and telomere length may be epigenetically mediated (histone acetylation). We therefore assessed whether the chromatin of neural stem cell or neuronal genes was similarly being altered by ZSCAN4 induction, potentially explaining the enhanced differentiation observed. Upon ZSCAN4 induction in T-MSCs, we found significant increases in histone acetylation at the gene bodies of the neural stem cell-associated gene NESTIN and the neuronal genes MAP2, TUBB3 (Beta-3-Tubulin), and PSD95 (Figure 20 A-D). These results demonstrate that, prior to neurogenic differentiation, the chromatin of neural stem cell and neuronal genes in ZSCAN4-induced cells is more acetylated and therefore more amenable to gene expression, potentially explaining the ZSCAN4-mediated enhancement of neurogenic potency.

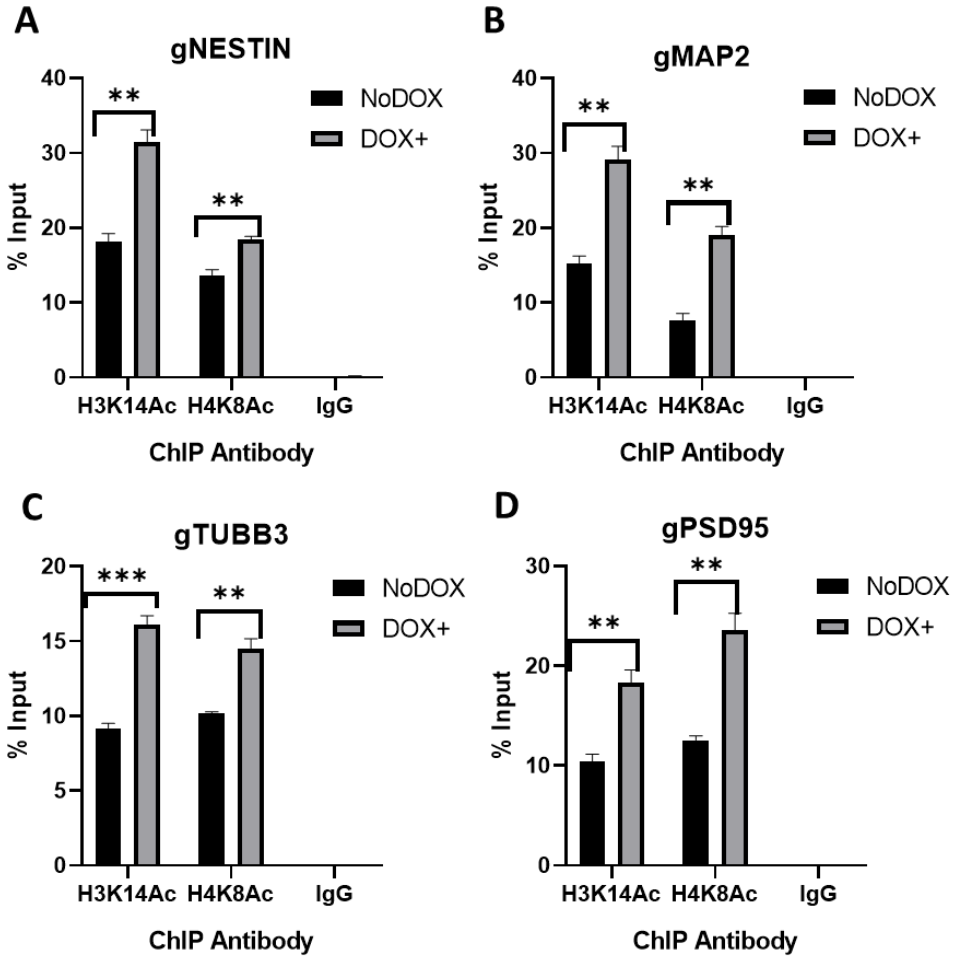

Figure 20: The effect of ZSCAN4 induction on histone acetylation at neurogenic genes in aged T-MSCs.

ChIP-PCR results after ZSCAN4 induction for 72h in aged T-MSCs show increases in histone acetylation at the gene bodies of A) Nestin, B) MAP2, C) TUBB3, and D) PSD95. Results presented as percentage of ChIP input chromatin. All data shown as mean ± S.E.M. *p<0.05, **p<0.01, ***p<0.001, ****P<0.0001. (Unpublished data generated by Robert Brown)

2.4. Discussion

Whether by cell replacement or stimulation of endogenous regeneration, MSC-based cell therapies have shown potential in neurodegenerative disease. Partially differentiate cells (neural stem cell-like) have shown improved outcomes compared to undifferentiated cells,

thus the ability of MSCs to differentiate to the neuronal lineage is integral to their effectiveness. The generation of neuron-like cells have been reported from BM-MSCs, adipose-derived MSC, and umbilical cord-derived MSCs. Recently, neuron-like cells from full-tonsillectomy derived MSCs have been described albeit only characterized for the motor neuron lineage (112). Here, we report for the first time the differentiation of small tonsil-biopsy derived MSCs (T-MSCs) to post-mitotic, neuron-like cells validating their neuropotency for potential therapeutic usage.

Basal neuropotency in MSCs varies depending on source of the cells (117). BM-MSCs are among the best characterized of MSC sources, however, they have been reported to have low neurogenic potency compared to other types of MSCs (123). As BM-MSCs remain the most common MSC source used in clinical trials, we compared the neurogenic capacity of our T-MSCs to that of commercially available BM-MSCs. Our results indicate that T-MSCs do show significantly increased neurogenic potency compared to BM-MSCs, at least through the neurosphere/neural stem cell stage of differentiation. It is worth noting that MSCs are derived from one of two developmental sources, either from mesoderm, or from neural crest cells (neuroectoderm)(9). BM-MSCs are derived from mesoderm, while T-MSCs, like all head and neck structural tissues, have a neural crest origin. T-MSC origin from neuroectoderm instead of mesoderm could potentially explain its superior neurogenic capacity compared to BM-MSCs.

Aside from improved neurogenesis, T-MSCs offer advantages over other MSC sources for cell therapy. T-MSCs generated from our extraction protocol result in 5 orders of magnitude more cells from 1 gram of tissue than reported extraction of MSCs from bone marrow aspirate(18). Coupled with their increased proliferative capacity, T-MScs appear

the best able of known MSC sources to meet the scale-up needs of clinical treatments and stem cell banking.

Previous studies on the neurogenic potential of MSCs have relied on expression of neuronal markers post-differentiation. In our study, we characterized differentiated cells at the neural stem cell stage, immature neuronal stage, and at the post-mitotic, mature neuronal stage. As mature neurons are not a viable source for stem cell transplantation, our characterization of T-MSCs at the neural stem cell-like stage suggests our cells can be partially differentiated prior to transplantation. Our study also evaluated expression of neurotransmitters, suggesting their differentiation potential to multiple neuronal sub-lineages. This is important for neurodegenerative cell replacement therapies in which a specific neuronal sub-type is often desired. Notably, our differentiation protocol was not optimized for a specific neuronal sub-lineage and thus, future work will be necessary to fully assess their dopaminergic, glutamatergic or other sub-lineage potential.

T-MSCs, like all MSCs, are still hindered by replicative aging and the associated loss of stem cell potency. Due to this constraint, clinical applications of MSCs are limited to low passage cells, making the cell numbers needed for therapeutic efficacy hard to achieve. Notably, highly passaged cells will often still proliferate well and express MSC markers, but no longer efficiently differentiate. Thus, methods to enhance MSC potency or to maintain it across many passages are needed.

Here we applied ZSCAN4 for the first time in human T-MSCs with the expectation it would similarly enhance stem cell potency. Our results show that the aspects of the stem cell phenotype enhanced by ZSCAN4 in PSCs, namely open chromatin, pluripotency gene expression, and telomere length, are similarly increased in T-MSCs. This conservation of

ZSCAN4's effects between species and between various stem cell types demonstrates its utility as a likely universal enhancer of stem cell potency. While our work revealed an enhancement in T-MSC differentiation to neural stem cells, ZSCAN4's effects on the phenotype of undifferentiated T-MSCs suggest a more general enhancement of stem cell potency. This is evidenced by concurrent work in our lab showing ZSCAN4 induction in T-MSCs also increases their osteogenic potency.

In total, this work demonstrates a novel stem cell source for cell therapies in neurodegenerative disease. It further reveals a novel method to enhance stem cell potency, bypassing the barrier imposed by cellular aging on MSC-based therapies.

2.5. Materials and Methods

Isolation and expansion of MSCs from human tonsillar biopsies

Tonsillar biopsy-derived MSC harvesting procedures were generated as previously described in detail(18). Briefly, the protocol was approved with informed consent by the University of Maryland, Baltimore institutional review board (IRB protocol #HP-00062781-1) and cell lines were characterized as we previously described(18). T-MSC lines were cultured in complete T-MSC medium: DMEM (Invitrogen) 10% FBS (Takara); 1 mM sodium pyruvate (Invitrogen), 0.1 mM non-essential amino acids (NEAA; Invitrogen), 2 mM GlutaMAX (Invitrogen), 0.1 mM beta-mercaptoethanol (Life Technologies/Gibco), and penicillin /streptomycin (50 U/50 μg/ml; Invitrogen). For all cell lines, medium was changed every 3 days and cells were routinely split every 4-7 days when 70% confluence was reached, using Accutase (EMD Millipore). Unless stated otherwise, cells from each expansion were cryopreserved and to maintain reproducibility of

differentiation, all cells were used up to eleven passages. Five donors were used in this research: 2 pediatric donors (3-7 years old): 1 female, 1 male, and 3 adult donors (20-35): 2 females, 1 male. Bone marrow derived MSCs (BM-MSCs) were purchased from Sigma and cultured alongside T-MSCs as above.

Generation of tetracycline-inducible ZSCAN4 T-MSC lines

Established T-MSC lines were transduced with a tetracycline inducible ZSCAN4 expression vector as previously described(124). Transduced lines were selected for 10 days with 1ug/mL Puromycin and expanded. Tet-inducible cells were cultured as above, albeit in media containing tetracycline-free FBS (Novus).

Neurosphere formation

Cells were harvested by using Accutase (EMD Millipore). To generate neurospheres, harvested T-MSCs or BM-MSCs were cultured at a density of $6x10^5$ cells per well in ultra-low attachment 6-well plates (Corning) in neurosphere medium containing DMEM/F12 (Invitrogen) and neurobasal medium (Invitrogen), (1:1 ratio), supplemented with 2 mM GlutaMAX, penicillin/streptomycin (50 U/50 μg/ml; Invitrogen), 0.5X B27 Supplement (Invitrogen), 0.5X N2 Supplement (Invitrogen), 20 ng/ml basic FGF (Biolegend) and 20 ng/ml Recombinant human EGF (Biolegend). These conditions were maintained for 72h, after which spheres were imaged on a light microscope and the size and number of spheres analyzed using ImageJ software.

Differentiation to a neural stem cell phenotype

Following 3 days of culture, neurospheres were collected, gently dissociated by Accutase and plated in 6-well cell culture plates (Corning) or on glass chamber slides (Fisher Scientific) pre-coated with a layer of Poly-D-lysine (30 min, room temperature; Sigma) and a second layer of Laminin (2 hours, 37° C; Sigma). The cells were then grown for 3 days in basal neuronal medium containing neurobasal medium, 1X B27 supplement, 2 mM GlutaMAX. Culture with penicillin and streptomycin at this stage appeared to cause significantly decreased viability. Therefore, cells were maintained instead in 100 µg/ml Ampicillin (American Bioanalytical).

Neuroblast differentiation and promotion of neuronal maturation

On day 6 of the procedure, following 48 hours of adherent culture, cells were supplemented with an enriched neuronal growth medium which included: the basal neuronal medium supplemented with 20 ng/ mL BDNF (Gibco), 20 ng/ mL GDNF (Gibco) and 500 µM Dibutyryl cAMP (Sigma) and 100ug/mL ampicillin (American Bioanalytical). Notably, a full media change after 3 days in these conditions often resulted in stress, cell death and loss of the culture, a phenomenon similar to that seen in primary neuron cell culture. Half of the medium was therefore removed and replaced every 3 days with fresh enriched neuronal growth medium.

RNA extraction and Reverse transcription

Total RNA was extracted from differentiated or undifferentiated control cells using the Qiagen RNeasy mini Kit, following the manufacturer instructions. cDNA was generated by using 1 µg of total RNA by Superscript III (Invitrogen) again following the manufacturer's protocol.

Quantitative reverse transcriptase polymerase chain reaction (RT-qPCR)

To determine the expression of neuronal differentiation related genes by RT-qPCR, 10ng cDNA was used per well in triplicates using Power-Up SYBR green (Applied Biosystems) following the manufacturer's protocol. Reactions were run on the QuantStudio 3 Real-Time PCR System (Applied Biosystems). Fold induction was calculated by the delta-delta Ct method using housekeeping genes RPLP0 or GAPDH as controls. Primers are listed in **Table 2**.

Immunocytochemistry

Cells were fixed in 4% PFA in DPBS with 10 ug/mL sucrose for 10 min at room temperature. Cells were then blocked for 10 min at room temperature in 1% BSA, 10% fetal bovine serum, and 0.2% Tween-20 in DPBS. Primary antibodies (**Table 1**) were incubated overnight at 4°C in blocking solution. Following washes, slides were then incubated for 90 min at room temperature with secondary antibodies (Thermo Fisher Scientific Inc.; diluted in block solution): Alexa 488 Donkey anti mouse (1:400) and Alexa 568 Donkey anti rabbit (1:800). Nuclei were stained with DAPI or TO-PRO-3 stain. Undifferentiated T-MSCs and cells without primary antibody were used as controls. All

samples were visualized under a Zeiss 510-confocal microscope or a Nikon CSU-W1 Spinning disk field scanning-confocal microscope system.

Surface membrane markers profiling by flow cytometry

Undifferentiated cells or differentiated neuroblasts were washed in phosphate-buffered saline (PBS) (Invitrogen), and fixed in 4% paraformaldehyde (Alfa Aesar) in DPBS for 10 minutes. Cells were then stained for 30 minutes on ice with PE-conjugated anti-CD73, Alexa-647 conjugated anti-CD90 and Alexa-488 conjugated anti-CD105 (Biolegend) (**Table 1**). Samples were washed twice and taken for analysis by a flow cytometer (FACS Canto II; BD Biosciences) and data analyzed using FCS Express 7 software.

Chromatin Immunoprecipitation (ChIP) and ChIP-qPCR

Chromatin Immunoprecipitations were performed using a SimpleChIP® Enzymatic Chromatin IP Kit (Cell signaling #9003) according to manufacturer's protocol. Antibodies used are listed in Table 1. Resultant DNA was used as qPCR template, and run using primers for pluripotency gene bodies and promoters (Table 2). Data was calculated as a percentage of ChIP Input DNA.

Genomic DNA extraction and telomere-PCR

For telomere length analysis, tet-ZSCAN4 T-MSCs were collected after 72h of Doxycycline treatment to induce ZSCAN4. Genomic DNA was extracted using a Wizard® Genomic DNA Purification Kit (Promega) and concentration determined via Nanodrop. 10ng of DNA from Doxycycline treated or untreated cells was used as template

for Telomere-qPCR as described by Cawthon(125). Telomere signal was normalized to that of the single copy gene RPLP0. Primers are listed in Table 2.

Statistical analysis

Data are shown as the mean±S.E.M of multiple independent experiments with multiple donors in biological replicates. Student's t-test or one-way ANOVAs were performed for statistical analyses. A significant result in ANOVA was followed by a Fisher LSD post-hoc test. In all statistical analyses, $p<0.05$ was considered statistically significant. Statistical analyses and graph generation were performed with GraphPad Prism 7.03 software.

Table 1: Antibody List

Antibody	Host species	Dilution	Source	Application
Pan-neurofilament (Smi-312)	Mouse	1:1000	Biolegend	IF
Beta 3-Tubulin (Tuj1)	rabbit	1:200	CST	IF
MAP2	rabbit	1:50	CST	IF
Synaptophysin	mouse	1:200	CST	IF
Neurofilament light	mouse	1:100	Biolegend	IF
PSD95	rabbit	1:250	CST	IF
Musashi-1	rabbit	1:500	Invitrogen	IF
Nestin	mouse	1:2000	CST	IF
CD73 (PE conjugate)	mouse	1:50	Biolegend	Flow
CD90 (Alexa 647 conjugate)	mouse	1:50	Biolegend	Flow
CD105 (Alexa 488 conjugate)	mouse	1:50	Biolegend	Flow
KI-67	rabbit	1:100	Invitrogen	IF
CyclinA2	rabbit	1:100	CST	IF
L-Dopamine	rabbit	1:200	Abcam	IF
L-Glutamate	rabbit	1:100	Sigma-Aldrich	IF
RBFOX3 (NeuN)	mouse	1:500	Novus	IF
H3K14Ac	Rabbit	1:50	CST	ChIP
H4K8Ac	Rabbit	1:50	CST	ChIP
Normal Rabbit IgG	Rabbit	1:50	CST	ChIP

Table 2:Primer List

	Forward (5'-3')	Reverse (5'-3')
Nestin	GCTACTGAAAAGTTCCAGCTGG	CTGAAAGCTGAGGGAAGTCTTG
DCX	GGAAGCACAAGGACCTGTAC	TAGGCTTGGATTTGTACTCTGG
ACTA2	GTTACTACTGCTGAGCGTGAGA	GATGCTGTTGTAGGTGGTTTCA
Beta3-tub	CATCTTTGGTCAGAGTGGGG	GTCGCAGTTTTCACACTCCT
NEFL	GAGATTGCAGCTTACAGGAAAC	GGTGGACATCAGATAGGAGCT
MAP2	TGGAGGTGGTAATGTCAAGATTG	GGGGACTGTGTAATGATCTCAG
PSD95	CCTGGAGAATGTGCTAGAGATT	GGTAGATCTCCTCAAAGCTGTC
MSI 1	GCCATGCTGATGTTC GACA	CTACGATGTCCTCGCTCTCA
CD73	CAG TAC CAG GGC ACT ATC TGG	AGT GGC CCC TTT GCT TTA AT
CD90	ATGAACCTGGCCATCAGCA	GTGTGCTCAGGCACCCC
CD105	CCA CTA GCC AGG TCT CGA AG	GAT GCA GGA AGA CAC TGC TG
SOX2	CAAGGAGAGGCTTCTTGCTGA	CACAGAGATGGTTCGCCAGT
RPLP0	CAGCAAGTGGGAAGGTGTAATCC	CCCATTCTATCATCAACGGGT
GAPDH	CAAGATCATCACGAATGCCTC	GCATGGACTGTGGTCATGAGTC
OCT4	TCT TCA GGA GAT ATG CAA AGC	ATC CTC TCG TTG TGC ATA GT
NANOG	AGC TAC AAA CAG GTG AAG AC	TAG GAA GAG TAA AGG CTG GG
pNANOG	GAAAGACATGACAAATCACCAGAC	CAA CTA GCT CCA TTT TCC TCT TTC
gNANOG	GGA ACA ATT CAA CCT GGA GCA	ATT ACA TTA AGG CCT TCC CCA G
pOCT4	TTACTTAAGTCGACAGAGGTCAGC	TGGTCTAGTGCTTGATTCTGTTTG
gOCT4	CTC ACT TCA CTG CAC TGT ACT C	TTG TGT TCC CAA TTC CTT CCT T
pSOX2	CGGTTGAATGAAGACAGTCTAGTG	CGACTAGAAGTTAGGAGACCCAAA
gSOX2	ACCTACATGAACGGCTCGC	GGGACATGTGAAGTCTGCTG
hTELO	GGTTTTTGAGGGTGAGGGTGAGGGT GAGGGTGAGGGT	TCCCGACTATCCCTATCCCTATCCCT ATCCCTATCCCTA
ZSCAN4	ATCCACCTGCCTTAGTCCAC	TCGAAGAACTGTTCCAGCCA

Chapter 3: Regulation of the cancer stem cell phenotype by ZSCAN4

3.1 Introduction

3.1A Stem Cells in Cancer

While cell stemness is an important consideration in regenerative medicine applications, it also plays a major role in malignancies. Many of the characteristics of stem cells that support their function can be appropriated by a small subpopulation of tumor cells that drive cancer progression, metastasis, drug resistance and thereby, cancer deaths. Like non-malignant stem cells, this population, known as Cancer stem cells (CSCs), are able to self-renew and to differentiate to all the various cell types that make up a bulk tumor. CSCs can be distinguished from bulk tumor cells by several aspects of stemness that they share with non-cancer stem cells, such as self-renewal, metabolic changes, open chromatin, telomere maintenance, pluripotency gene expression, and expression of drug resistance genes.

3.1.B. CSC phenotype

Compared to bulk tumor cells CSCs are distinguished by a capacity for self-renewal and the ability to (re)generate an entire tumor from a single cell. Outside of these attributes, CSCs are characterized by more open chromatin signatures, differential gene expression, and enhanced telomere maintenance (68, 70, 71, 73, 74, 76, 126)

In non-cancer stem cells, there is a well-established association between open chromatin and increased stem cell potency. Starting from a totipotent or pluripotent stem cell, during differentiation chromatin is gradually closed and gene expression resultantly silenced, until a differentiated cell is left with open chromatin only at the genes needed for its specialized function(27). This is paralleled in the tumor environment, with CSCs

harboring more open chromatin which is closed upon differentiation to a bulk tumor cell phenotype. One important difference is that the differentiated, non-CSC, tumor cells still retain significantly more open chromatin and generalized gene expression than a differentiated somatic cell would. Finally, unlike somatic cells, where differentiation is unidirectional, tumor cells have significant plasticity and can often shift back and forth between a CSC phenotype and a non-CSC phenotype, depending on microenvironmental cues (127).

Gene expression patterns are often quite distinct in CSCs compared to non-CSCs. While these patterns differ between CSCs in different types of tumors, the common threads are increased expression of pluripotency-associated genes, increased metabolic genes involved in oxidative phosphorylation, genes involved in drug-resistance, DNA damage response genes, and cell surface receptor genes that mediate immune evasion and migration. Increased expression of those genes confers the CSC phenotype on a given cancer cell and that expression is dependent on having open chromatin.

Both CSCs and non-CSCs express high levels of telomere extension-related proteins. In the vast majority of cancers, telomere maintenance is accomplished by telomerase expression and activity, with those not expressing telomerase seeing an increase in ALT-pathway proteins(51). Compared to somatic cells in the tissue of origin, cancer cells can have either shorter, similar, or longer telomeres, which are stable regardless of the telomere extension mechanisms employed (73, 128). Several reports have shown that CSCs harbor upregulated telomerase compared to bulk tumor cells (73, 75, 81). Thus, telomere maintenance is also an important characteristic of the CSC population.

3.1.C. CSC targeting therapies

Given the role of CSCs in promoting tumor characteristics that drive cancer progression and death, the selecting targeting of CSCs is an area of intensive study in oncology. While more generalized cancer therapies can be quite effective at killing non-CSC, bulk tumor cells, the survival of CSCs enables tumor recurrence and metastasis post-treatment. Thus, an approach targeting CSCs, with (or even without) concomitant targeting of bulk tumor cells has the potential to more effectively cure cancers. While there are no (as of yet) FDA-approved drugs specifically targeting cancer stem cells, clinical trials are ongoing, primarily with monoclonal antibodies targeting CSC-associated cell surface receptors (129) Another avenue of CSC treatment is differentiation therapy, wherein a CSC can be induced to differentiate and thereby become more benign. A notable success story is the use of retinoids to treat Acute Promyelocytic Leukemia (APL), with retinoic acid treatment inhibiting self-renewal and forcing differentiation of the CSC-like population(130). Targeting CSCs in additional cancers and using additional CSC markers, is thus a promising approach for cancer therapy **(Figure 21**).

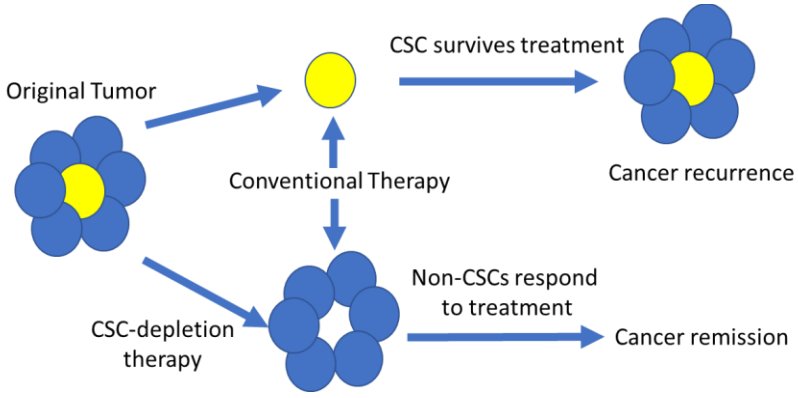

Figure 21: CSC targeting as a therapeutic approach
Tumor cells are heterogeneous, holding a majority of non/low tumorigenic cells and a small subset of CSCs. CSCs can be experimentally identified by their ability to generate differentiated tumors after transplantation into an immunocompromised mouse or generate 3D tumorspheres *in vitro*. This model suggests CSC-specific therapies in combination with conventional chemotherapies may kill both CSC and bulk tumor populations, thereby preventing cancer recurrence.

Therapeutic targeting of CSCs is a promising strategy for cancer treatment. While more selective than the chemotherapies aimed at highly proliferative, bulk tumor cells, CSC-targeting therapies are still not fully selective for CSCs, potentially damaging healthy cells (particularly healthy stem cells). This is due to many reported CSC-markers not being specific to cancers, as they are typically also expressed in both somatic and germline stem cells. Thus, there is a continuing need to refine anti-CSC therapies by identifying and characterizing novel (ideally CSC-specific) factors that underlie cancer stemness.

3.1D ZSCAN4 in cancer

As described previously, ZSCAN4 is an early developmental gene whose expression is confined to the early embryo, with negligible expression in somatic cells. Unpublished work in our lab by Dr. Alex Meltzer demonstrated that ZSCAN4 is aberrantly re-expressed in many human cancers and in human cancer cell lines. Furthermore, ZSCAN4 in stem cells appears to regulate stem cell potency in ESCs, iPSCs, and, per our results in Chapter 2, in somatic T-MSCs. We therefore hypothesized that ZSCAN4 may be playing a similar role in human cancers, with its expression conferring a CSC phenotype. As in Chapter 2, we expected ZSCAN4 to: 1) increase open chromatin, 2) increase pluripotency gene expression and 3) extend the telomeres, together leading to increased cancer stemness.

3.1.E. Ring Finger Protein 20 (RNF20)

To target cancer stemness by way of ZSCAN4, a better mechanistic understanding of how ZSCAN4 may promote stemness is needed. While ZSCAN4 expression in cancer cells is transient and thereby harder to target, ZSCAN4 does interact with many other proteins in the cell. Previous data in our lab demonstrated an interaction between ZSCAN4 and the

E3 Ubiquitin ligase RNF20(124). Previous characterization of this interaction determined that RNF20 regulated ZSCAN4 stability by polyubiquitinating the latter, leading to proteasomal degradation (124). RNF20's ubiquitin ligase activity, however, does not end with polyubiquitination of cellular proteins. RNF20 is also responsible for mono-ubiquitination of Histone H2B, an important step in converting closed chromatin to a more open conformation (131). While histone acetylation and methylation levels determine the strength of the interaction between DNA and the histone octamer it wraps around, histone mono-ubiquitination levels determine how separated nucleosomes are from each other (132). To have truly open, transcriptionally accessible chromatin, both intra-nucleosomal and inter-nucleosomal effects must work in concert.

3.2 Results

3.2A ZSCAN4 is associated with cancer stem cells in HNSCC lines

Given the role of ZSCAN4 in promoting the stem cell phenotype, in this part of the work, we set to define the significance of its interaction with the ubiquitin ligase RNF20, and the role both factors play in chromatin remodeling at pluripotency genes. Previous findings in the lab have established that ZSCAN4 is aberrantly re-expressed in a variety of humans cancers and human cancer cell lines. Given the role of ZSCAN4 in underlying stem cell potency, reported in PSCs by others and in T-MSCs in Chapter 2, we hypothesized that ZSCAN4 may similarly underlie stemness in human cancer lines. We first assessed whether ZSCAN4 was associated with stemness in human Head and Neck squamous cell carcinoma (HNSCC) lines as HNSCC have been reported to harbor a significant CSC population, as well as express the core pluripotency factors (133, 134). As ZSCAN4 is

transiently expressed and only in a small number of cells at a time, we transduced, and subsequently selected, the HNSCC lines Tu167 and 012SCC with a promoter-reporter lentivector where mCherry expression is driven by the ZSCAN4 promoter (Figure 22A). To enrich for cancer stem cells, we cultured both lines in spheroid conditions to generate 3D-tumorspheres. Culturing both lines as tumorspheres resulted in substantially increased percentages of mCherry+ cells, indicating that CSCs were associated with ZSCAN4 expression (Figure 22B-C). Several markers of CSCs have been reported in HNSCC, including the cell surface marker CD44 and the enzyme ALDH1A1 (135). We thus immuno-stained our pZSCAN4-mCherry cells for these markers and assessed their expression in mCherry-positive (ZSCAN4+) and mCherry-negative (ZSCAN4-) cells by flow cytometry. In both HNSCC lines, mCherry+ (ZSCAN4+) cells had significantly higher percentages of both CD44+ and ALDH1A1+ cells (Figure 22D-G). Furthermore, mCherry+ cells also had a higher percentage of CD44+/ALDH1A1+ co-positive cells, likely representing true cancer stem cells. Together, this data suggests that ZSCAN4 expression is associated with cancer stem cells.

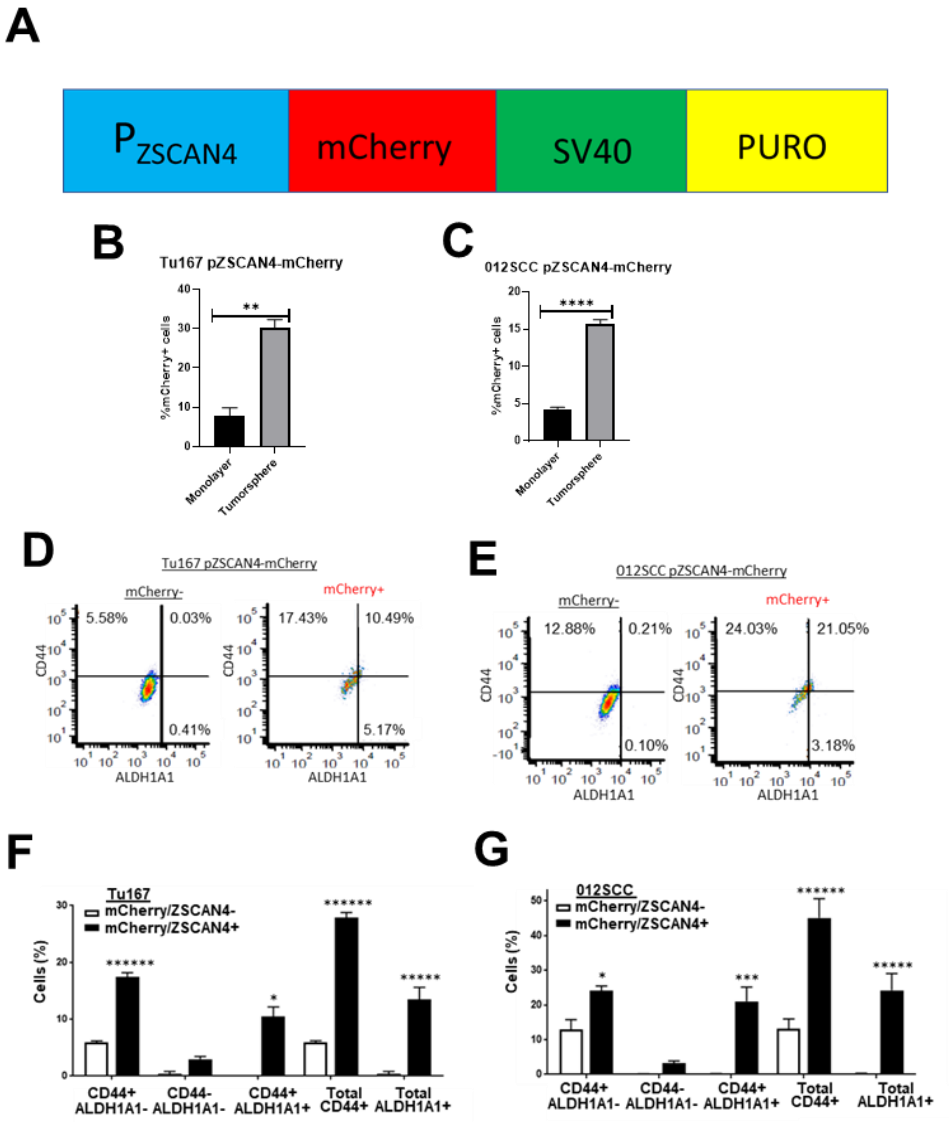

Figure 22: ZSCAN4 is associated with cancer stem cells in head and neck cancer lines.

Illustration of ZSCAN4 promoter reporter system where mCherry expression is driven by the ZSCAN4 promoter. **B)** Flow cytometry results of mCherry expression in cell cultured as monolayers or tumorspheres in Tu167 and **C)** 012SCC. Statistical significance determined by student's t-tests. **D)** Flow cytometry analysis (FCS Express) showing the expression distributions of CD44 and ALDH1A1 in mCherry+ and mCherry- populations in Tu167 and **E)** 012SCC cells. **F)** Quantification of flow cytometry data showing percentage of cells positive and co-positive for CD44 and ALDH1A1 in mCherry+ and mCherry negative Tu167 and **G)** 012SCC cells. Statistical significance determined by independent student t-tests. All data shown as mean ± S.E.M. *p<0.05, **p<0.01, ***p<0.001, ****P<0.0001, *****p<0.00001, ******p<0.000001. (Adapted from Portney BA, Arad M, Gupta A, Brown RA, et al. Oncogene (2020). Data generated by Robert Brown. (97))

3.2.B. ZSCAN4 regulates pluripotency and CSC-associated gene expression

Given the chromatin changes mediated by ZSCAN4 at pluripotency gene promoters, we next asked whether those changes were functional, that is, would they affecting gene expression. Using our tet-inducible HNSCC lines (Tu167 and 012SCC) we found that ZSCAN4 induction for 48h led to robust, significant increases in the pluripotency genes Nanog, OCT4, and SOX2. (Figure 23A-B). This supports concurrent work in the lab which found pluripotency genes are upregulated in HNSCC lines in response to ZSCAN4(101). We further found that the CSC-associated genes BMI1, MDR1, and ABCG2 were also upregulated, suggesting ZSCAN4 is driving both pluripotency and CSC gene expression in HNSCC. To determine if ZSCAN4's effects were specific to HNSCC, we also induced ZSCAN4 in the additional tet-inducible cancer lines U2OS (Osteosarcoma), SW480 (Colorectal cancer), and SKBR-3 (Breast Cancer). Despite some variability, at least one pluripotency gene was significantly upregulated in each cell line, with most of the CSC-associated genes also upregulated in response to ZSCAN4 induction. (Figure 23C-E). This data suggests ZSCAN4 may regulate pluripotency gene expression and CSC gene expression across multiple distinct cancer backgrounds.

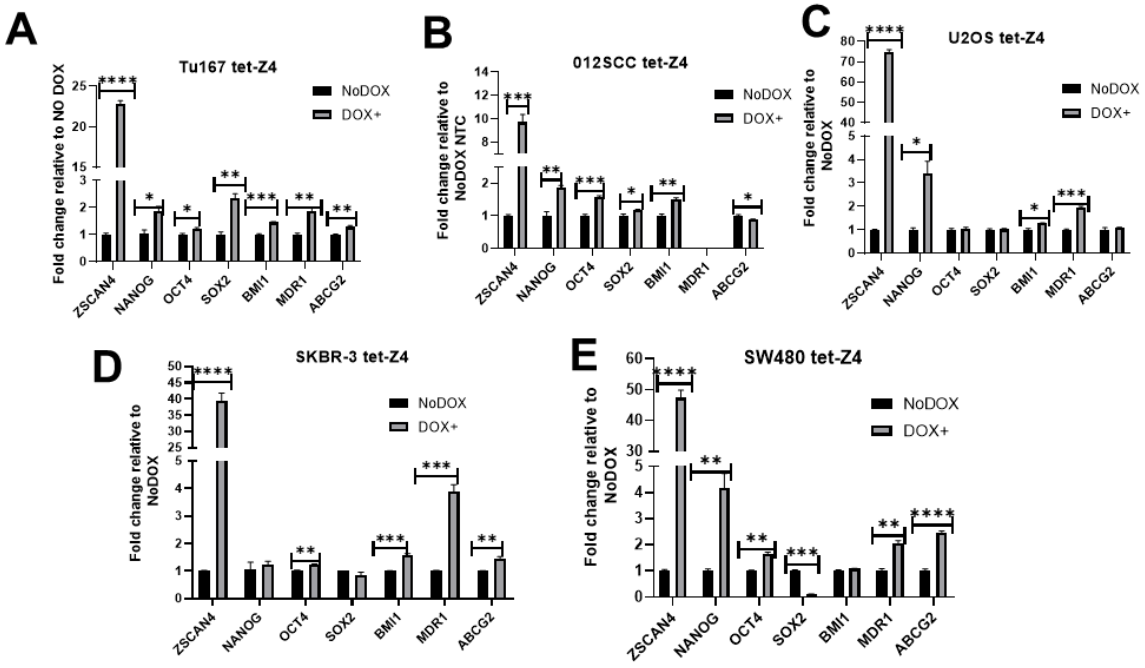

Figure 23: ZSCAN4 induction leads to increased CSC-associated gene expression.
RT-qPCR in ZSCAN4-induced and uninduced cells in **A)** Tu167**, B)** 012SCC, **C)** U2OS, **D)** SKBR-3, **E)** SW480 cell lines. Data presented as fold change relative to uninduced cells, with all genes normalized to the housekeeping gene RPLP0. Statistical significance was determined by independent student t-tests. All data shown as mean ± S.E.M. *p<0.05, **p<0.01, ***p<0.001, ****P<0.0001. (Unpublished data generated by Robert Brown)

While ectopic overexpression of ZSCAN4 in cancer lines led to increased pluripotency gene expression, parallel experiments in the lab demonstrated that shRNA depletion of ZSCAN4 in HNSCC lines resulted in diminished pluripotency gene expression (97). To assess whether ZSCAN4 is necessary for such gene expression, we desired a more robust ZSCAN4 depletion system. In collaboration with the UMB's CRISPR Core facility and the laboratory of Tami Kingsbury, we were able to generate multiple ZSCAN4 knockouts in both Tu167 and U2OS, validated by Sanger sequencing and ICE analysis, as well as by Western blot. We then assessed pluripotency gene expression in these validated lines by RT-qPCR. Our results revealed significant clonal variation, with two clones of Tu167 showing a trend of reduced Nanog and SOX2 expression, while one clone showed increased Nanog and SOX2 compared to WT cells. (Figure 24A) As the functions of the

core pluripotency genes are co-operative, the observed increases in NANOG and SOX2, while OCT4 remained unchanged potentially reflects differentiation, rather than a true increase in pluripotency. In our U2OS cells, Nanog expression was unchanged, while both KO clones demonstrated reductions in OCT4 and SOX2. (Fig. 24B). The discrepancies among our KO clones led us to hypothesize that clonal variation could also be masking the true effect of ZSCAN4-KO on pluripotency gene expression. As an alternative approach, we used a tet-inducible CRISPR-Cas9 KO system for ZSCAN4 in U2OS. In response to incubation with Doxycycline, the Cas9 protein and ZSCAN4-targeting sgRNA are expressed, leading to gene knockout. This system allows us to assess cells both shortly after ZSCAN4-KO, as well as generating a bulk knockout population to avoid clonal variation. Remarkably, inducing ZSCAN4 knockout in these cells led to major reductions in the expression of Nanog, OCT4, and SOX2, compared to the empty sgRNA control (Fig.24C). We further assessed this effect by immunostaining and found that the pluripotency markers OCT4 and KLF4 were reduced on the protein level as well. (Fig.24D) Our results suggest that ZSCAN4 depletion does indeed lead to reduced pluripotency gene expression, though long term culture in the absence of ZSCAN4 (as occurs with KO clones) may allow for compensatory mechanisms to alter their expression.

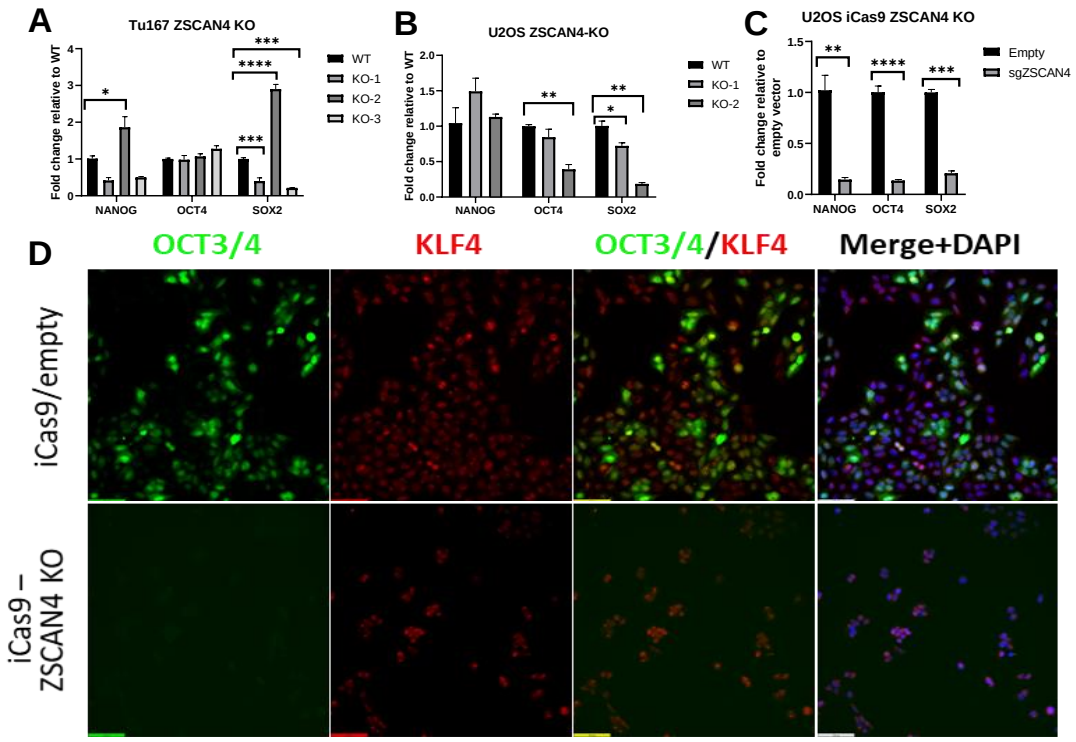

Figure 24: ZSCAN4 depletion leads to reduction in pluripotency gene expression. RT-qPCR results showing pluripotency gene expression in **A)** Tu167 CRISPR-Cas9 knockout clones and **B)** U2OS CRISPR-Cas9 knockout clones. Data is presented as fold change relative to WT with expression normalized to the housekeeping gene RPLP0. Statistical significance was determined by one way ANOVA and Fisher's LSD**. C)** RT-PCR results showing pluripotency gene expression in U2OS inducible ZSCAN4 knockout cells. Data is expressed as fold change relative to empty vector control, with expression normalized to the housekeeping gene RPLP0. Statistical significance was determined by independent student t-tests. **D)** Representative immunofluorescence images showing expression of the pluripotency genes OCT4 and KLF4 in U2OS inducible ZSCAN4 knockout cells. All data shown as mean ± S.E.M. *p<0.05, **p<0.01, ***p<0.001, ****P<0.0001 (Unpublished data generated by Robert Brown)

3.2.C. ZSCAN4 positively regulates open chromatin at pluripotency genes

Our findings that ZSCAN4 positively regulates pluripotency gene expression led us to ask how ZSCAN4 may be doing so. Work in mESC and iPSC, as well as our results in T-MSCs (Chapter 2), led us to hypothesize that ZSCAN4 may enhance cancer stemness by inducing open chromatin, thereby enhancing pluripotency gene expression. Concurrent work in our lab revealed that ZSCAN4 induction in HNSCC lines leads to increased open chromatin marks, both globally and at Nanog and OCT4 promoters (97). While open chromatin marks are suggestive of open chromatin, to further assess chromatin accessibility at pluripotency

gene loci, we performed Chromatin Accessibility by Real Time PCR (ChART-PCR). In this technique, fully natured chromatin is digested *in situ* by an endonuclease (DNaseI or MNase). The digested chromatin is then extracted, with DNA purified and used as template for RT-qPCR. More open, accessible chromatin is more easily digested by the endonuclease and therefore yields a weaker signal by PCR. This signal, relative to an undigested input control, can be compared across treatment conditions to determine differences in chromatin accessibility. In our tet-inducible ZSCAN4 Tu167 line, we cultured cells with or without Doxycycline for 72h and then performed a DNaseI digest on extracted nuclei. Our results indicate a robust increase in chromatin accessibility at the promoters of Nanog, SOX2, and OCT4, in response to ZSCAN4 expression. (Fig.25A). Conversely, we digested two CRISPR-Cas9 ZSCAN4 KO clones of Tu167 cells with DNaseI. Our results demonstrate a remarkable reduction in chromatin accessibility in Tu167 ZSCAN4 KO cells (Fig.25B), which, when coupled with the data from ZSCAN4 overexpression in Tu167, suggest ZSCAN4 is indeed regulating the chromatin accessibility of pluripotency gene promoters. In an effort to extend our findings beyond HNSCC, we also performed a DNaseI digest of two KO clones of U2OS. As with ZSCAN4 KO in Tu167, we found that ZSCAN4 KO in U2OS resulted in significantly reduced chromatin accessibility at pluripotency gene promoters (Fig.25C), yet further evidence that ZSCAN4 regulates pluripotency genes epigenetically. Additionally, we utilized a tet-inducible Cas9 system in U2OS cells. Treatment of these cells with Doxycycline leads to expression of Cas9 protein and ZSCAN4-targeting sgRNA. Thus, these cells give temporal control over the knockout of ZSCAN4, compared to our clonal KO lines which have been ZSCAN4 depleted for dozens of cell divisions during expansion. After knockout induction, we

performed ChIP for open chromatin marks. Our induced-KO cells demonstrated significant reductions in the open chromatin marks H3K18Ac and H4K8Ac (Fig.25D-F), further confirming that ZSCAN4 appears to regulate open chromatin, both across cell lines and across modes of depletion.

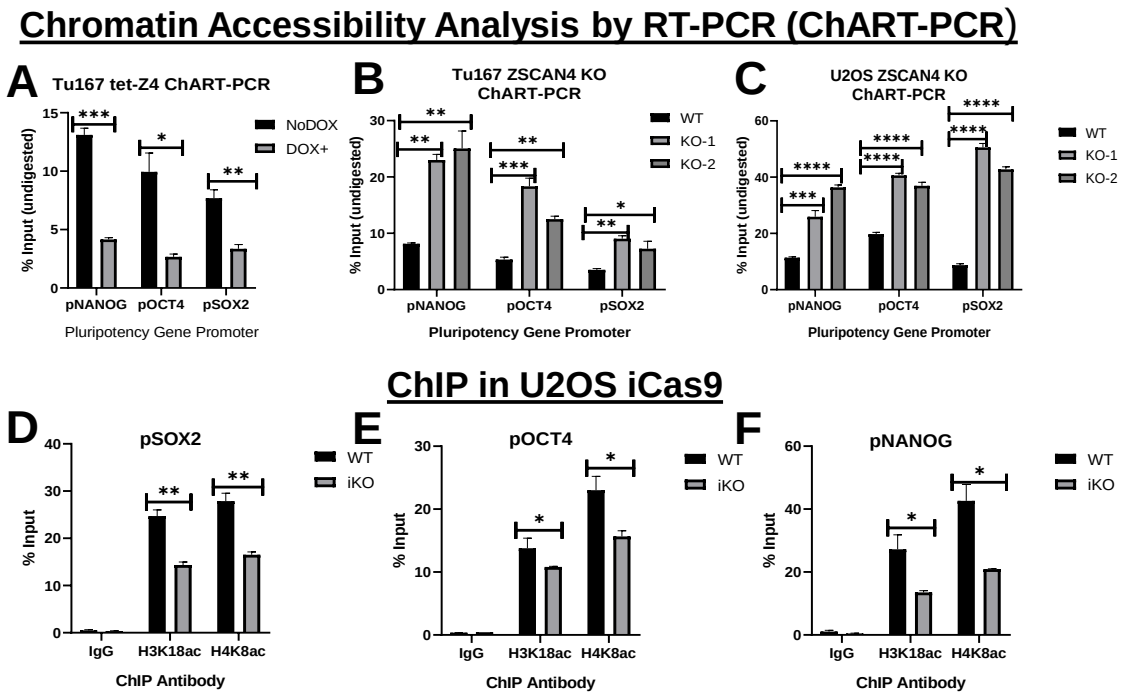

Figure 25: ZSCAN4's effect on chromatin accessibility and histone acetylation at pluripotency gene promoters.

A) ChART-qPCR results in Tu167 tet-ZSCAN4 cells showing chromatin accessibility at pluripotency gene promoters. Results presented as a percentage of undigested input DNA. Statistical significance determined by student t-tests. **B)** ChART-PCR results in Tu167 ZSCAN4 knockout cells and **C)** U2OS ZSCAN4 knockout cells showing chromatin accessibility at pluripotency gene promoters. Results presented as a percentage of undigested input DNA. Statistical significance determined by one way ANOVA with Fisher's LSD. **D-F)** ZSCAN4 depletion leads to reduction in histone acetylation at pluripotency gene promoters. ChIP-qPCR in U2OS inducible ZSCAN4 knockout cells showing histone acetylation levels at pluripotency gene promoters. Results presented as a percentage of ChIP Input. Statistical significance determined by student t-tests. All data shown as mean ± S.E.M. *p<0.05, **p<0.01, ***p<0.001, ****P<0.0001. (Unpublished data generated by Robert Brown)

3.2.D. ZSCAN4 positively regulates telomeric open chromatin and telomere length

As mentioned in the introduction, maintenance of telomere length across cell divisions is a characteristic of both pluripotent stem cells and cancer cells, particularly cancer stem cells. Given ZSCAN4's association with cancer stem cells in HNSCC and its role in

regulating pluripotency and cancer stem cell gene expression, as well as ZSCAN4's regulation of telomeres in T-MSCs (Chapter 2) and mESC (83), we assessed whether ZSCAN4 also regulates the telomeres of cancer cells. Excitingly, just 48h of ZSCAN4 induction in both Tu167 and U2OS tet-inducible lines, led to significant increases in telomere length as assessed by Telomere RT-qPCR. (Fig.26A-B). As Tu167 cells are telomerase-positive, while U2OS cells are telomerase-negative, this suggests ZSCAN4-mediated telomere extension is independent of telomerase, a finding that has been reported in mESC (83, 122) and implied by telomere extension in our telomerase-negative T-MSCs (Figure 18). As both Tu167 and U2OS do express endogenous ZSCAN4, we also assessed whether ZSCAN4 depletion would lead to telomere shortening. Using our CRISPR-Cas9 ZSCAN4 KO clonal lines, we assessed the effect of ZSCAN4-KO on Tu167 and U2OS telomere length. Remarkably, all three ZSCAN4-KO clones in Tu167 showed significantly reduced telomere length. (Fig.26C) The two ZSCAN4-KO clones in U2OS displayed some variation, with one clone showing significantly reduced telomeres while the other showed no significant change in telomere length. (Fig.26D). To gain insights into the mechanism ZSCAN4 may be employing to regulate telomere length, we next looked at telomeric chromatin. The relative compaction of telomeric chromatin governs its accessibility to both telomerase and homologous recombination enzymes in ALT (34, 54). As ZSCAN4 appears to regulate pluripotency gene expression by epigenetic changes, we anticipated that ZSCAN4 may open the telomeric chromatin, facilitating telomere elongation. Our findings by ChIP-PCR in tet-inducible Tu167 reveal that induction of ZSCAN4 results in increased histone acetylation (H3K27, H4K5, and H4K8) as well as the euchromatin associated tri-methylation mark,

H3K4Me3 (Fig. 26E). These data reveal that ZSCAN4 is indeed opening telomeric chromatin, and suggest that enhancement of telomere accessibility may be the mechanism behind ZSCAN4-mediated telomere regulation.

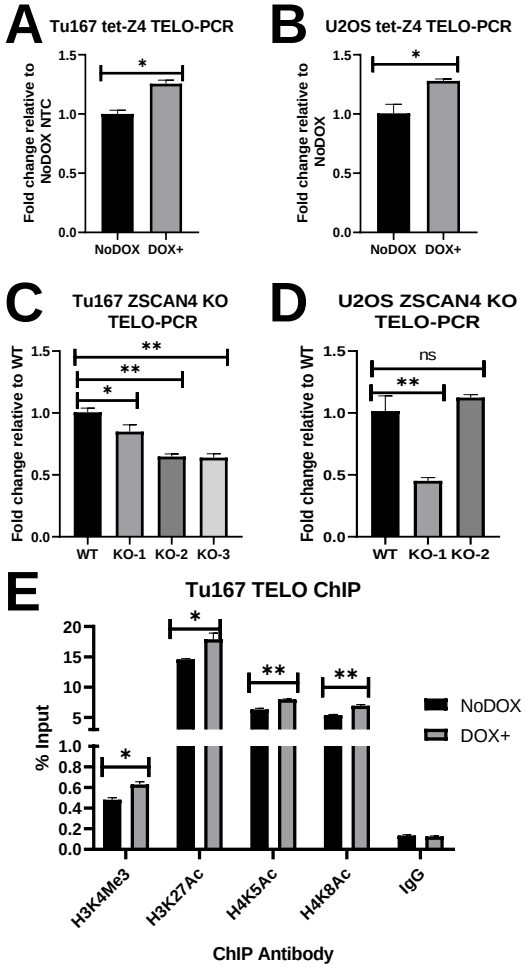

Figure 26: ZSCAN4 positively regulates telomere length and histone acetylation at the telomere.

Telomere-qPCR showing relative telomere length in **A)** Tu167 tet-ZSCAN4 cells and **B)** U2OS tet-ZSCAN4 cells. Results are presented as fold change relative to uninduced cells (NoDOX) with telomeres normalized to the expression of the single-copy gene RPLP0. Statistical significance was determined by student t-tests**. C)** Telomere-qPCR showing relative telomere length in Tu167 ZSCAN4 knockout cells and **D)** U2OS ZSCAN4 knockout cells. Results presented as fold change relative to WT cells with telomeres normalized to the expression of the single-copy gene RPLP0. Statistical significance was determined by one way ANOVA with Fisher's LSD**. E)** ChIP-qPCR in Tu167 tet-ZSCAN4 cells showing levels of open chromatin marks at the telomere. Results are presented as a percentage of ChIP input. Statistical significance was determined by student t-tests. All data shown as mean ± S.E.M. *p<0.05, **p<0.01, ***p<0.001, ****P<0.0001. (Unpublished data generated by Robert Brown)

3.2E: ZSCAN4 regulates *in vitro* cancer stemness in HNSCC lines

Thus far we have demonstrated that ZSCAN4 regulates the chromatin of cancer cell lines, with such epigenetic changes potentially responsible for ZSCAN4-mediated pluripotency gene expression and telomere extension. As its effects are all characteristics of cancer stem cells, we next wanted to determine if ZSCAN4 would regulate functional cancer stemness. Since CSCs have the ability to self-renew and generate a tumor from a single cell, relative cancer stemness can be assessed *in vitro* by an extreme limiting dilution assay (ELDA). Adherent cells in culture are detached into a single cell solution and then serial dilutions of cells are made and added to wells of an ultra-low attachment plate. Upon culture in non-adherent, serum-free conditions, CSCs will generate 3D tumorspheres, while non-CSCs will not. Thus, by quantifying the number of wells per dilution containing at least one tumorsphere, we can calculate the frequency of tumorsphere-forming cells (CSCs) and compare between conditions. For our *in vitro* ELDA, we made serial dilutions of Tu167 WT and ZSCAN4-KO clonal lines and plated them. After 10 days in non-adherent culture, we quantified the resultant wells containing tumorspheres. Remarkably, both ZSCAN4-KO clones showed significant reductions in CSC frequency (Fig.27A), suggesting that endogenous levels of ZSCAN4 promote cancer stemness. To further confirm this finding, we performed ELDA in Tu167 cells using an shRNA mediated ZSCAN4-knockdown system. Compared to a scrambled shRNA control, and consistent with our findings in ZSCAN4-KO cells, ZSCAN4-KD cells also showed a significant reduction in CSC frequency (Fig.27B), further bolstering the idea that ZSCAN4 is important for cancer stemness. To explore the converse, that is, does ZSCAN4 overexpression increase cancer

stemness, we induced ZSCAN4 in our tet-inducible Tu167 and 012SCC lines and then plated them for ELDA. While ZSCAN4-induction in both cells lines resulted in increased CSC frequencies, they did not reach significance (Fig.27C-D). Taken with the depletion data from KO and KD, however, our data suggest a role for ZSCAN4 in the regulation of *in vitro* cancer stemness.

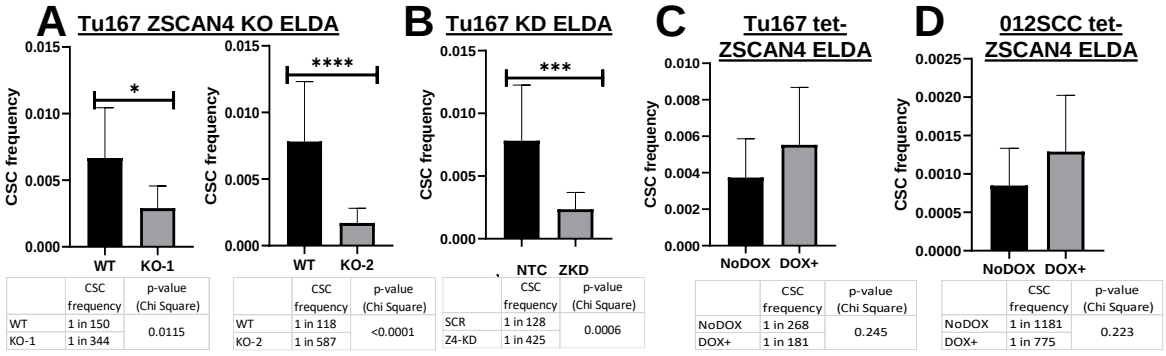

	CSC frequency	p-value (Chi Square)
WT	1 in 150	0.0115
KO-1	1 in 344	

	CSC frequency	p-value (Chi Square)
WT	1 in 118	<0.0001
KO-2	1 in 587	

	CSC frequency	p-value (Chi Square)
SCR	1 in 128	0.0006
Z4-KD	1 in 425	

	CSC frequency	p-value (Chi Square)
NoDOX	1 in 268	0.245
DOX+	1 in 181	

	CSC frequency	p-value (Chi Square)
NoDOX	1 in 1181	0.223
DOX+	1 in 775	

Figure 27: ZSCAN4 regulates in vitro cancer stemness in head and neck cancer lines. **A)** In vitro extreme limiting dilution assay results in Tu167 WT and ZSCAN4 knockout cells showing calculated cancer stem cell frequency. **B)** In vitro ELDA results in Tu167 ZSCAN4 knockdown cells and scrambled control. **C)** In vitro ELDA results in Tu167 tet-ZSCAN4 and **D)** 012SCC tet-ZSCAN4 cells. Cancer stem cell frequency calculations for all experiments were performed via L-Calc software and statistical significance determined by Chi-square test. All data presented as mean frequency with range representing a 95% confidence interval. *p<0.05, **p<0.01, ***p<0.001, ****P<0.0001. (Unpublished data generated by Robert Brown)

3.2.G. ZSCAN4 is required for maintenance of H2B-Ub levels at pluripotency genes

Prior work in our lab had revealed that ZSCAN4 and the E3 Ubiquitin ligase RNF20 co-localize and co-immunoprecipitate (124). That work also found that RNF20 is responsible for the polyubiquitylation and degradation of ZSCAN4 (124). RNF20 also plays an important role in chromatin structure via its mono-ubiquitylation of Histone H2B (H2BUb). Therefore, to assess significance of RNF20 in mediating ZSCAN4 in chromatin modifications, we performed Westerns blots for H2BUb across our ZSCAN4 depletion cell lines. In Tu167 ZSCAN4-KD cells (**Fig.29A**), there does appear to be reduced H2BUb and RNF20, yet in Tu167-KO cells only one clone shows reduction in H2BUb (Fig.29B).

Likewise in U2OS-KO, H2BUb is substantially reduced in one clone, but increased in the other, while RNF20 is unchanged and increased, respectively (Fig.29C). Our inducible KO U2OS cells show increased H2BUb and RNF20 (Fig.29D). Our results demonstrate that, at least on the global level, neither H2BUb nor RNF20 is consistently reduced when ZSCAN4 is depleted.

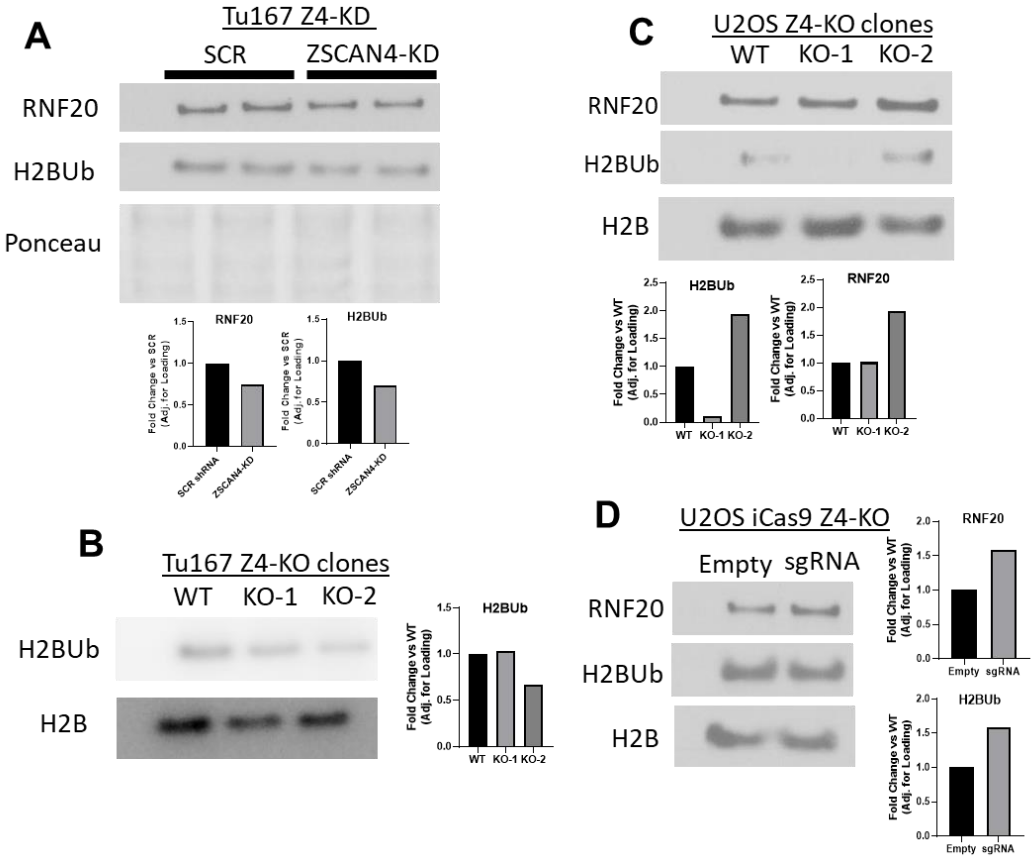

Figure 28: ZSCAN4 depletion does not consistently affect RNF20 or H2BUb levels.
Immuno-blotting for RNF20 and H2B-Ub levels in A) Tu167 ZSCAN4 knockdown and scrambled control, B) Tu167 ZSCAN4 knockout clones, C) U2OS ZSCAN4 knockout clones, and D) U2OS inducible ZSCAN4 knockout cells and empty vector control. Quantification shows relative expression after normalization to either total Histone H2B or Total Protein quantification (TPQ) via Ponceau staining. (Unpublished data generated by Robert Brown)

H2BUb and RNF20 levels being unaltered globally, however, does not necessarily reflect the situation at specific genes. We therefore performed ChIP to determine whether the

localization of RNF20 and H2BUb at pluripotency gene was affected by loss of ZSCAN4. We first performed ChIP in our Tu167 ZSCAN4-KD cells and found that both H2BUb and RNF20 were reduced at the promoters of NANOG, OCT4, and SOX2 (Fig 30A-C). We subsequently performed ChIP in our Tu167 ZSCAN4-KO lines. Here, again, the results demonstrated clonal variability with one clone showing significant changes in both H2B and RNF20 and the other did not. In the clone that did show changes, the results were very interesting. Here, there was significantly reduced H2BUb at pluripotency promoters, while also having increased RNF20 levels at those same promoters. (Fig 30D-F). This data, coupled with the Tu167-KD data, suggests that even when RNF20 is present or even increased, its activity on H2B ubiquitylation may be impaired. To exclude clonal variation and assess this effect in a different cell background, we finally performed this ChIP in our U2OS inducible KO line. Here, we found robust reductions in both RNF20 and H2BUb at pluripotency gene promoters. (Fig 30G-I). This suggests there may be a temporal component to how ZSCAN4 depletion affects RNF20 function. Both Tu167-KD and U2OS inducible KO cells have been without ZSCAN4 for a relatively short period of time. Tu167 KO clones, on the other hand, have undergone dozens of cell divisions in the absence of ZSCAN4. Thus, early on, ZSCAN4 depletion may lead to reduced RNF20 and H2BUb at pluripotency promoters, but over a longer period, compensatory mechanisms may rescue RNF20 localization, but not necessarily its function (H2B mono-ubiquitylation). Intriguingly, we also found that there was reduced RNA Polymerase II (POLR2A) at pluripotency gene promoters in our U2OS inducible KO cells. (Fig 30G-I). As RNA polymerase II is required for gene transcription, its reduction provides one possible mechanism for the reduced pluripotency gene expressed seen with ZSCAN4

depletion (Figure 24). Independently, both RNF20 and H2BUb have been reported to promote RNA Polymerase transcriptional activity. Thus, the loss of localization of one or both factors may underlie both the lack of RNA polymerase recruitment and the lack of pluripotency gene expression in the absence of ZSCAN4.

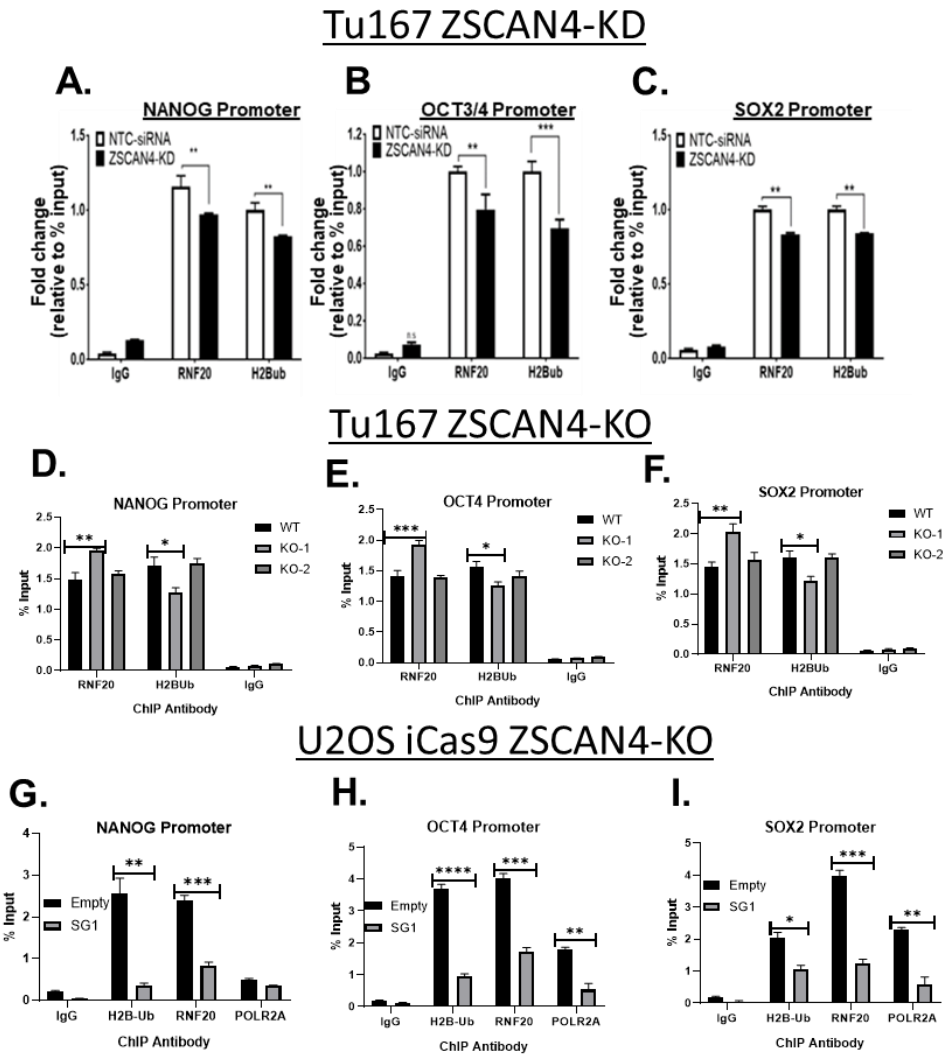

Figure 29: ZSCAN4 depletion impairs H2BUb at pluripotency gene promoters.
(A-C) ChIP-qPCR in Tu167 ZSCAN4-knockdown cells showing RNF20 and H2B-Ub levels at pluripotency gene promoters. Data shown as percentage of ChIP input DNA, with statistical significance determined by independent t-tests. **D-F)** ChIP-qPCR in Tu167 ZSCAN4-knockout clones showing RNF20 and H2B-Ub levels at pluripotency gene promoters. Data shown as percentage of ChIP Input DNA, with statistical significance determined by one way ANOVA with Fisher's LSD**. G-I)** ChIP-PCR in U2OS inducible ZSCAN4 KO cells showing H2B-Ub, RNF20, and POLR2A levels at pluripotency gene promoters. Data shown as percentage of ChIP input DNA, with statistical significance determined by independent student t-tests. All data shown as mean ± S.E.M. *p<0.05, **p<0.01, ***p<0.001, ****P<0.0001. (Unpublished data generated by Robert Brown and Dr. Benjamin Portney)

3.2.H. ZSCAN4's effects on pluripotency gene expression require RNF20

As ZSCAN4 appears necessary for optimal H2B monoubiquitylation and RNA polymerase localization at pluripotency genes, we next asked whether RNF20 was necessary for ZSCAN4's effects on pluripotency genes. We previously (Fig 23) showed that ZSCAN4 overexpression in multiple cell lines leads to increased pluripotency gene expression. To assess RNF20's potential contribution to ZSCAN4-induced gene expression, we knocked down RNF20 by siRNA transfection in our tet-inducible Tu167, 012SCC, and U2OS lines. 24h transfecting cells with either RNF20 siRNA or a universal non-targeting control (NTC), we treated cells with Doxycycline for 48h. Thus, ZSCAN4 expression occurred against a backdrop of RNF20 depletion, allowing us to determine whether RNF20 was required for ZSCAN4-induced gene expression. Notably, we found that, while ZSCAN4 induction led to increased pluripotency gene expression as expected, this effect was abolished when RNF20 was knocked down. This effect was seen across pluripotency genes and among all cell lines tested. (Fig 31A-C) ZSCAN4's effects on pluripotency gene expression thus appear to be RNF20-dependent.

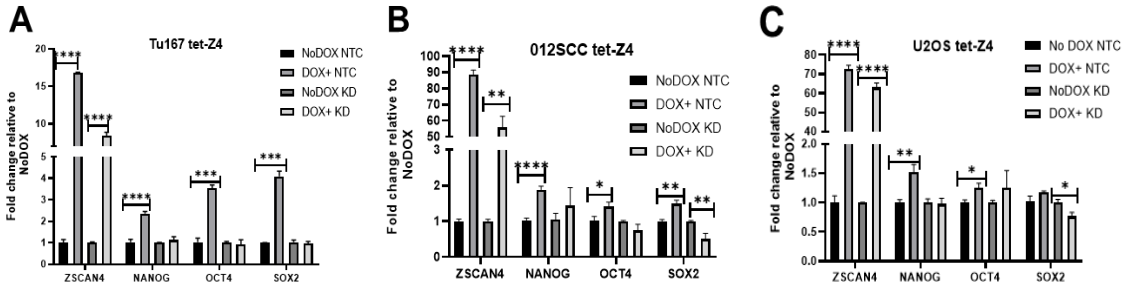

Figure 30: ZSCAN4 effect on pluripotency gene expression is RNF20-dependent.
Gene expression RT-qPCR in **A)** Tu167 tet-ZSCAN4, **B)** 012SCC tet-ZSCAN4, and **C)** U2OS tet-ZSCAN4 cells transfected with either NTC or RNF20-KD siRNA for 24h and then treated with Doxycycline for an additional 48h. Results are presented as fold change relative to the uninduced conditions (NoDOX). All data shown as mean ± S.E.M. Statistical significance was determined by one way ANOVA with Fisher's LSD for comparisons: *p<0.05, **p<0.01, ***p<0.001, ****p<0.0001. (Unpublished data generated by Robert Brown)

3.2.I. ZSCAN4 can facilitate histone acetylation independent of RNF20

In both T-MSCs and cancer lines, ZSCAN4's exerts an epigenetic effect on pluripotency genes, inducing open chromatin and allowing for gene expression. Given that ZSCAN4 requires RNF20 for pluripotency gene expression, we next looked for a potential mechanism. We first assessed whether ZSCAN4's effect on global chromatin as we reported previously(97) was RNF20-dependent. Again, we induced ZSCAN4 in 3 tet-inducible cell lines after prior transfection with either RNF20 siRNA or NTC. We then performed Western blotting to determine RNF20's contribution to global histone modifications. As shown in Figure 9, both RNF20 and H2BUb were massively decreased by RNF20-KD across all three cell lines. In 012SCC cells (Fig.32A), H3K14ac and H3K18ac were clearly increased in response to ZSCAN4 whether or not RNF20 was present. H4K5Ac and H4K8Ac also showed an increase, albeit somewhat blunted, in response to ZSCAN4 when RNF20 was depleted. In Tu167 cells (Fig 32B), this was not the case, with H3K18ac, H3K4me3, H4K5Ac, and H4K8Ac all increasing with ZSCAN4, regardless of RNF20 status. In U2OS cells (Fig. 32C), H4K8ac did appear blunted or even reduced when ZSCAN4 was induced in RNF20 knockdown, but H3K18ac, H3K4me3, and H4K5ac all appeared RNF20-independent. On the whole, then, ZSCAN4-induced open chromatin marks are not dependent on RNF20, at least globally speaking.

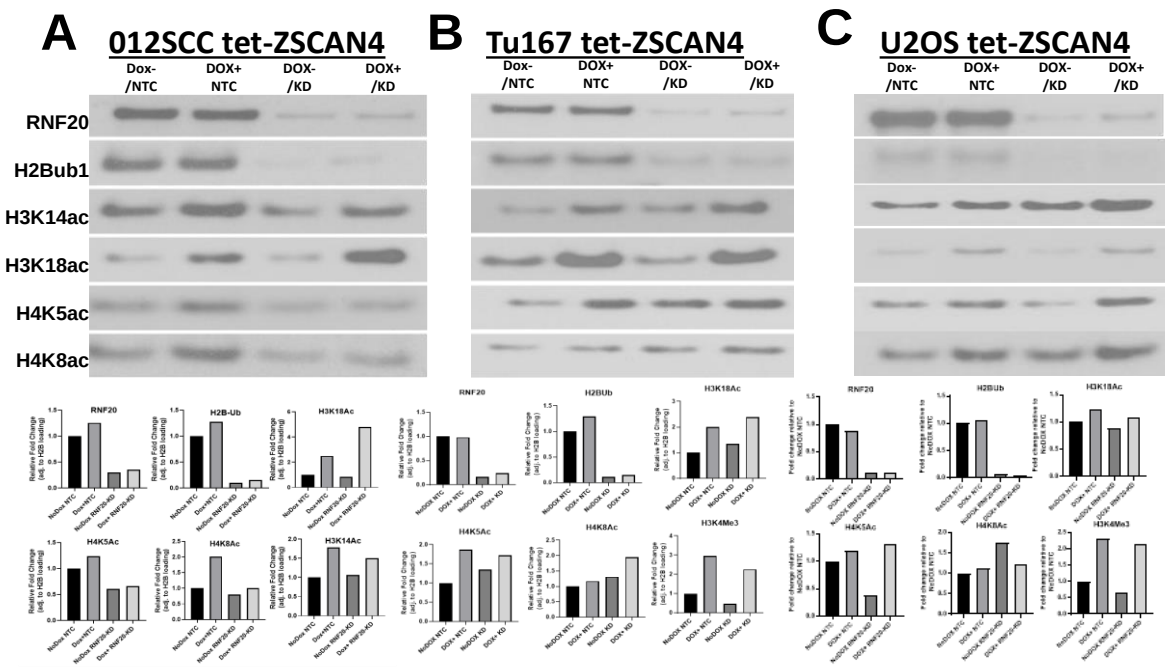

Figure 31: ZSCAN4 increases open histone marks *is not dependent on* RNF20.
Immuno-blotting was performed in **A)** 012SCC tet-ZSCAN4 cells, **B)** Tu167 tet-ZSCAN4 cells, and **C)** U2OS tet-ZSCAN4 cells transfected with either NTC or RNF20-KD siRNA for 24h and then treated with Doxycycline for an additional 48h. Total Histone H2B or total protein quantification (by Ponceau stain) were used as loading controls. Quantification is relative to respective loading control from the same experiment. (Unpublished data generated by Robert Brown)

Given that there were significant differences between global levels of H2BUb and their level at pluripotency gene promoters, we next wanted to assess ZSCAN4's effects on open chromatin marks at specific gene targets, with or without RNF20 knockdown. For this experiment we performed a ChIP on tet-inducible Tu167 cells with or without concurrent RNF20 knockdown. Our results on the promoters of NANOG and OCT4 demonstrate that increases in the open chromatin marks H3K4me3, H3K14ac, H3K18ac, H4K5ac and H4K8ac occur whether or not RNF20 is depleted, and are therefore RNF20-independent (Figure 33A-B) One histone mark (H3K27Ac) did appear RNF20-dependent, though in the context of so many RNF20-independent marks, its importance remains unclear. To confirm that the RNF20-dependence of ZSCAN4-mediated histone changes was functional, we performed a DNaseI digest and ChART-PCR on tet-inducible 012SCC

cells, with or without concomitant RNF20KD. Consistent with Western and ChIP results showing open chromatin mark increases regardless of RNF20, we found that the NANOG and OCT4 promoters were significantly more accessible in response to ZSCAN4, an effect that was also independent of RNF20 (Fig 33C). ZSCAN4 therefore induces open chromatin in an RNF20-independent manner and epigenetics therefore do not explain the RNF20-dependent transcription of pluripotency genes.

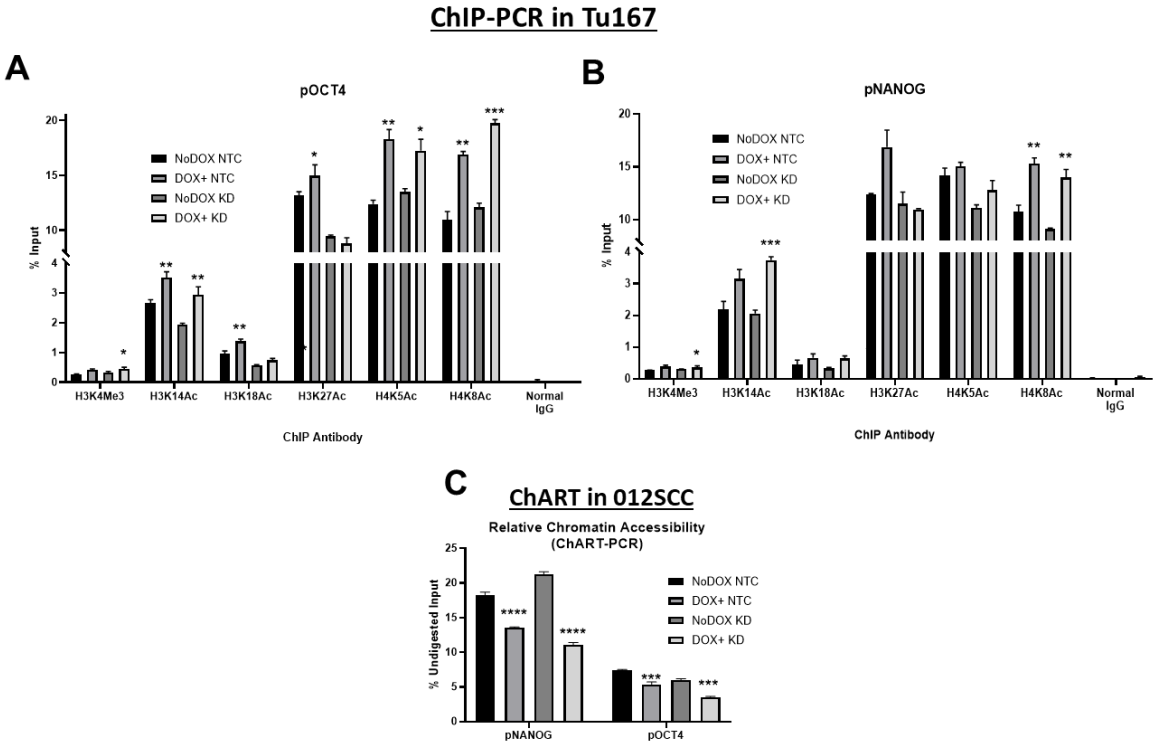

Figure 32: ZSCAN4 mediated induction of open chromatin is RNF20-independent.
ChIP-qPCR in Tu167 tet-ZSCAN4 cells transfected with either NTC or RNF20-KD siRNA for 24h and then treated with Doxycycline for an additional 48h. After ChIP using antibodies for H4K4me3, H3K14ac, H3K18ac, H3K27ac, H4K5ac, H4K8ac, or control rabbit IgG, ChIP'd DNA was used as template for RT-PCR using primers for the promoters of **A)** OCT4 or **B)** NANOG. Data presented as percentage of ChIP input from the same treatment condition. **C)** ChART-PCR in 012SCC tet-ZSCAN4 cells transfected with either NTC or RNF20-KD siRNA for 24h and then treated with Doxycycline for an additional 48h. After digestion, RT-PCR was performed on digested DNA using primers for promoters of NANOG and OCT4. Data shown as percentage of undigested input DNA from the same treatment condition. All data shown as mean ± S.E.M. Statistical significance was determined by one way ANOVA with Fisher's LSD for comparisons: *p<0.05, **p<0.01, ***p<0.001. (Unpublished data generated by Robert Brown)

3.2.J. RNF20 is necessary for RNA polymerase localization at pluripotency genes

A potential explanation for ZSCAN4's failure to increase pluripotency gene expression comes from the biology of RNF20 itself. RNF20 and its mono-ubiquitination of H2B have been reported to positively regulate general transcription(136-139). Various mechanisms for this have been reported, falling into two camps: independent facilitation of transcriptional accessibility via RNF20/H2B-Ub opening the chromatin for subsequent POLR2A transcription, or an actual interaction between RNF20 or H2BUb and POLR2A itself. In our cells, the former mechanism would mean POLR2A would still be present at target genes, but simply unable to transcribe when RNF20 is knocked down. In the latter mechanism of interaction/recruitment, loss of RNF20 should lead to a loss of POLR2A localization and a loss of transcription and gene expression. To determine how RNF20 may be affecting transcription, we performed ChIP in tet-inducible Tu167 cells with or without RNF20-KD. Our results indicate that RNF20 depletion led not just to reduced RNF20 at pluripotency gene promoters, but also to a substantial, significant reduction in POLR2A at these same promoters (Fig 34A-C). This indicates that RNF20 is not just required to effectively prime these genes for POLR2A transcription, but is actually needed for proper localization of POLR2A, either through recruitment or a yet to be identified mechanism. The consequence of this for ZSCAN4-induced gene expression is that ZSCAN4 can induce open chromatin marks and physically open pluripotency gene promoters, but in the absence of RNF20, POLR2A does not localize to that open chromatin and thus, more open chromatin does not translate to increased gene expression. Together, our data suggest that RNF20 is requisite for ZSCAN4-mediated increases in pluripotency gene expression.

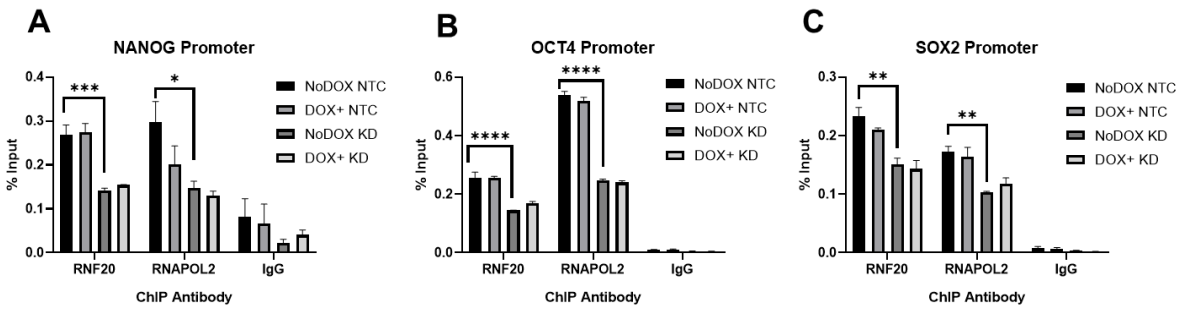

Figure 33: RNF20 is required for RNA Polymerase localization at pluripotency gene promoters.

ChIP-qPCR in Tu167 tet-ZSCAN4 cells transfected with either NTC or RNF20-KD siRNA for 24h and then treated with Doxycycline for an additional 48h. After ChIP using antibodies for RNF20, RNAPOL II, or control rabbit IgG, ChIP'd DNA was used as template for RT-PCR using primers for the promoters of **A)**Nanog, **B)**OCT4, **C)**SOX2. Data is shown as percentage of ChIP input from the same treatment condition. Statistical significance was determined by one way ANOVA with Fisher's LSD for relevant comparisons: *p<0.05, **p<0.01, ***p<0.001, ****p<0.0001. (Unpublished data generated by Robert Brown)

3.2.K. RNF20 is required for ZSCAN4-mediated telomere extension

Having established the relationship between ZSCAN4 and RNF20 on pluripotency gene expression and chromatin dynamics, we finally wanted to study a third aspect of the stem cell phenotype, the telomeres. We previously illustrated that ZSCAN4 induces telomere extension, both in T-MSCs (Figure 18) and in cancer cell lines (Figure 26A-B), appearing to do so by increasing the openness of telomeric chromatin (Figure 26 E). RNF20 and resultant H2B mono-ubiquitination have been reported to play a significant role at the telomeres, with loss of RNF20 or H2BUb leading to telomere shortening and increased H2BUb levels leading to telomere lengthening(140). Like ZSCAN4, RNF20/H2BUb appear to regulate telomere length by increasing telomere accessibility, whether to telomerase, homologous recombination machinery, or other ALT mechanisms(141). We thus hypothesized that, given its known importance at the telomere, RNF20 may be required by ZSCAN4 to exert its effect on telomere extension. To test this, using our tet-inducible Tu167 and 012SCC lines, we induced ZSCAN4 expression with or without

concomitant RNF20-KD. Our results in both cell lines show a significant increase in telomere length in response to ZSCAN4, but no ZSCAN4-induced extension occurred when RNF20 was depleted.(Figure 35A-B) We then assessed whether ZSCAN4's effects on telomeric chromatin may be likewise RNF20-dependent. We therefore performed a DNaseI digest and subsequent ChART-PCR to determine relative telomere accessibility. ZSCAN4 induction alone was able to cause a modest, yet significant increase in telomeric sensitivity to DNaseI, indicative of more open chromatin (Figure 35C). When RNF20 was knocked down, this ZSCAN4 mediated effect was lost. Notably, RNF20 knockdown led to a massive increase in telomere accessibility, possibly masking a more mild effect of ZSCAN4. This unexpected finding merits further study in the future as the consensus of reports is that RNF20 increases telomere accessibility. Overall our data reveal that ZSCAN4 requires RNF20 for its effects on telomere extension and telomeric chromatin accessibility.

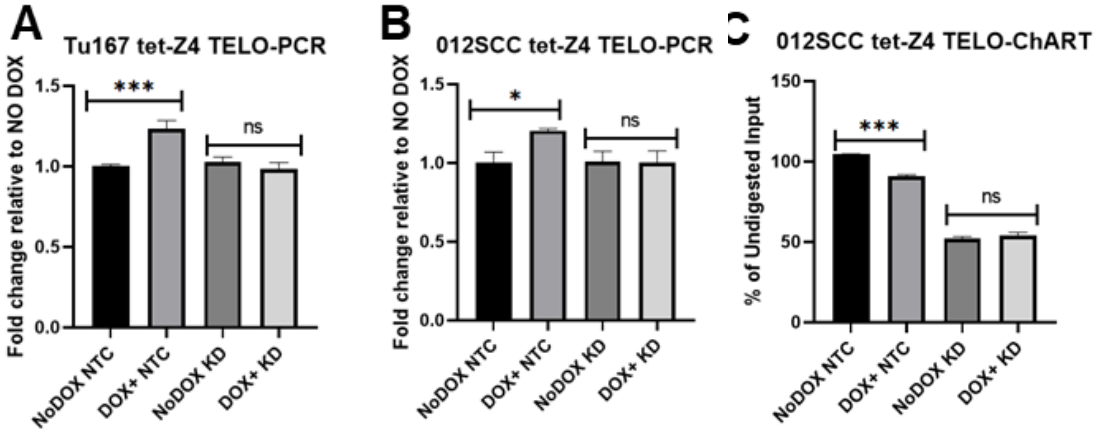

Figure 34: ZSCAN4 effects on telomere chromatin are RNF20-dependent.
A) Telomere-qPCR in Tu167 tet-ZSCAN4 cells and B) 012SCC tet-ZSCAN4 cells after either RNF20 siRNA or NTC for 72h and ZSCAN4 induction for 48h showing telomere signal normalized to the single copy gene RPLP0. Results presented as fold change relative to uninduced (NoDOX) cells. **C)** Telomere ChART-PCR in 012SCC tet-ZSCAN4 cells following DNaseI digest on native chromatin. Results presented as percentage of undigested input. All Data are shown as mean ± S.E.M Statistical significance determined by one way ANOVA with significant results followed by Fisher's LSD: *p<0.05, **p<0.01, ***p<0.001. (Unpublished data generated by Robert Brown)

3.3 Discussion

Cancer stem cells are drivers of cancer progression, recurrence and deaths in many different tumor types, including head and neck cancers (HNSCC). CSCs demonstrate increased tumorigenicity in both *in vitro* and *in vivo* research models, and expression of CSC-associated markers are prognostic for treatment response, metastatic potential, and mortality across cancer types. Thus, identifying regulators of the CSC phenotype is important, both as prognostic biomarkers and as targets for developing future cancer treatments.

As discussed, ZSCAN4 is aberrantly re-expressed in many human cancers and cancer cell lines. ZSCAN4's otherwise restricted expression to the early embryo posits it as a specific marker in human cancer. Similar to reports in murine ESCs and iPSCs, ZSCAN4 expression in cancers is restricted to a small percentage of cells, a characteristic suggestive of CSCs. Our findings in HNSCC cell lines demonstrate that ZSCAN4 expression in enriched for, but enriching for CSCs, with ZSCAN4 expression further associated with classical HNSCC CSC markers. ZSCAN4 expression therefore has potential as a biomarker for relative cancer stemness, at least in HNSCC.

Current cancer therapies are generally efficacious against bulk tumor cells, but less so against CSCs, making the targeting of mediators of the CSC phenotype key for reducing tumor recurrence, metastasis and thereby cancer deaths. Our findings that ZSCAN4 is not just associated with the cancer stem cell phenotype, but actually drives it by inducing open chromatin, pluripotency gene expression and telomere elongation, identify it as a potential drug target. The research into targeting of CSCs has focused primarily on cancer stem cell surface markers like CD44, CD133 or EpCAM. These markers, however, are not specific

to CSCs, being shared by many types of non-cancer stem cells as well. Thus, by depleting these populations with monoclonal antibodies, one's normal stem cell populations are also depleted, resulting in potential side effects, particularly in the long term. Additionally, many cell surface markers may be dispensable to the CSC phenotype, allowing CSCs that do not express these markers to promote cancer progression instead(142). Our results position ZSCAN4 as an upstream regulator of many cancer stem cell characteristics, suggesting its inhibition may be more efficacious than targeting downstream pathways. Indeed our results show ZSCAN4 depletion leads to compromised CSC frequency in HNSCC lines, both *in vitro* (Figure 5) and *in vivo* (97). ZSCAN4 as a drug target is beset with some drawbacks. ZSCAN4's localization is intracellular (nuclear) making it inaccessible to monoclonal antibodies. Further, ZSCAN4's structure is not solved, nor has its effect on the chromatin been fully elucidated. Thus, rational drug design targeting ZSCAN4 is difficult. Finding factors necessary for ZSCAN4 to exert its effects is thus a promising avenue to inhibit ZSCAN4 indirectly.

An interaction between ZSCAN4 and the E3 ubiquitin ligase RNF20 was previously reported by our lab(124). Here, RNF20 negatively regulated ZSCAN4 levels via polyubiquitylation and degradation. ZSCAN4 and RNF20 were shown to co-localize in the nucleus, as well as co-immunoprecipitate.(124) Recent unpublished work in our lab has revealed that ZSCAN4 and RNF20 directly interact *in vitro*, suggesting a direct binding mechanism. We thus explored the relationship between these two proteins, thinking that their protein-protein interaction may be important for ZSCAN4's effects. By way of ZSCAN4 depletion, we found that RNF20 was still able to perform global H2B mono-ubiquitylation, suggesting RNF20 does not require ZSCAN4 for this effect. This makes

sense as, unlike ZSCAN4, RNF20 is a widely expressed protein responsible for maintenance ubiquitylations throughout the genome and the loss of a rarely expressed protein like ZSCAN4 may not affect this function. However, ZSCAN4 depletion did lead to reduced H2B mono-ubiquitylation at pluripotency genes, known genomic targets of ZSCAN4 regulation. Given the interaction between ZSCAN4 and RNF20 we first thought ZSCAN4, when expressed, may be recruiting RNF20 to pluripotency genes. While this idea was supported by our results in short-term ZSCAN4 depletion systems where both RNF20 and H2BUb levels were reduced at pluripotency genes, long-term ZSCAN4 depletion (clonal knockout lines) showed RNF20 levels were actually higher at these loci, despite still showing reduced H2BUb. Thus direct recruitment by ZSCAN4 could play a role in RNF20 localization and H2BUb at pluripotency genes early on, but even when RNF20 levels are adequate, its function is impaired. This suggests RNF20 may require some effect (likely epigenetic) of ZSCAN4 as a pre-requisite for its ubiquitylation activities on H2B.

Conversely, we found that ZSCAN4's effects on the chromatin at pluripotency genes are RNF20-independent. Even when RNF20 is depleted, induction of ZSCAN4 increases both global histone acetylation and histone acetylation at pluripotency genes, suggesting this effect is independent of and potentially upstream to H2BUb. However, our finding that ZSCAN4's enhancement of pluripotency gene expression requires RNF20 suggests H2BUb is still required for ZSCAN4-mediated gene expression. RNF20 itself has been reported to recruit RNA polymerase II during gene transcription(143). Our results show that when RNF20 is depleted, RNA polymerase localization at pluripotency genes is also reduced. This reduction is present whether or not ZSCAN4 is overexpressed,

suggesting RNA Polymerase II recruitment is independent of ZSCAN4 or ZSCAN4-induced histone acetylation. Taken together, this data suggests that RNF20 must be present at pluripotency genes for ZSCAN4's effects on transcription.

Our understanding of the interplay between RNF20 and ZSCAN4's effects on the chromatin of and expression of pluripotency genes may allow for the development of therapeutic targets. RNF20, due to its multiple roles in the cell and near ubiquitous expression, is not an ideal target for inhibition. Indeed knockout of RNF20 has been shown to be embryonic lethal in mice and RNF20 knockout in cell lines has been reported to be deleterious(144). As both RNF20 mediated H2B ubiquitylation and ZSCAN4-mediated histone acetylation appear necessary for pluripotency gene expression, countering their epigenetic effects may be beneficial. Either ablating ZSCAN4-induced histone acetylation by promoting HDAC activity, or ablating RNF20-induced histone ubiquitylation by promoting DUB activity, could blunt their CSC-promoting effects on gene expression.

In total, our work reveals ZSCAN4 as a driver of the CSC phenotype and characterizes its functional relationship with its previously reported interactor RNF20, with our mechanistic understanding paving the way for potential therapeutic targeting.

3.4 Materials and Methods

Cancer Cell Line Culture

Head and neck squamous cell carcinoma (HNSCC) cell lines TU167 were obtained from the University of Texas MD Anderson Cancer Center (Houston, TX, USA). The cells used in our laboratory were originally generated by Dr. Gary Clayman and were reported to be free of cross contamination (145). The cell line 012SCC was donated by Bert O'Malley from the University of Pennsylvania School of Medicine (Philadelphia, PA, USA). U2OS,

SKBR-3, and SW480 cell lines were obtained from ATCC. All cell lines were routinely tested for mycoplasma or treated with PlasmoCure (InvivoGen) and tested as negative. All tumor cell lines were cultured in complete DMEM medium (Invitrogen) supplemented with 10% fetal bovine serum (Novus), 2 mM GlutaMAX, penicillin (100 U/mL), streptomycin (100 μg/mL).

Generation of mCherry promoter-reporter lines

The genomic region containing the ZSCAN4 promoter (2.5 Kb upstream of transcriptional start codon, and 299 base pairs downstream) was cloned into a lentiviral vector (pEZX-LvPM02; GeneCopoeia) in which the mCherry reporter gene is downstream to the reported ZSCAN4 promoter, with the puromycin resistance gene under control of the constitutive promoter SV40. Tu167 and 012SCC cell lines were transduced with pZSCAN4-mCherry lentivirus and selected with puromycin.

Generation of tetracycline inducible ZSCAN4 lines

Cancer cell lines were transduced with a tetracycline inducible ZSCAN4 expression vector as previously described(124). Transduced lines were selected for 10 days with 1ug/mL Puromycin and expanded. Tet-inducible cells were cultured as above, albeit in media containing tetracycline-free FBS (Novus).

Generation of ZSCAN4 shRNA knockdown lines

ZSCAN4 shRNAs vectors as previously described (97) were stably transfected into Tu167 or 012SCC cells by Effectene (QIAGEN) according to the manufacturer's protocol. As controls, isogenic cell lines were also generated expressing a non-targeting control shRNA (NTC-shRNA). Cell lines were selected with 1 μg/ml Puromycin (ThermoFisher Scientific). Knockdown was confirmed by immunostaining and by qPCR.

Generation of CRISPR-Cas9 ZSCAN4 knockout lines

In Collaboration with the CRISPR Services Core at University of Maryland Baltimore's Center for Innovative Biomedical Resources (CIBR) and the lab of Dr. Tami Kingsbury, clonal CRISPR-Cas9 knockout lines were generated in Tu167 and U2OS cell lines. For both lines, cells were nucleofected with Cas9 mRNA and sgRNA targeting Exon 3 of ZSCAN4. Bulk cell populations were screened for successful ZSCAN4 gene edits by Sanger sequencing and plated as single cells for generation of clones. Ater expansion, clonal lines were tested for successful gene edits by Sanger sequencing and subsequent ICE analysis. Successful knockout of ZSCAN4 was further confirmed via Western Blot. After clonal expansion, cells were expanded and used for experiments between passages 3 and 6. For inducible ZSCAN4 knockout cells, U2OS cells were transduced with lentivirus containing tetracycline-inducible Cas9 expression vector with sgRNA targeting Exon 3 of ZSCAN4. Cells were selected with puromycin. After inducing with Doxycycline for 72h, cells were evaluated for gene edits by Sanger sequencing and ICE analysis. The inducible Cas9 vector without an sgRNA (Empty) was used as control.

RNA extraction and RT-qPCR

Total RNA was extracted from cells by RNAEasy Kit (Qiagen) with 1 µg of total RNA reverse transcribed by Superscript III (Invitrogen) following the manufacturer's protocols. Then, 10 ng cDNA was used per well in triplicates using Power-Up SYBR green PCR master mix (Applied Biosystems) following the manufacturer's protocol. Real time PCR was performed via a Quantstudio 3 system (Applied Biosystems)). Fold induction was calculated by the ddCt method. Gene expression was normalized to the housekeeping gene RPLP0. Primers are listed in Table 4.

Genomic DNA extraction and Telomere PCR

For telomere length analysis, treated cells were collected, genomic DNA was extracted using a Wizard® Genomic DNA Purification Kit (Promega) and concentration determined via Nanodrop. 10ng of DNA from each condition was used as template for Telomere-PCR as described by Cawthon(125). Telomere signal was normalized to that of the single copy gene RPLP0. Primers are listed in Table 4.

Immunofluorescence staining

Cells were fixed in 4% Paraformaldehyde in PBS for 15 minutes, washed and then blocked/permeabilized in 5% FBS/1.5% BSA and 0.2% Tween-20 in PBS for 30 minutes. Primary antibodies were diluted in blocking buffer and incubated overnight at 4 degrees C. The following day, cells were washed, and incubated with secondary antibodies for 1h in PBS. Cells were then washed, incubated with 1ug/mL DAPI (Fisher Scientific) for 10 minutes, washed again, then mounted with Vectashield Antifade Mounting media (Vector Labs). Stainings were imaged on a DMi8b fluorescent microscope (Leica). All antibodies listed in Table 3.

Chromatin Immunoprecipitation (ChIP)

Chromatin Immunoprecipitations were performed using a SimpleChIP® Enzymatic Chromatin IP Kit (Cell signaling #9003) according to manufacturer's protocol. Antibodies are listed in table 3. Resultant DNA was used as RT-PCR template, and run using primers for pluripotency gene bodies and promoters (Table 4). Data was calculated as a percentage of ChIP Input DNA.

Chromatin Accessibility by RT-PCR (ChART-PCR)

~5 million cell nuclei were lysed in a hypotonic chromatin lysis buffer (10mM Tris HCl 7.5pH, 5mM MgCl2, 1mM CaCl2, 10mM KCl, 300mM sucrose, 0.1% Triton-X) and nuclei isolated. Nuclei were re-suspended in DNase digestion buffer (10mM Tris HCl 7.5pH, 5mM MgCl2, 1mM CaCl2, 10mM KCl, 300mM sucrose) and volume divided evenly between tubes, with each tube receiving either various amounts (1Unit, 2Unit, or 4Units) of DNaseI enzyme (Promega) or no enzyme for the undigested control. Digestion was halted by the addition of 0.05M EDTA and heating to 70 degrees C for 15 minutes. Digested DNA or undigested control DNA was then extracted using a Wizard Genomic DNA extraction kit (Promega) and concentration determined by Nanodrop One (ThermoFisher). 50ng of gDNA was used as template for RT-PCR, with digested samples calculated as a percentage of their undigested control. Primers are listed in Table 4.

In vitro Extreme Limiting Dilution Assay (ELDA)

Cells were dissociated with 0.25% Trypsin into single cell solution and serial dilutions made, such that each well of a 96-well plate received 4000, 2000, 1000, 500, 250, 125, 62.5, 31.25, 15.625, 7.8125, or 3.90625 cells each. Each dilution was plated in octuplicate. Cells were cultured for up to 10 days in a serum-free tumorsphere media consisting of DMEM/F12, 1X B-27 Supplement, 20ng/mL bFGF, 20ng/mL EGF, and 50ug/mL Ampicillin. Individual wells were then assessed for the presence or absence of 3D spheres >50um.. Results were then analyzed with L-calc software (STEMCELL technologies) to determine the CSC frequencies in each treatment condition and to compare frequencies between conditions via Chi-squared test.

Protein Extraction and Western Blotting

Cells were lysed in Cytoskeleton buffer (10 mM PIPES, 300 mM sucrose, 100 mM NaCl, 3 mM MgCl2, 1 mM EGTA, and 0.5% Triton X100), and the nuclear fraction was isolated. Next, pellets were lysed in urea solution (8 M Urea in 0.01 Tris pH 8 + 0.1 M NaH2PO4) and sonicated. Samples were electrophoresed in polyacrylamide gels. PVDF membranes were blocked with 5% nonfat milk or Superblock (Thermo Fisher Scientific) for 1 h, then incubated overnight at 4 °C with the indicated primary antibodies in blocking solution (Supplementary Table 2). Membranes were washed and incubated with secondary antibodies (1:5000) for 1 h. Secondary antibodies were visualized by ECL Chemiluminescence (ThermoFisher Scientific) by developing on film. Primary antibodies listed in table 3.

Statistical Analysis

Data are shown as the mean±S.E.M of multiple independent experiments with multiple donors in biological replicates. Student's t-test or one-way ANOVAs were performed for statistical analyses. A significant result in ANOVA was followed by a Fisher LSD post-hoc test. In all statistical analyses, $p<0.05$ was considered statistically significant. Statistical analyses and graph generation were performed with GraphPad Prism 7.03 software.

Table 3-Antibody list

Antibody	Host species	Dilution	Source	Application
H3K14Ac	rabbit	1:50/1:1000	CST	ChIP/Western
H3K18Ac	rabbit	1:50/1:1000	CST	ChIP/Western
H3K27Ac	rabbit	1:50/1:1000	CST	ChIP
H4K5Ac	rabbit	1:50/1:1000	CST	ChIP/Western
H4K8Ac	rabbit	1:50/1:1000	CST	ChIP/Western
H3K4me3	rabbit	1:50/1:1000	CST	ChIP/Western
Normal rabbit IgG	rabbit	1:50/1:1000	CST	ChIP/Western
H2B	rabbit	1:1000	CST	Western
H2B-Ub	rabbit	1:50/1:1000	CST	ChIP/Western
RNF20	rabbit	1:50/1:1000	CST	ChIP/Western
POLR2A	rabbit	1:50/1:1000	CST	ChIP/Western
OCT4	mouse	1:100	BD	IF
KLF4	rabbit	1:200	CST	IF
CD44 (eFluor450 conjugate)	mouse	1:100	eBiosciences	Flow
ALDH1A1 (Alexa647 conjugate)	recombinant	1:50	Abcam	Flow

Table 4-Primers Used

	Forward (5'-3')	Reverse (5'-3')
SOX2	CAAGGAGAGGCTTCTTGCTGA	CACAGAGATGGTTCGCCAGT
RPLP0	CAGCAAGTGGGAAGGTGTAATCC	CCCATTCTATCATCAACGGGT
OCT4	TCT TCA GGA GAT ATG CAA AGC	ATC CTC TCG TTG TGC ATA GT
NANOG	AGC TAC AAA CAG GTG AAG AC	TAG GAA GAG TAA AGG CTG GG
pNANOG	GAA AGA CAT GAC AAA TCA CCA GAC	CAA CTA GCT CCA TTT TCC TCT TTC
pOCT4	TTA CTT AAG TCG ACA GAG GTC AGC	TGG TCT AGT GCT TGA TTC TGT TTG
pSOX2	CGG TTG AAT GAA GAC AGT CTA GTG	CGA CTA GAA GTT AGG AGA CCC AAA
hTELO	GGTTTTTGAGGGTGAGGGTGAGGGTGAGG GTGAGGGT	TCCCGACTATCCCTATCCCTATCCCTATCC CTATCCCTA
ZSCAN4	ATCCACCTGCCTTAGTCCAC	TCGAAGAACTGTTCCAGCCA
BMI1	GGC TCG CAT TCA TTT TCT GCT	GAA CAA TAC ACG TTT TAC AGA AGG A
ABCG2	GCC ACA GAG ATC ATA GAG CCT	TCA CCC CCG GAA AGT TGA TG
MDR1	GGG AGC TTA ACA CCC GAC TT	CAG CAG CTG ACA GTC CAA GA

Chapter 4: Conclusions and Future Directions

4.1 Stem Cell Potency and therapeutic use of T-MSCs

Several types of MSCs have been reported to differentiate to the neuronal lineage, neurogenic potency being a requirement for their use in cell replacement therapies. Our T-MSCs were previously reported to have superior extraction efficiency over other sources of MSCs, along with equivalent or superior proliferative capacity and differentiation capacity to mesenchymal lineages, compared to BM-MSCs(18). Thus, even in an undifferentiated state, T-MSC's are an excellent candidate for cell therapies or for cell replacement therapies involving differentiation to mesenchymal cell types. Our results characterizing the neurogenic potential of T-MSCs support their use in replacement therapies of CNS disease, in particular.

4.2 Therapeutic use of T-MSCs in Neurodegenerative Disease

For cell replacement therapies in neurodegenerative disease, the transplanted cells must be able to differentiate to the type of cells requiring replacement. Complete neuronal differentiation includes loss of their original MSC phenotype, cessation of proliferation, expression of mature neuronal markers, and expression of neurotransmitters. Our results indicate that T-MSCs, upon differentiation in our protocol, results in post-mitotic, neuron-like cells with neurotransmitter expression. This recommends them as an excellent stem cell source for replacement therapies in neurodegenerative disease. To further characterize these cells, future work will be required to direct their differentiation to specific neuronal sub-lineages, as well as to assess secretion of expressed neurotransmitters as well as electrophysiologic maturity, the gold standard in proving functionality(146).

4.3 Using ZSCAN4 to enhance cell stemness

While T-MSCs possess advantages over other MSC sources, their use is still constrained by issues of cellular aging, either physiologic aging with older donors or in vitro aging with cell culture. ZSCAN4, consistent with its established role in supporting stem cell potency in murine pluripotent stem cells, enhances the stem cell potency of T-MSCs, bypassing an otherwise critical barrier to the widespread therapeutic use of these cells. Our evaluation of several aspects of stem cell potency (epigenetics, pluripotency gene expression and telomere length) with ZSCAN4 induction in aged T-MSCs gives further insight into the mechanism underlying its conserved effects across species and across cell types. Future work will more completely assess ZSCAN4's enhancement of neurogenic differentiation in T-MSCs, as well as determine whether ZSCAN4 improves differentiation to other lineages. Future mechanistic analysis will hopefully elucidate the exact mechanism by which ZSCAN4 exerts its effects, offering a target for pharmaceutical intervention, either activating ZSCAN4 to increase stem cell potency or inhibiting it to decrease potency.

4.4 ZSCAN4 as a cancer stem cell marker and target

CSCs are drivers of cancer progression, metastasis, drug resistance and thereby cancer deaths. The use of CSC specific biomarkers to identify CSCs in tumor samples can help to guide the intensity and type of treatment regimen used, as well as provide a prognostic marker for likelihood of progression. Current CSC markers are neither entirely specific to cancer cells, nor expressed in all CSCs. Thus, treatments based around them can be expected to adversely impact a patient's normal stem cell reserves, as well as not eliminate all CSCs. ZSCAN4, due to its transient expression is even more rarely expressed than

other CSC markers. This characteristic makes it a more specific potential biomarker for bona fide CSCs than commonly used markers (CD44, CD133, etc.). Our findings that ZSCAN4 is a driver of the CSC phenotype, inducing open chromatin, pluripotency gene expression, telomere elongation and *in vitro* stemness, suggest its expression is integral to CSCs, and is therefore a therapeutic target. Future work on determining the exact mechanism by which ZSCAN4 exerts its effects may give insight into strategies to inhibit its function in cancer, thereby impairing CSCs. Together with traditional bulk tumor chemoradiation therapies, such a strategy should lead to increased treatment response, decreased relapse rates and increased survival in HNSCC. The fact that ZSCAN4 is expressed in, and some of its effects appear conserved in, disparate cancer lines, suggests ZSCAN4 targeting could be efficacious in reducing cancer stemness in a variety of cancers, though more evidence will be needed in each specific type of cancer.

4.5 Co-operative effects of RNF20 and ZSCAN4

Aside from targeting ZSCAN4 directly, it could be indirectly inhibited identifying and blocking necessary co-factors needed for its effects. One potential co-factor is RNF20, previously reported to interact with and negatively regulate ZSCAN4 levels. Both ZSCAN4 and RNF20 appear to independently alter the epigenetics of the cell, with ZSCAN4 facilitating histone acetylations and RNF20 causing histone mono-ubiquitylation. Our work to elucidate the relationship between the two proteins suggests that ZSCAN4 does not require RNF20 or H2BUb for its effects on histone acetylation globally or at pluripotency gene promoters. RNF20, while not requiring ZSCAN4 or ZSCAN4-mediated acetylation for its effect on global H2B-Ub, does appear to require

them for H2B-Ub at pluripotency genes. Given the known interaction between RNF20 and ZSCAN4, and our results in short term ZSCAN4 depletion, ZSCAN4 may be responsible for recruitment of RNF20 to pluripotency genes, where it exerts its effect on H2B-Ub. In longer term ZSCAN4-depletion, however, RNF20 is able to localize to pluripotency genes, but H2B-Ub levels remain down, as does gene expression. While not mutually exclusive, our results suggest that it is the lack of ZSCAN4's function (histone acetylation at pluripotency genes) that impairs H2BUb levels, not necessarily the lack of ZSCAN4 as a recruitment factor for RNF20. Conversely, RNF20 is necessary for ZSCAN4-induced pluripotency gene expression, appearing to do so by recruiting RNA Polymerase II. Thus, both ZSCAN4 and RNF20 are necessary for pluripotency gene expression, a key factor in the cancer stem cell phenotype. Telomere length, another important aspect of the cancer stem cell phenotype, appears to be similarly regulated. This knowledge can be used to inform future therapeutic approaches to reduce cancer stemness.

4.6 Targeting RNF20-ZSCAN4 in cancers

ZSCAN4 alone is an excellent therapeutic target in cancer. Its negligible expression in post-embryonic cells portend a low side effect profile with systemic inhibition. However, as it is localized to the nucleus, monoclonal antibodies are unlikely to be helpful. RNF20 on the other hand has a solved structure and known enzymatic activity, but its ubiquitous expression across cell types and multiple functions in the cell augur a significant side effect profile. Indeed, RNF20 knockout models have shown embryonic lethality and deleterious effects in cell culture(144). If ZSCAN4 recruits RNF20 to pluripotency genes, then their direct interaction can be targeted and inhibited. Our data showing RNF20 can still localize,

but not function, in the absence of ZSCAN4 suggests it is the lack of ZSCAN4-induced histone acetylation that impairs RNF20 function. All is not lost, however, as each protein's chromatin effects offer potential treatment targets. As ZSCAN4's effects on histone acetylation appear to be responsible for its effects on gene expression and telomere elongation, blocking or reversing these effects with epigenetic therapies, such as small molecule histone acetyltransferase (HAT) inhibitors or histone deacetylase (HDAC) activators. Without ZSCAN4-based histone acetylation, pluripotency gene expression would likely be hindered, as would cancer stemness. One other potential avenue would be to target ZSCAN4 by increasing RNF20 levels or activity. Previous work found RNF20 negatively regulates ZSCAN4 levels, significantly reducing its protein half-life(124). By clearing ZSCAN4, induced high levels of RNF20 could prevent it from exerting its effects on cancer stemness. In total, the mechanistic insights into the ZSCAN4-RNF20 relationship gained from this work, can help to guide future development of therapeutics to inhibit cancer stemness.

Overall, means to alter stem cell potency are of great importance to the fields of both regenerative medicine and oncology. In this work we have identified ZSCAN4 as one such factor and demonstrated its use as a tool to increase the stem cell potency of tonsil-derived MSCs for future neuro-regenerative applications. Conversely, we defined ZSCAN4 as a mediator of cancer stemness in HNSCC (and potentially other cancers) which posits it as a target to impair CSCs. Mechanistic insights into the relationship between ZSCAN4 and RNF20 further our understanding of ZSCAN4 biology, guiding the development of future therapeutics.

References

1. Zakrzewski W, Dobrzyński M, Szymonowicz M, Rybak Z. Stem cells: past, present, and future. Stem Cell Res Ther. 2019;10(1):68. Epub 20190226. doi: 10.1186/s13287-019-1165-5. PubMed PMID: 30808416; PubMed Central PMCID: PMC6390367.

2. Niwa H, Burdon T, Chambers I, Smith A. Self-renewal of pluripotent embryonic stem cells is mediated via activation of STAT3. Genes Dev. 1998;12(13):2048-60. doi: 10.1101/gad.12.13.2048. PubMed PMID: 9649508; PubMed Central PMCID: PMC316954.

3. Itskovitz-Eldor J, Schuldiner M, Karsenti D, Eden A, Yanuka O, Amit M, et al. Differentiation of human embryonic stem cells into embryoid bodies compromising the three embryonic germ layers. Mol Med. 2000;6(2):88-95. PubMed PMID: 10859025; PubMed Central PMCID: PMC1949933.

4. Chambers SM, Fasano CA, Papapetrou EP, Tomishima M, Sadelain M, Studer L. Highly efficient neural conversion of human ES and iPS cells by dual inhibition of SMAD signaling. Nat Biotechnol. 2009;27(3):275-80. Epub 20090301. doi: 10.1038/nbt.1529. PubMed PMID: 19252484; PubMed Central PMCID: PMC2756723.

5. Mummery CL, Zhang J, Ng ES, Elliott DA, Elefanty AG, Kamp TJ. Differentiation of human embryonic stem cells and induced pluripotent stem cells to cardiomyocytes: a methods overview. Circ Res. 2012;111(3):344-58. doi: 10.1161/circresaha.110.227512. PubMed PMID: 22821908; PubMed Central PMCID: PMC3578601.

6. Lim WF, Inoue-Yokoo T, Tan KS, Lai MI, Sugiyama D. Hematopoietic cell differentiation from embryonic and induced pluripotent stem cells. Stem Cell Res Ther. 2013;4(3):71. Epub 20130618. doi: 10.1186/scrt222. PubMed PMID: 23796405; PubMed Central PMCID: PMC3706875.

7. Barker N, van de Wetering M, Clevers H. The intestinal stem cell. Genes Dev. 2008;22(14):1856-64. doi: 10.1101/gad.1674008. PubMed PMID: 18628392; PubMed Central PMCID: PMC2735277.

8. Pittenger MF, Discher DE, Péault BM, Phinney DG, Hare JM, Caplan AI. Mesenchymal stem cell perspective: cell biology to clinical progress. NPJ Regen Med. 2019;4:22. Epub 20191202. doi: 10.1038/s41536-019-0083-6. PubMed PMID: 31815001; PubMed Central PMCID: PMC6889290.

9. Sheng G. The developmental basis of mesenchymal stem/stromal cells (MSCs). BMC Dev Biol. 2015;15:44. Epub 20151120. doi: 10.1186/s12861-015-0094-5. PubMed PMID: 26589542; PubMed Central PMCID: PMC4654913.

10. Pittenger MF, Mackay AM, Beck SC, Jaiswal RK, Douglas R, Mosca JD, et al. Multilineage potential of adult human mesenchymal stem cells. Science. 1999;284(5411):143-7. doi: 10.1126/science.284.5411.143. PubMed PMID: 10102814.

11. Oedayrajsingh-Varma MJ, van Ham SM, Knippenberg M, Helder MN, Klein-Nulend J, Schouten TE, et al. Adipose tissue-derived mesenchymal stem cell yield and growth characteristics are affected by the tissue-harvesting procedure. Cytotherapy. 2006;8(2):166-77. doi: 10.1080/14653240600621125. PubMed PMID: 16698690.

12. Ke F, Zhang L, Liu Z, Liu J, Yan S, Xu Z, et al. Autocrine interleukin-6 drives skin-derived mesenchymal stem cell trafficking via regulating voltage-gated Ca(2+) channels. Stem Cells. 2014;32(10):2799-810. doi: 10.1002/stem.1763. PubMed PMID: 24906203.

13. Testa S, Riera CS, Fornetti E, Riccio F, Fuoco C, Bernardini S, et al. Skeletal Muscle-Derived Human Mesenchymal Stem Cells: Influence of Different Culture Conditions on Proliferative and Myogenic Capabilities. Front Physiol. 2020;11:553198. Epub 20200916. doi: 10.3389/fphys.2020.553198. PubMed PMID: 33041857; PubMed Central PMCID: PMC7526461.

14. Huang GT, Gronthos S, Shi S. Mesenchymal stem cells derived from dental tissues vs. those from other sources: their biology and role in regenerative medicine. J Dent Res. 2009;88(9):792-806. doi: 10.1177/0022034509340867. PubMed PMID: 19767575; PubMed Central PMCID: PMC2830488.

15. Wouters G, Grossi S, Mesoraca A, Bizzoco D, Mobili L, Cignini P, et al. Isolation of amniotic fluid-derived mesenchymal stem cells. J Prenat Med. 2007;1(3):39-40. PubMed PMID: 22470826; PubMed Central PMCID: PMC3309337.

16. Ishige I, Nagamura-Inoue T, Honda MJ, Harnprasopwat R, Kido M, Sugimoto M, et al. Comparison of mesenchymal stem cells derived from arterial, venous, and Wharton's jelly explants of human umbilical cord. Int J Hematol. 2009;90(2):261-9. Epub 20090806. doi: 10.1007/s12185-009-0377-3. PubMed PMID: 19657615.

17. Kim YH, Park M, Cho KA, Kim BK, Ryu JH, Woo SY, et al. Tonsil-Derived Mesenchymal Stem Cells Promote Bone Mineralization and Reduce Marrow and Visceral Adiposity in a Mouse Model of Senile Osteoporosis. Stem Cells Dev. 2016;25(15):1161-71. Epub 20160627. doi: 10.1089/scd.2016.0063. PubMed PMID: 27245267.

18. Khatri R, Arad M, Ortlip T, Portney BA, Meltzer WA, Diaconu S, et al. Harvesting multipotent progenitor cells from a small sample of tonsillar biopsy for clinical applications. Stem Cell Res Ther. 2017;8(1):174. Epub 20170727. doi: 10.1186/s13287-017-0619-x. PubMed PMID: 28750664; PubMed Central PMCID: PMC5531028.

19. Chen Z, Kuang Q, Lao XJ, Yang J, Huang W, Zhou D. Differentiation of UC-MSCs into hepatocyte-like cells in partially hepatectomized model rats. Exp Ther Med.

2016;12(3):1775-9. Epub 20160726. doi: 10.3892/etm.2016.3543. PubMed PMID: 27602090; PubMed Central PMCID: PMC4998204.

20. Zanini C, Bruno S, Mandili G, Baci D, Cerutti F, Cenacchi G, et al. Differentiation of mesenchymal stem cells derived from pancreatic islets and bone marrow into islet-like cell phenotype. PLoS One. 2011;6(12):e28175. Epub 20111216. doi: 10.1371/journal.pone.0028175. PubMed PMID: 22194812; PubMed Central PMCID: PMC3241623.

21. Scintu F, Reali C, Pillai R, Badiali M, Sanna MA, Argiolu F, et al. Differentiation of human bone marrow stem cells into cells with a neural phenotype: diverse effects of two specific treatments. BMC Neurosci. 2006;7:14. Epub 20060216. doi: 10.1186/1471-2202-7-14. PubMed PMID: 16483379; PubMed Central PMCID: PMC1397850.

22. Marmorstein R, Zhou MM. Writers and readers of histone acetylation: structure, mechanism, and inhibition. Cold Spring Harb Perspect Biol. 2014;6(7):a018762. Epub 20140701. doi: 10.1101/cshperspect.a018762. PubMed PMID: 24984779; PubMed Central PMCID: PMC4067988.

23. Bannister AJ, Kouzarides T. Regulation of chromatin by histone modifications. Cell Res. 2011;21(3):381-95. Epub 20110215. doi: 10.1038/cr.2011.22. PubMed PMID: 21321607; PubMed Central PMCID: PMC3193420.

24. Miller JL, Grant PA. The role of DNA methylation and histone modifications in transcriptional regulation in humans. Subcell Biochem. 2013;61:289-317. doi: 10.1007/978-94-007-4525-4_13. PubMed PMID: 23150256; PubMed Central PMCID: PMC6611551.

25. Greenberg MVC, Bourc'his D. The diverse roles of DNA methylation in mammalian development and disease. Nat Rev Mol Cell Biol. 2019;20(10):590-607. Epub 20190809. doi: 10.1038/s41580-019-0159-6. PubMed PMID: 31399642.

26. Fournier A, Sasai N, Nakao M, Defossez PA. The role of methyl-binding proteins in chromatin organization and epigenome maintenance. Brief Funct Genomics. 2012;11(3):251-64. Epub 20111219. doi: 10.1093/bfgp/elr040. PubMed PMID: 22184333.

27. Ugarte F, Sousae R, Cinquin B, Martin EW, Krietsch J, Sanchez G, et al. Progressive Chromatin Condensation and H3K9 Methylation Regulate the Differentiation of Embryonic and Hematopoietic Stem Cells. Stem Cell Reports. 2015;5(5):728-40. Epub 20151017. doi: 10.1016/j.stemcr.2015.09.009. PubMed PMID: 26489895; PubMed Central PMCID: PMC4649257.

28. May D, Yun S, Gonzalez DG, Park S, Chen Y, Lathrop E, et al. Live imaging reveals chromatin compaction transitions and dynamic transcriptional bursting during stem cell differentiation in vivo. Elife. 2023;12. Epub 20230307. doi: 10.7554/eLife.83444. PubMed PMID: 36880644; PubMed Central PMCID: PMC10027315.

29. Sun L, Yu R, Dang W. Chromatin Architectural Changes during Cellular Senescence and Aging. Genes (Basel). 2018;9(4). Epub 20180416. doi: 10.3390/genes9040211. PubMed PMID: 29659513; PubMed Central PMCID: PMC5924553.

30. Hattori N, Imao Y, Nishino K, Ohgane J, Yagi S, Tanaka S, et al. Epigenetic regulation of Nanog gene in embryonic stem and trophoblast stem cells. Genes Cells. 2007;12(3):387-96. doi: 10.1111/j.1365-2443.2007.01058.x. PubMed PMID: 17352742.

31. Hattori N, Nishino K, Ko YG, Ohgane J, Tanaka S, Shiota K. Epigenetic control of mouse Oct-4 gene expression in embryonic stem cells and trophoblast stem cells. J Biol Chem. 2004;279(17):17063-9. Epub 20040204. doi: 10.1074/jbc.M309002200. PubMed PMID: 14761969.

32. Song Y, van den Berg PR, Markoulaki S, Soldner F, Dall'Agnese A, Henninger JE, et al. Dynamic Enhancer DNA Methylation as Basis for Transcriptional and Cellular Heterogeneity of ESCs. Mol Cell. 2019;75(5):905-20.e6. Epub 20190815. doi: 10.1016/j.molcel.2019.06.045. PubMed PMID: 31422875; PubMed Central PMCID: PMC6731151.

33. Friman ET, Deluz C, Meireles-Filho AC, Govindan S, Gardeux V, Deplancke B, et al. Dynamic regulation of chromatin accessibility by pluripotency transcription factors across the cell cycle. Elife. 2019;8. Epub 20191203. doi: 10.7554/eLife.50087. PubMed PMID: 31794382; PubMed Central PMCID: PMC6890464.

34. Jezek M, Green EM. Histone Modifications and the Maintenance of Telomere Integrity. Cells. 2019;8(2). Epub 20190225. doi: 10.3390/cells8020199. PubMed PMID: 30823596; PubMed Central PMCID: PMC6407025.

35. Li J, Chen B. Oct4 was a novel target of Wnt signaling pathway. Mol Cell Biochem. 2012;362(1-2):233-40. Epub 20111126. doi: 10.1007/s11010-011-1148-z. PubMed PMID: 22120493.

36. Atlasi Y, van Dorsten RT, Sacchetti A, Joosten R, Oosterhuis JW, Looijenga LHJ, et al. Ectopic activation of WNT signaling in human embryonal carcinoma cells and its effects in short- and long-term in vitro culture. Sci Rep. 2019;9(1):11928. Epub 20190815. doi: 10.1038/s41598-019-48396-7. PubMed PMID: 31417131; PubMed Central PMCID: PMC6695393.

37. Cho JH, Dimri M, Dimri GP. A positive feedback loop regulates the expression of polycomb group protein BMI1 via WNT signaling pathway. J Biol Chem. 2013;288(5):3406-18. Epub 20121213. doi: 10.1074/jbc.M112.422931. PubMed PMID: 23239878; PubMed Central PMCID: PMC3561559.

38. López-Arribillaga E, Rodilla V, Pellegrinet L, Guiu J, Iglesias M, Roman AC, et al. Bmi1 regulates murine intestinal stem cell proliferation and self-renewal downstream of Notch. Development. 2015;142(1):41-50. Epub 20141205. doi: 10.1242/dev.107714. PubMed PMID: 25480918.

39. Xu R, Chen L, Yang WT. Aberrantly elevated Bmi1 promotes cervical cancer tumorigenicity and tumor sphere formation via enhanced transcriptional regulation of Sox2 genes. Oncol Rep. 2019;42(2):688-96. Epub 20190606. doi: 10.3892/or.2019.7188. PubMed PMID: 31173263; PubMed Central PMCID: PMC6609343.

40. Rodda DJ, Chew JL, Lim LH, Loh YH, Wang B, Ng HH, et al. Transcriptional regulation of nanog by OCT4 and SOX2. J Biol Chem. 2005;280(26):24731-7. Epub 20050427. doi: 10.1074/jbc.M502573200. PubMed PMID: 15860457.

41. Gökbuget D, Blelloch R. Epigenetic control of transcriptional regulation in pluripotency and early differentiation. Development. 2019;146(19). Epub 20190925. doi: 10.1242/dev.164772. PubMed PMID: 31554624; PubMed Central PMCID: PMC6803368.

42. Lu H, Lyu Y, Tran L, Lan J, Xie Y, Yang Y, et al. HIF-1 recruits NANOG as a coactivator for TERT gene transcription in hypoxic breast cancer stem cells. Cell Rep. 2021;36(13):109757. doi: 10.1016/j.celrep.2021.109757. PubMed PMID: 34592152.

43. Allen ND, Baird DM. Telomere length maintenance in stem cell populations. Biochim Biophys Acta. 2009;1792(4):324-8. Epub 20090212. doi: 10.1016/j.bbadis.2009.02.004. PubMed PMID: 19419691.

44. Rossiello F, Jurk D, Passos JF, d'Adda di Fagagna F. Telomere dysfunction in ageing and age-related diseases. Nat Cell Biol. 2022;24(2):135-47. Epub 20220214. doi: 10.1038/s41556-022-00842-x. PubMed PMID: 35165420; PubMed Central PMCID: PMC8985209.

45. Blackburn EH, Greider CW, Henderson E, Lee MS, Shampay J, Shippen-Lentz D. Recognition and elongation of telomeres by telomerase. Genome. 1989;31(2):553-60. PubMed PMID: 2698831.

46. Shippen-Lentz D, Blackburn EH. Functional evidence for an RNA template in telomerase. Science. 1990;247(4942):546-52. PubMed PMID: 1689074.

47. Greider CW, Blackburn EH. Identification of a specific telomere terminal transferase activity in Tetrahymena extracts. Cell. 1985;43(2 Pt 1):405-13. doi: 0092-8674(85)90170-9 [pii]. PubMed PMID: 3907856.

48. Lupatov AY, Yarygin KN. Telomeres and Telomerase in the Control of Stem Cells. Biomedicines. 2022;10(10). Epub 20220920. doi: 10.3390/biomedicines10102335. PubMed PMID: 36289597; PubMed Central PMCID: PMC9598777.

49. Bryan TM, Englezou A, Dalla-Pozza L, Dunham MA, Reddel RR. Evidence for an alternative mechanism for maintaining telomere length in human tumors and tumor-derived cell lines. Nat Med. 1997;3(11):1271-4. PubMed PMID: 9359704.

50. Yeager TR, Neumann AA, Englezou A, Huschtscha LI, Noble JR, Reddel RR. Telomerase-negative immortalized human cells contain a novel type of promyelocytic leukemia (PML) body. Cancer Res. 1999;59(17):4175-9. PubMed PMID: 10485449.

51. Zhang JM, Zou L. Alternative lengthening of telomeres: from molecular mechanisms to therapeutic outlooks. Cell Biosci. 2020;10:30. Epub 20200310. doi: 10.1186/s13578-020-00391-6. PubMed PMID: 32175073; PubMed Central PMCID: PMC7063710.

52. Zhao S, Wang F, Liu L. Alternative Lengthening of Telomeres (ALT) in Tumors and Pluripotent Stem Cells. Genes (Basel). 2019;10(12). Epub 20191210. doi: 10.3390/genes10121030. PubMed PMID: 31835618; PubMed Central PMCID: PMC6947546.

53. Dan J, Yang J, Liu Y, Xiao A, Liu L. Roles for Histone Acetylation in Regulation of Telomere Elongation and Two-cell State in Mouse ES Cells. J Cell Physiol. 2015;230(10):2337-44. doi: 10.1002/jcp.24980. PubMed PMID: 25752831; PubMed Central PMCID: PMC4711819.

54. Episkopou H, Draskovic I, Van Beneden A, Tilman G, Mattiussi M, Gobin M, et al. Alternative Lengthening of Telomeres is characterized by reduced compaction of telomeric chromatin. Nucleic Acids Res. 2014;42(7):4391-405. Epub 20140205. doi: 10.1093/nar/gku114. PubMed PMID: 24500201; PubMed Central PMCID: PMC3985679.

55. Liu L. Linking Telomere Regulation to Stem Cell Pluripotency. Trends Genet. 2017;33(1):16-33. Epub 20161123. doi: 10.1016/j.tig.2016.10.007. PubMed PMID: 27889084.

56. Marión RM, Montero JJ, López de Silanes I, Graña-Castro O, Martínez P, Schoeftner S, et al. TERRA regulate the transcriptional landscape of pluripotent cells through TRF1-dependent recruitment of PRC2. Elife. 2019;8. Epub 20190820. doi: 10.7554/eLife.44656. PubMed PMID: 31426913; PubMed Central PMCID: PMC6701927.

57. Lim JE, Son Y. Endogenous Stem Cells in Homeostasis and Aging. Tissue Eng Regen Med. 2017;14(6):679-98. Epub 20171120. doi: 10.1007/s13770-017-0097-3. PubMed PMID: 30603520; PubMed Central PMCID: PMC6171667.

58. Behrens A, van Deursen JM, Rudolph KL, Schumacher B. Impact of genomic damage and ageing on stem cell function. Nat Cell Biol. 2014;16(3):201-7. doi: 10.1038/ncb2928. PubMed PMID: 24576896; PubMed Central PMCID: PMC4214082.

59. Overton M, Pihlsgård M, Elmståhl S. Prevalence and Incidence of Mild Cognitive Impairment across Subtypes, Age, and Sex. Dement Geriatr Cogn Disord. 2019;47(4-6):219-32. Epub 20190716. doi: 10.1159/000499763. PubMed PMID: 31311017.

60. Morales AV, Mira H. Adult Neural Stem Cells: Born to Last. Front Cell Dev Biol. 2019;7:96. Epub 20190604. doi: 10.3389/fcell.2019.00096. PubMed PMID: 31214589; PubMed Central PMCID: PMC6557982.

61. Nicaise AM, Willis CM, Crocker SJ, Pluchino S. Stem Cells of the Aging Brain. Front Aging Neurosci. 2020;12:247. Epub 20200806. doi: 10.3389/fnagi.2020.00247. PubMed PMID: 32848716; PubMed Central PMCID: PMC7426063.

62. Brown SJ, Boussaad I, Jarazo J, Fitzgerald JC, Antony P, Keatinge M, et al. PINK1 deficiency impairs adult neurogenesis of dopaminergic neurons. Sci Rep. 2021;11(1):6617. Epub 20210323. doi: 10.1038/s41598-021-84278-7. PubMed PMID: 33758225; PubMed Central PMCID: PMC7988014.

63. Awad O, Panicker LM, Deranieh RM, Srikanth MP, Brown RA, Voit A, et al. Altered Differentiation Potential of Gaucher's Disease iPSC Neuronal Progenitors due to Wnt/β-Catenin Downregulation. Stem Cell Reports. 2017;9(6):1853-67. Epub 20171130. doi: 10.1016/j.stemcr.2017.10.029. PubMed PMID: 29198828; PubMed Central PMCID: PMC5785733.

64. Coronel R, Lachgar M, Bernabeu-Zornoza A, Palmer C, Domínguez-Alvaro M, Revilla A, et al. Neuronal and Glial Differentiation of Human Neural Stem Cells Is Regulated by Amyloid Precursor Protein (APP) Levels. Mol Neurobiol. 2019;56(2):1248-61. Epub 20180607. doi: 10.1007/s12035-018-1167-9. PubMed PMID: 29881946.

65. Kwak YD, Brannen CL, Qu T, Kim HM, Dong X, Soba P, et al. Amyloid precursor protein regulates differentiation of human neural stem cells. Stem Cells Dev. 2006;15(3):381-9. doi: 10.1089/scd.2006.15.381. PubMed PMID: 16846375.

66. Wang C, Najm R, Xu Q, Jeong DE, Walker D, Balestra ME, et al. Gain of toxic apolipoprotein E4 effects in human iPSC-derived neurons is ameliorated by a small-molecule structure corrector. Nat Med. 2018;24(5):647-57. Epub 20180409. doi: 10.1038/s41591-018-0004-z. PubMed PMID: 29632371; PubMed Central PMCID: PMC5948154.

67. Hayat H, Dwan BF, Gudi M, Bishop JO, Wang P. A Concise Review: The Role of Stem Cells in Cancer Progression and Therapy. Onco Targets Ther. 2021;14:2761-72. Epub 20210420. doi: 10.2147/ott.s260391. PubMed PMID: 33907419; PubMed Central PMCID: PMC8068480.

68. Wainwright EN, Scaffidi P. Epigenetics and Cancer Stem Cells: Unleashing, Hijacking, and Restricting Cellular Plasticity. Trends Cancer. 2017;3(5):372-86. Epub

20170505. doi: 10.1016/j.trecan.2017.04.004. PubMed PMID: 28718414; PubMed Central PMCID: PMC5506260.

69. Feng Y, Liu X, Pauklin S. 3D chromatin architecture and epigenetic regulation in cancer stem cells. Protein Cell. 2021;12(6):440-54. Epub 20210116. doi: 10.1007/s13238-020-00819-2. PubMed PMID: 33453053; PubMed Central PMCID: PMC8160035.

70. Robinson M, Gilbert SF, Waters JA, Lujano-Olazaba O, Lara J, Alexander LJ, et al. Characterization of SOX2, OCT4 and NANOG in Ovarian Cancer Tumor-Initiating Cells. Cancers (Basel). 2021;13(2). Epub 20210112. doi: 10.3390/cancers13020262. PubMed PMID: 33445692; PubMed Central PMCID: PMC7828139.

71. Swain N, Thakur M, Pathak J, Swain B. SOX2, OCT4 and NANOG: The core embryonic stem cell pluripotency regulators in oral carcinogenesis. J Oral Maxillofac Pathol. 2020;24(2):368-73. Epub 20200909. doi: 10.4103/jomfp.JOMFP_22_20. PubMed PMID: 33456249; PubMed Central PMCID: PMC7802841.

72. Müller M, Hermann PC, Liebau S, Weidgang C, Seufferlein T, Kleger A, et al. The role of pluripotency factors to drive stemness in gastrointestinal cancer. Stem Cell Res. 2016;16(2):349-57. Epub 20160203. doi: 10.1016/j.scr.2016.02.005. PubMed PMID: 26896855.

73. Walter K, Rodriguez-Aznar E, Ferreira MSV, Frappart PO, Dittrich T, Tiwary K, et al. Telomerase and Pluripotency Factors Jointly Regulate Stemness in Pancreatic Cancer Stem Cells. Cancers (Basel). 2021;13(13). Epub 20210623. doi: 10.3390/cancers13133145. PubMed PMID: 34201898; PubMed Central PMCID: PMC8268125.

74. Castelo-Branco P, Zhang C, Lipman T, Fujitani M, Hansford L, Clarke I, et al. Neural tumor-initiating cells have distinct telomere maintenance and can be safely targeted for telomerase inhibition. Clin Cancer Res. 2011;17(1):111-21. doi: 10.1158/1078-0432.ccr-10-2075. PubMed PMID: 21208905.

75. Joseph I, Tressler R, Bassett E, Harley C, Buseman CM, Pattamatta P, et al. The telomerase inhibitor imetelstat depletes cancer stem cells in breast and pancreatic cancer cell lines. Cancer Res. 2010;70(22):9494-504. Epub 20101109. doi: 10.1158/0008-5472.can-10-0233. PubMed PMID: 21062983.

76. Bojovic B, Booth RE, Jin Y, Zhou X, Crowe DL. Alternative lengthening of telomeres in cancer stem cells in vivo. Oncogene. 2015;34(5):611-20. Epub 20140217. doi: 10.1038/onc.2013.603. PubMed PMID: 24531712; PubMed Central PMCID: PMC4135038.

77. Mazzoldi EL, Pastò A, Pilotto G, Minuzzo S, Piga I, Palumbo P, et al. Comparison of the Genomic Profile of Cancer Stem Cells and Their Non-Stem Counterpart: The Case

of Ovarian Cancer. J Clin Med. 2020;9(2). Epub 20200129. doi: 10.3390/jcm9020368. PubMed PMID: 32013179; PubMed Central PMCID: PMC7073612.

78. Zhu X, Chen HH, Gao CY, Zhang XX, Jiang JX, Zhang Y, et al. Energy metabolism in cancer stem cells. World J Stem Cells. 2020;12(6):448-61. doi: 10.4252/wjsc.v12.i6.448. PubMed PMID: 32742562; PubMed Central PMCID: PMC7360992.

79. Mani C, Reddy PH, Palle K. DNA repair fidelity in stem cell maintenance, health, and disease. Biochim Biophys Acta Mol Basis Dis. 2020;1866(4):165444. Epub 20190404. doi: 10.1016/j.bbadis.2019.03.017. PubMed PMID: 30953688; PubMed Central PMCID: PMC6935429.

80. Schulz A, Meyer F, Dubrovska A, Borgmann K. Cancer Stem Cells and Radioresistance: DNA Repair and Beyond. Cancers (Basel). 2019;11(6). Epub 20190621. doi: 10.3390/cancers11060862. PubMed PMID: 31234336; PubMed Central PMCID: PMC6627210.

81. Serrano D, Bleau AM, Fernandez-Garcia I, Fernandez-Marcelo T, Iniesta P, Ortiz-de-Solorzano C, et al. Inhibition of telomerase activity preferentially targets aldehyde dehydrogenase-positive cancer stem-like cells in lung cancer. Mol Cancer. 2011;10:96. Epub 20110809. doi: 10.1186/1476-4598-10-96. PubMed PMID: 21827695; PubMed Central PMCID: PMC3199900.

82. Falco G, Lee SL, Stanghellini I, Bassey UC, Hamatani T, Ko MS. Zscan4: a novel gene expressed exclusively in late 2-cell embryos and embryonic stem cells. Dev Biol. 2007;307(2):539-50. Epub 20070508. doi: 10.1016/j.ydbio.2007.05.003. PubMed PMID: 17553482; PubMed Central PMCID: PMC1994725.

83. Zalzman M, Falco G, Sharova LV, Nishiyama A, Thomas M, Lee SL, et al. Zscan4 regulates telomere elongation and genomic stability in ES cells. Nature. 2010;464(7290):858-63. Epub 20100324. doi: 10.1038/nature08882. PubMed PMID: 20336070; PubMed Central PMCID: PMC2851843.

84. Vassena R, Boué S, González-Roca E, Aran B, Auer H, Veiga A, et al. Waves of early transcriptional activation and pluripotency program initiation during human preimplantation development. Development. 2011;138(17):3699-709. Epub 20110720. doi: 10.1242/dev.064741. PubMed PMID: 21775417; PubMed Central PMCID: PMC4074286.

85. Storm MP, Kumpfmueller B, Bone HK, Buchholz M, Sanchez Ripoll Y, Chaudhuri JB, et al. Zscan4 is regulated by PI3-kinase and DNA-damaging agents and directly interacts with the transcriptional repressors LSD1 and CtBP2 in mouse embryonic stem cells. PLoS One. 2014;9(3):e89821. Epub 20140303. doi: 10.1371/journal.pone.0089821. PubMed PMID: 24594919; PubMed Central PMCID: PMC3940611.

86. Ko MS. Zygotic Genome Activation Revisited: Looking Through the Expression and Function of Zscan4. Curr Top Dev Biol. 2016;120:103-24. Epub 20160531. doi: 10.1016/bs.ctdb.2016.04.004. PubMed PMID: 27475850.

87. Lee MT, Bonneau AR, Giraldez AJ. Zygotic genome activation during the maternal-to-zygotic transition. Annu Rev Cell Dev Biol. 2014;30:581-613. Epub 20140811. doi: 10.1146/annurev-cellbio-100913-013027. PubMed PMID: 25150012; PubMed Central PMCID: PMC4303375.

88. Takahashi K, Ross PJ, Sawai K. The necessity of ZSCAN4 for preimplantation development and gene expression of bovine embryos. J Reprod Dev. 2019;65(4):319-26. Epub 20190425. doi: 10.1262/jrd.2019-039. PubMed PMID: 31019155; PubMed Central PMCID: PMC6708851.

89. Akiyama T, Xin L, Oda M, Sharov AA, Amano M, Piao Y, et al. Transient bursts of Zscan4 expression are accompanied by the rapid derepression of heterochromatin in mouse embryonic stem cells. DNA Res. 2015;22(5):307-18. Epub 20150831. doi: 10.1093/dnares/dsv013. PubMed PMID: 26324425; PubMed Central PMCID: PMC4596397.

90. Eckersley-Maslin MA, Svensson V, Krueger C, Stubbs TM, Giehr P, Krueger F, et al. MERVL/Zscan4 Network Activation Results in Transient Genome-wide DNA Demethylation of mESCs. Cell Rep. 2016;17(1):179-92. doi: 10.1016/j.celrep.2016.08.087. PubMed PMID: 27681430; PubMed Central PMCID: PMC5055476.

91. Akiyama T, Xin L, Oda M, Sharov AA, Amano M, Piao Y, et al. Transient bursts of Zscan4 expression are accompanied by the rapid derepression of heterochromatin in mouse embryonic stem cells. DNA research : an international journal for rapid publication of reports on genes and genomes. 2015. Epub 2015/09/02. doi: 10.1093/dnares/dsv013. PubMed PMID: 26324425.

92. Eckersley-Maslin Mélanie A, Svensson V, Krueger C, Stubbs TM, Giehr P, Krueger F, et al. MERVL/Zscan4 Network Activation Results in Transient Genome-wide DNA Demethylation of mESCs. Cell reports. 2016;17(1):179-92. doi: 10.1016/j.celrep.2016.08.087. PubMed PMID: PMC5055476.

93. Zalzman M. Zscan4 regulates cellular immortality and response to DNA damage of mouse embryonic stem cells. Journal of Cell Science and Therapy. 2012;3(8):129-31.

94. Dan J, Zhou Z, Wang F, Wang H, Guo R, Keefe DL, et al. Zscan4 Contributes to Telomere Maintenance in Telomerase-Deficient Late Generation Mouse ESCs and Human ALT Cancer Cells. Cells. 2022;11(3). Epub 20220128. doi: 10.3390/cells11030456. PubMed PMID: 35159266; PubMed Central PMCID: PMC8834411.

95. Le R, Huang Y, Zhang Y, Wang H, Lin J, Dong Y, et al. Dcaf11 activates Zscan4-mediated alternative telomere lengthening in early embryos and embryonic stem cells. Cell Stem Cell. 2021;28(4):732-47.e9. Epub 20201223. doi: 10.1016/j.stem.2020.11.018. PubMed PMID: 33357405.

96. Hirata T, Amano T, Nakatake Y, Amano M, Piao Y, Hoang HG, et al. Zscan4 transiently reactivates early embryonic genes during the generation of induced pluripotent stem cells. Sci Rep. 2012;2:208. Epub 20120104. doi: 10.1038/srep00208. PubMed PMID: 22355722; PubMed Central PMCID: PMC3250575.

97. Portney BA, Arad M, Gupta A, Brown RA, Khatri R, Lin PN, et al. ZSCAN4 facilitates chromatin remodeling and promotes the cancer stem cell phenotype. Oncogene. 2020;39(26):4970-82. Epub 20200607. doi: 10.1038/s41388-020-1333-1. PubMed PMID: 32507861; PubMed Central PMCID: PMC7314663.

98. Storm MP, Kumpfmueller B, Thompson B, Kolde R, Vilo J, Hummel O, et al. Characterization of the phosphoinositide 3-kinase-dependent transcriptome in murine embryonic stem cells: identification of novel regulators of pluripotency. Stem Cells. 2009;27(4):764-75. doi: 10.1002/stem.3. PubMed PMID: 19350676.

99. Jiang J, Lv W, Ye X, Wang L, Zhang M, Yang H, et al. Zscan4 promotes genomic stability during reprogramming and dramatically improves the quality of iPS cells as demonstrated by tetraploid complementation. Cell Res. 2013;23(1):92-106. Epub 20121113. doi: 10.1038/cr.2012.157. PubMed PMID: 23147797; PubMed Central PMCID: PMC3541664.

100. Amano T, Hirata T, Falco G, Monti M, Sharova LV, Amano M, et al. Zscan4 restores the developmental potency of embryonic stem cells. Nat Commun. 2013;4:1966. doi: 10.1038/ncomms2966. PubMed PMID: 23739662; PubMed Central PMCID: PMC3682791.

101. Beane OS, Fonseca VC, Cooper LL, Koren G, Darling EM. Impact of aging on the regenerative properties of bone marrow-, muscle-, and adipose-derived mesenchymal stem/stromal cells. PLoS One. 2014;9(12):e115963. Epub 20141226. doi: 10.1371/journal.pone.0115963. PubMed PMID: 25541697; PubMed Central PMCID: PMC4277426.

102. Yang YK, Ogando CR, Wang See C, Chang TY, Barabino GA. Changes in phenotype and differentiation potential of human mesenchymal stem cells aging in vitro. Stem Cell Res Ther. 2018;9(1):131. Epub 20180511. doi: 10.1186/s13287-018-0876-3. PubMed PMID: 29751774; PubMed Central PMCID: PMC5948736.

103. Bonab MM, Alimoghaddam K, Talebian F, Ghaffari SH, Ghavamzadeh A, Nikbin B. Aging of mesenchymal stem cell in vitro. BMC Cell Biol. 2006;7:14. Epub 20060310. doi: 10.1186/1471-2121-7-14. PubMed PMID: 16529651; PubMed Central PMCID: PMC1435883.

104. Cantor EL, Shen F, Jiang G, Tan Z, Cunningham GM, Wu X, et al. Passage number affects differentiation of sensory neurons from human induced pluripotent stem cells. Sci Rep. 2022;12(1):15869. Epub 20220923. doi: 10.1038/s41598-022-19018-6. PubMed PMID: 36151116; PubMed Central PMCID: PMC9508090.

105. Wilson DM, 3rd, Cookson MR, Van Den Bosch L, Zetterberg H, Holtzman DM, Dewachter I. Hallmarks of neurodegenerative diseases. Cell. 2023;186(4):693-714. doi: 10.1016/j.cell.2022.12.032. PubMed PMID: 36803602.

106. Björklund A, Stenevi U. Reconstruction of the nigrostriatal dopamine pathway by intracerebral nigral transplants. Brain Res. 1979;177(3):555-60. doi: 10.1016/0006-8993(79)90472-4. PubMed PMID: 574053.

107. Freed WJ, Perlow MJ, Karoum F, Seiger A, Olson L, Hoffer BJ, et al. Restoration of dopaminergic function by grafting of fetal rat substantia nigra to the caudate nucleus: long-term behavioral, biochemical, and histochemical studies. Ann Neurol. 1980;8(5):510-9. doi: 10.1002/ana.410080508. PubMed PMID: 7436393.

108. Perlow MJ, Freed WJ, Hoffer BJ, Seiger A, Olson L, Wyatt RJ. Brain grafts reduce motor abnormalities produced by destruction of nigrostriatal dopamine system. Science. 1979;204(4393):643-7. doi: 10.1126/science.571147. PubMed PMID: 571147.

109. Maiti P, Manna J, Dunbar GL. Current understanding of the molecular mechanisms in Parkinson's disease: Targets for potential treatments. Transl Neurodegener. 2017;6:28. Epub 20171025. doi: 10.1186/s40035-017-0099-z. PubMed PMID: 29090092; PubMed Central PMCID: PMC5655877.

110. Stoker TB, Barker RA. Cell therapies for Parkinson's disease: how far have we come? Regen Med. 2016;11(8):777-86. Epub 20161125. doi: 10.2217/rme-2016-0102. PubMed PMID: 27885887; PubMed Central PMCID: PMC5221268.

111. Jung N, Park S, Choi Y, Park JW, Hong YB, Park HH, et al. Tonsil-Derived Mesenchymal Stem Cells Differentiate into a Schwann Cell Phenotype and Promote Peripheral Nerve Regeneration. Int J Mol Sci. 2016;17(11). Epub 20161109. doi: 10.3390/ijms17111867. PubMed PMID: 27834852; PubMed Central PMCID: PMC5133867.

112. Park S, Kim JY, Myung S, Jung N, Choi Y, Jung SC. Differentiation of Motor Neuron-Like Cells from Tonsil-Derived Mesenchymal Stem Cells and Their Possible Application to Neuromuscular Junction Formation. Int J Mol Sci. 2019;20(11). Epub 20190601. doi: 10.3390/ijms20112702. PubMed PMID: 31159418; PubMed Central PMCID: PMC6600529.

113. Al-Azab M, Safi M, Idiiatullina E, Al-Shaebi F, Zaky MY. Aging of mesenchymal stem cell: machinery, markers, and strategies of fighting. Cell Mol Biol Lett.

2022;27(1):69. Epub 20220819. doi: 10.1186/s11658-022-00366-0. PubMed PMID: 35986247; PubMed Central PMCID: PMC9388978.

114. Hass R, Kasper C, Böhm S, Jacobs R. Different populations and sources of human mesenchymal stem cells (MSC): A comparison of adult and neonatal tissue-derived MSC. Cell Commun Signal. 2011;9:12. Epub 20110514. doi: 10.1186/1478-811x-9-12. PubMed PMID: 21569606; PubMed Central PMCID: PMC3117820.

115. Nishimori M, Yamada Y, Hoshi K, Akiyama Y, Hoshi Y, Morishima Y, et al. Health-related quality of life of unrelated bone marrow donors in Japan. Blood. 2002;99(6):1995-2001. doi: 10.1182/blood.v99.6.1995. PubMed PMID: 11877271.

116. Buckner CD, Clift RA, Sanders JE, Stewart P, Bensinger WI, Doney KC, et al. Marrow harvesting from normal donors. Blood. 1984;64(3):630-4. PubMed PMID: 6380620.

117. Urrutia DN, Caviedes P, Mardones R, Minguell JJ, Vega-Letter AM, Jofre CM. Comparative study of the neural differentiation capacity of mesenchymal stromal cells from different tissue sources: An approach for their use in neural regeneration therapies. PLoS One. 2019;14(3):e0213032. Epub 20190311. doi: 10.1371/journal.pone.0213032. PubMed PMID: 30856179; PubMed Central PMCID: PMC6437714.

118. Arad M, Brown RA, Khatri R, Taylor RJ, Zalzman M. Direct differentiation of tonsillar biopsy-derived stem cells to the neuronal lineage. Cell Mol Biol Lett. 2021;26(1):38. Epub 20210818. doi: 10.1186/s11658-021-00279-4. PubMed PMID: 34407767; PubMed Central PMCID: PMC8371824.

119. Guo X, Tang Y, Zhang P, Li S, Chen Y, Qian B, et al. Effect of ectopic high expression of transcription factor OCT4 on the "stemness" characteristics of human bone marrow-derived mesenchymal stromal cells. Stem Cell Res Ther. 2019;10(1):160. Epub 20190603. doi: 10.1186/s13287-019-1263-4. PubMed PMID: 31159871; PubMed Central PMCID: PMC6547465.

120. Han SM, Han SH, Coh YR, Jang G, Chan Ra J, Kang SK, et al. Enhanced proliferation and differentiation of Oct4- and Sox2-overexpressing human adipose tissue mesenchymal stem cells. Exp Mol Med. 2014;46(6):e101. Epub 20140620. doi: 10.1038/emm.2014.28. PubMed PMID: 24946789; PubMed Central PMCID: PMC4081551.

121. Han J, Mistriotis P, Lei P, Wang D, Liu S, Andreadis ST. Nanog reverses the effects of organismal aging on mesenchymal stem cell proliferation and myogenic differentiation potential. Stem Cells. 2012;30(12):2746-59. doi: 10.1002/stem.1223. PubMed PMID: 22949105; PubMed Central PMCID: PMC3508087.

122. Markiewicz-Potoczny M, Lobanova A, Loeb AM, Kirak O, Olbrich T, Ruiz S, et al. TRF2-mediated telomere protection is dispensable in pluripotent stem cells. Nature.

2021;589(7840):110-5. Epub 20201125. doi: 10.1038/s41586-020-2959-4. PubMed PMID: 33239785; PubMed Central PMCID: PMC9161009.

123. Chung CS, Fujita N, Kawahara N, Yui S, Nam E, Nishimura R. A comparison of neurosphere differentiation potential of canine bone marrow-derived mesenchymal stem cells and adipose-derived mesenchymal stem cells. J Vet Med Sci. 2013;75(7):879-86. Epub 20130219. doi: 10.1292/jvms.12-0470. PubMed PMID: 23419261.

124. Portney BA, Khatri R, Meltzer WA, Mariano JM, Zalzman M. ZSCAN4 is negatively regulated by the ubiquitin-proteasome system and the E3 ubiquitin ligase RNF20. Biochem Biophys Res Commun. 2018;498(1):72-8. Epub 20180302. doi: 10.1016/j.bbrc.2018.02.155. PubMed PMID: 29477841; PubMed Central PMCID: PMC5928792.

125. Cawthon RM. Telomere measurement by quantitative PCR. Nucleic Acids Res. 2002;30(10):e47. doi: 10.1093/nar/30.10.e47. PubMed PMID: 12000852; PubMed Central PMCID: PMC115301.

126. Toh TB, Lim JJ, Chow EK. Epigenetics in cancer stem cells. Mol Cancer. 2017;16(1):29. Epub 20170201. doi: 10.1186/s12943-017-0596-9. PubMed PMID: 28148257; PubMed Central PMCID: PMC5286794.

127. Shimokawa M, Ohta Y, Nishikori S, Matano M, Takano A, Fujii M, et al. Visualization and targeting of LGR5(+) human colon cancer stem cells. Nature. 2017;545(7653):187-92. Epub 20170329. doi: 10.1038/nature22081. PubMed PMID: 28355176.

128. Hirashima K, Migita T, Sato S, Muramatsu Y, Ishikawa Y, Seimiya H. Telomere length influences cancer cell differentiation in vivo. Mol Cell Biol. 2013;33(15):2988-95. Epub 20130528. doi: 10.1128/mcb.00136-13. PubMed PMID: 23716593; PubMed Central PMCID: PMC3719673.

129. Shibata M, Hoque MO. Targeting Cancer Stem Cells: A Strategy for Effective Eradication of Cancer. Cancers (Basel). 2019;11(5). Epub 20190527. doi: 10.3390/cancers11050732. PubMed PMID: 31137841; PubMed Central PMCID: PMC6562442.

130. Tallman MS, Andersen JW, Schiffer CA, Appelbaum FR, Feusner JH, Ogden A, et al. All-trans-retinoic acid in acute promyelocytic leukemia. N Engl J Med. 1997;337(15):1021-8. doi: 10.1056/nejm199710093371501. PubMed PMID: 9321529.

131. Wood A, Krogan NJ, Dover J, Schneider J, Heidt J, Boateng MA, et al. Bre1, an E3 ubiquitin ligase required for recruitment and substrate selection of Rad6 at a promoter. Mol Cell. 2003;11(1):267-74. doi: 10.1016/s1097-2765(02)00802-x. PubMed PMID: 12535539.

132. Peterson CL. Chromatin: a ubiquitin crowbar opens chromatin. Nat Chem Biol. 7. United States2011. p. 68-9.

133. Picon H, Guddati AK. Cancer stem cells in head and neck cancer. Am J Stem Cells. 2021;10(3):28-35. Epub 20210815. PubMed PMID: 34552815; PubMed Central PMCID: PMC8449141.

134. Muraki Y, Hasegawa T, Takeda D, Ueha T, Iwata E, Saito I, et al. Induced Pluripotent Stem Cell-related Genes Correlate With Poor Prognoses of Oral Squamous Cell Carcinoma. Anticancer Res. 2019;39(3):1205-16. doi: 10.21873/anticanres.13231. PubMed PMID: 30842151.

135. Leinung M, Ernst B, Döring C, Wagenblast J, Tahtali A, Diensthuber M, et al. Expression of ALDH1A1 and CD44 in primary head and neck squamous cell carcinoma and their value for carcinogenesis, tumor progression and cancer stem cell identification. Oncol Lett. 2015;10(4):2289-94. Epub 20150729. doi: 10.3892/ol.2015.3542. PubMed PMID: 26622836; PubMed Central PMCID: PMC4579825.

136. Wang L, Xu Z, Liu C, Wei H, Zhang R, Chen Y, et al. Histone H2B ubiquitination mediated chromatin relaxation is essential for the induction of somatic cell reprogramming. Cell Prolif. 2021;54(8):e13080. Epub 20210622. doi: 10.1111/cpr.13080. PubMed PMID: 34155716; PubMed Central PMCID: PMC8349662.

137. Wu C, Cui Y, Liu X, Zhang F, Lu LY, Yu X. The RNF20/40 complex regulates p53-dependent gene transcription and mRNA splicing. J Mol Cell Biol. 2020;12(2):113-24. doi: 10.1093/jmcb/mjz045. PubMed PMID: 31152661; PubMed Central PMCID: PMC7109600.

138. Tanny JC, Erdjument-Bromage H, Tempst P, Allis CD. Ubiquitylation of histone H2B controls RNA polymerase II transcription elongation independently of histone H3 methylation. Genes Dev. 2007;21(7):835-47. Epub 20070320. doi: 10.1101/gad.1516207. PubMed PMID: 17374714; PubMed Central PMCID: PMC1838534.

139. Shema E, Tirosh I, Aylon Y, Huang J, Ye C, Moskovits N, et al. The histone H2B-specific ubiquitin ligase RNF20/hBRE1 acts as a putative tumor suppressor through selective regulation of gene expression. Genes Dev. 2008;22(19):2664-76. doi: 10.1101/gad.1703008. PubMed PMID: 18832071; PubMed Central PMCID: PMC2559905.

140. Wu Z, Liu J, Zhang QD, Lv DK, Wu NF, Zhou JQ. Rad6-Bre1-mediated H2B ubiquitination regulates telomere replication by promoting telomere-end resection. Nucleic Acids Res. 2017;45(6):3308-22. doi: 10.1093/nar/gkx101. PubMed PMID: 28180293; PubMed Central PMCID: PMC5389628.

141. So CC, Ramachandran S, Martin A. E3 Ubiquitin Ligases RNF20 and RNF40 Are Required for Double-Stranded Break (DSB) Repair: Evidence for Monoubiquitination of Histone H2B Lysine 120 as a Novel Axis of DSB Signaling and Repair. Mol Cell Biol. 2019;39(8). Epub 20190402. doi: 10.1128/mcb.00488-18. PubMed PMID: 30692271; PubMed Central PMCID: PMC6447412.

142. Oh SY, Kang HJ, Kim YS, Kim H, Lim YC. CD44-negative cells in head and neck squamous carcinoma also have stem-cell like traits. Eur J Cancer. 2013;49(1):272-80. Epub 20120706. doi: 10.1016/j.ejca.2012.06.004. PubMed PMID: 22770891.

143. Wu L, Li L, Zhou B, Qin Z, Dou Y. H2B ubiquitylation promotes RNA Pol II processivity via PAF1 and pTEFb. Mol Cell. 2014;54(6):920-31. Epub 20140515. doi: 10.1016/j.molcel.2014.04.013. PubMed PMID: 24837678; PubMed Central PMCID: PMC4065619.

144. Tarcic O, Pateras IS, Cooks T, Shema E, Kanterman J, Ashkenazi H, et al. RNF20 Links Histone H2B Ubiquitylation with Inflammation and Inflammation-Associated Cancer. Cell Rep. 2016;14(6):1462-76. Epub 20160204. doi: 10.1016/j.celrep.2016.01.020. PubMed PMID: 26854224; PubMed Central PMCID: PMC4761112.

145. Zhao M, Sano D, Pickering CR, Jasser SA, Henderson YC, Clayman GL, et al. Assembly and initial characterization of a panel of 85 genomically validated cell lines from diverse head and neck tumor sites. Clin Cancer Res. 2011;17(23):7248-64. Epub 2011/08/25. doi: 10.1158/1078-0432.CCR-11-0690. PubMed PMID: 21868764; PubMed Central PMCID: PMC3229662.

146. Goparaju SK, Kohda K, Ibata K, Soma A, Nakatake Y, Akiyama T, et al. Rapid differentiation of human pluripotent stem cells into functional neurons by mRNAs encoding transcription factors. Sci Rep. 2017;7:42367. Epub 20170213. doi: 10.1038/srep42367. PubMed PMID: 28205555; PubMed Central PMCID: PMC5304326.